NASA Contractor Report 159124

Evaluation of Aero Commander Propeller Acoustic Data: Taxi Operations

A. G. Piersol
E. G. Wilby
J. F. Wilby

BOLT BERANEK AND NEWMAN INC.
Canoga Park, Ca. 91303

CONTRACT NO. NAS1-14611-26
JULY 1979

National Aeronautics and
Space Administration

Langley Research Center
Hampton, Virginia 23665

NASA Contractor Report 159124

Evaluation of Aero Commander Propeller Acoustic Data: Taxi Operations

A. G. Piersol
E. G. Wilby
J. F. Wilby

BOLT BERANEK AND NEWMAN INC.
Canoga Park, Ca. 91303

CONTRACT NO. NAS1-14611-26
JULY 1979

National Aeronautics and
Space Administration

Langley Research Center
Hampton, Virginia 23665

ABSTRACT

This report is the second in a series covering the analyses of acoustic data from ground tests performed on an Aero Commander propeller-driven aircraft with an array of microphones flush-mounted on the side of the fuselage. The analyses of data acquired during static operations are summarized in NASA CR-158919. This document details results for taxi operations. The analyses were concerned with the propeller blade passage noise during operations at several different taxi speeds and included calculations of the magnitude and phase of the blade passage tones, the amplitude stability of the tones, and the spatial phase and coherence of the tones. The results confirm the basic conclusion deduced from the static operations data in CR-158919 that the pressure field impinging on the fuselage represents primarily aerodynamic (near field) effects in the plane of the propeller at all frequencies. Forward and aft of the propeller plane, aerodynamic effects still dominate the pressure field below 200 Hz, but at the higher frequencies, the pressure field is acoustic in character and falls in magnitude dramatically as the airplane acquires forward velocity. The aerodynamic pressure field in the plane of the propeller does not diminish significantly with forward velocity up through the fifteenth harmonic of the propeller blade passage frequency. A number of comparisons of the measured results to theoretical predictions for propeller noise are presented, as well as various evaluations which reveal important details of propeller noise characteristics.

TABLE OF CONTENTS

TABLE OF CONTENTS (Cont'd)

LIST OF FIGURES

LIST OF FIGURES (Cont'd)

LIST OF TABLES

EVALUATION OF AERO COMMANDER PROPELLER ACOUSTIC DATA DURING TAXI OPERATIONS

1. INTRODUCTION AND OBJECTIVES

Considerable quantities of vibration and acoustic data have been collected by the NASA Langley Research Center (LRC) on a reciprocating engine propeller driven Aero Commander airplane during static ground runup and taxi operations. Among the data acquired were pressure signals from an array of microphones flush mounted on the starboard side of the fuselage. Some analyses of the resulting acoustic data were performed by LRC personnel [1], and more detailed analyses of the data collected during static operations have been carried out by Bolt Beranek and Newman (BBN) [2]. This report is concerned with additional analyses of the acoustic data collected during taxi operations at various taxi speeds. The specific data of interest are as follows:

a) The magnitude of all significant propeller blade passage tones at various locations on the fuselage for various taxi speeds.

b) The magnitude stability of the propeller blade passage tones at selected locations on the fuselage for various taxi speeds.

c) The phase of the propeller blade passage tones at each of several selected locations on the fuselage for various taxi speeds.

d) The spatial correlation and velocity of the propeller blade passage tones over the fuselage for various taxi speeds.

This report summarizes the procedures and results of the data analysis designed to obtain the above desired information. The analyses were performed by BBN for LRC under Task Assignment No. 26 of Contract NAS1-14611.

2. DATA AND INSTRUMENTATION

The data were provided for analysis by LRC in the form of frequency modulated magnetic tape recordings of sound pressure levels on 14-channel tape. These recordings were transcribed from the original recordings which were made using a 4-channel FM recorder. Hence, for any given test run, only four microphone locations were simultaneously recorded. The frequency range for the data after dubbing operations was 0 to 10 kHz.

2.1 Summary of Data

The recorded data were divided into two parts, each part including four channels representing four different measurement locations for various taxi runs, as summarized in Table 1. The measurement locations indicated in Table 1 are detailed in Figure 1. Note that microphone No. 5 (at the center of the array) was included in both sets of data and, hence, represents the only common measurement for all speed conditions. Further note that microphones No. 2,6,7, and 10 were not recorded for these experiments.

Table 1. Summary of Aero Commander Taxi Runs

Run Number	Taxi Speed (Knots)	Engine Speed (rpm)	Blade Passage Frequency (Hz)	Measurement Locations (Figure 1)
1	Static	2600	81.8	1 5 8 9
2	30	2600	81.8	1 5 8 9
3	40	2690	84.6	1 5 8 9
4	Static	2580	81.4	3 4 5 11
5	40	2710	85.4	3 4 5 11
6	55	2770	87.2	3 4 5 11
7	70	2620	82.6	3 4 5 11

Location	1	2	3	4	5	6	7	8	9	10	11*
x (Meters)	-.622	-.368	0	0	0	0	.368	.622	1.841	2.785	0
y (Meters)	0	0	.584	.279	0	-.305	0	0	.152	.152	.279

Propeller Diameter = 2.36 m

Distance From Microphone to Propeller Tip (Along Radius)	3	4	5	6
	.140	.121	.178	.330

* Location 11 is inside the fuselage 0.25 meters directly left of Location 4

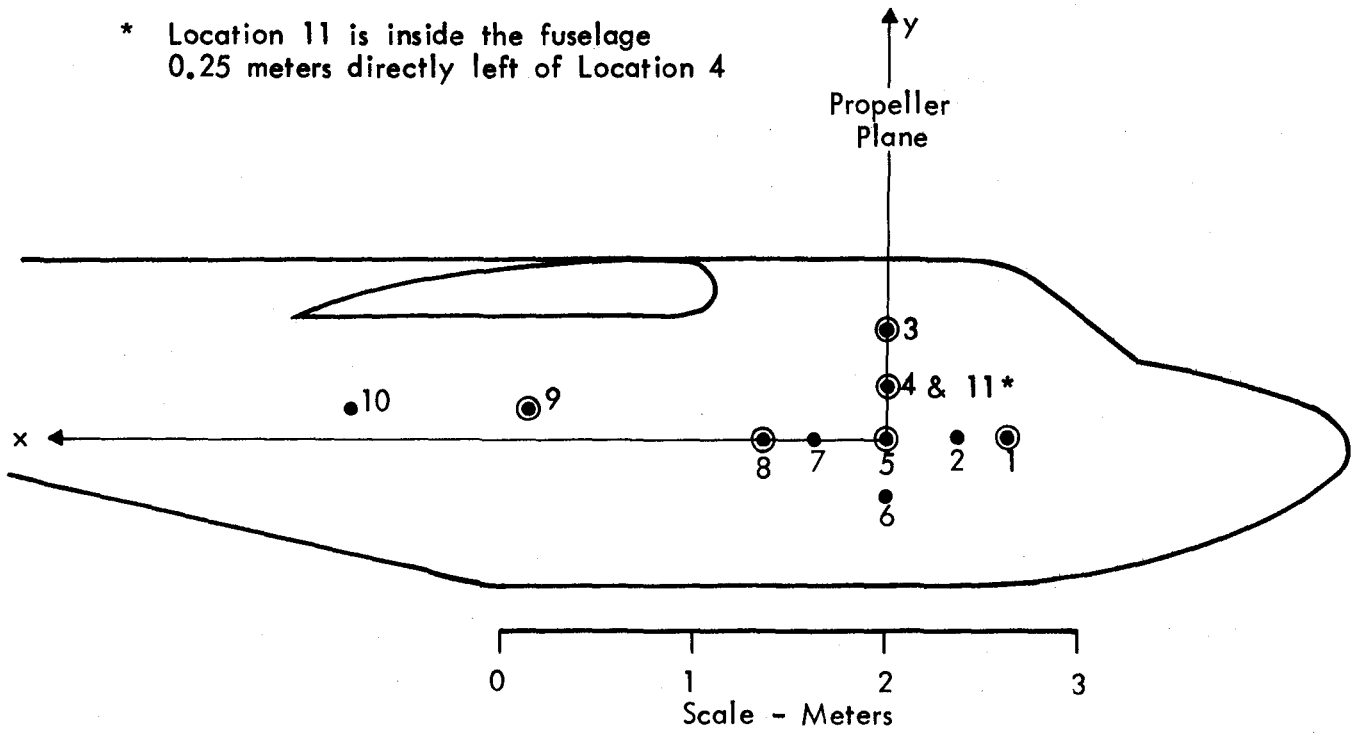

◉ Microphone Locations for Taxi Runs

FIGURE 1. LOCATION OF MICROPHONES FOR AERO COMMANDER TEST RUNS

Each channel of recording was preceded by a 124 dB acoustic calibration signal at 250 Hz. Other calibrations were carried out by LRC on various elements in the data collection system to assure that the frequency response of the system is reasonably flat from 0 to 10 kHz, and that the four channels for a given recording are in phase.

The various test runs were accomplished as follows:

1. With airplane held by its brakes, power was established on both engines at approximately 40% of rated 320 hp (2600 rpm nominal).
2. The brakes were then released permitting the airplane to accelerate to the desired taxi speed.
3. Upon reaching the desired taxi speed, the brakes were again applied as required to maintain an approximately constant speed with full engine power.
4. This full power constant speed taxi condition was maintained for at least 30 seconds and data were recorded.

For all runs except No. 7 (the 70 knot run), the propeller pitch was maintained on the stops at full pitch. As seen from Table 1, the engine rpm did tend to increase somewhat above the nominal 2600 rpm at the higher taxi speeds. For the 70 knot run, the engine rpm could not be stabilized under these conditions, so the propeller pitch was freed from the stops for this run.

During these tests, the ambient wind speed reached a maximum of 20 knots, which was significantly higher than the 5 knot speed associated with the tests reported in [2]. Furthermore, during the static tests reported herein, the airplane orientation relative to the wind direction was not the same for all test runs.

2.2 Summary of Analysis Instrumentation

The data analysis instrumentation used for these studies were basically the same as used previously for the analysis of the static operations data [2]. Specifically, the data records were reproduced for analysis using a Hewlett Packard 3924B magnetic tape recorder with appropriate FM reproduce electronics. All analyses were performed using the appropriate function on a Spectral Dynamics Model SD360 Digital Signal Processor. The stability studies of the propeller blade passage tones required a narrowband analog filtering operation prior to the SD360 Processor. This was provided by a General Radio Model 1564A Sound and Vibration Analyzer. Exact frequencies were generated using a General Radio Model 204D oscillator and calculated with a General Radio Model 1192B counter. A schematic diagram of the instrumentation for these general analysis is shown in Figure 2.

As part of the propeller blade passage tone stability studies, signal enhancement (ensemble averaging) analysis was also performed. Since the recorded data did not include a propeller position indicator pulse, it was necessary to define the approximate propeller position using the propeller blade passage signal which was isolated with the General Radio Model 1564A Sound and Vibration Analyzer. The isolated blade passage tone was used to drive a clamp circuit which in turn triggered the digital signal processor. A schematic diagram of the instrumentation for the signal enhancement analysis is shown in Figure 3.

It should be mentioned that the above technique for generating the time base for signal enhancement is not wholly satisfactory since slight amounts of noise in the fundamental blade passage tone used to trigger the analyzer will translate into time base

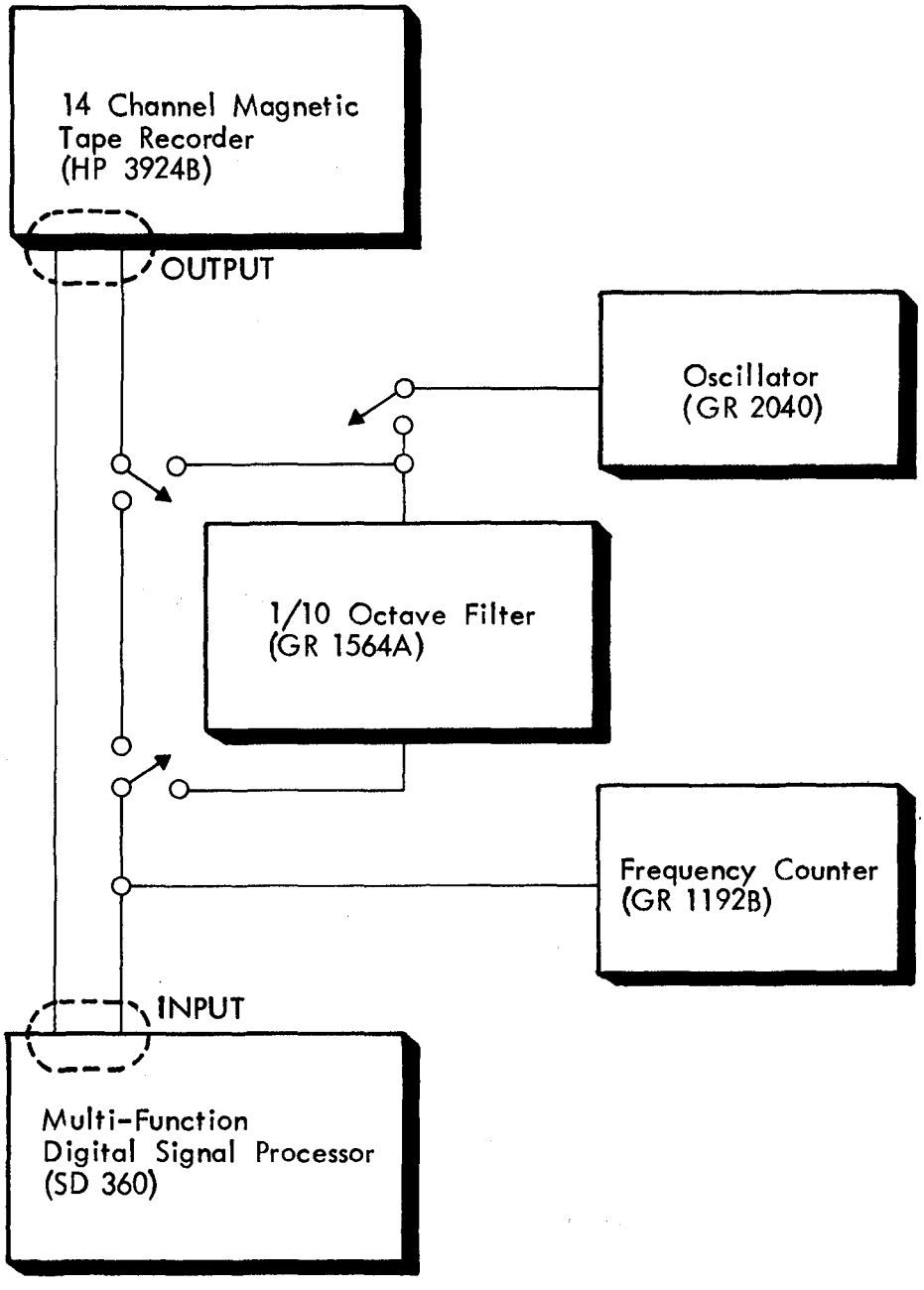

FIGURE 2. SCHEMATIC DIAGRAM OF GENERAL ANALYSIS INSTRUMENTATION

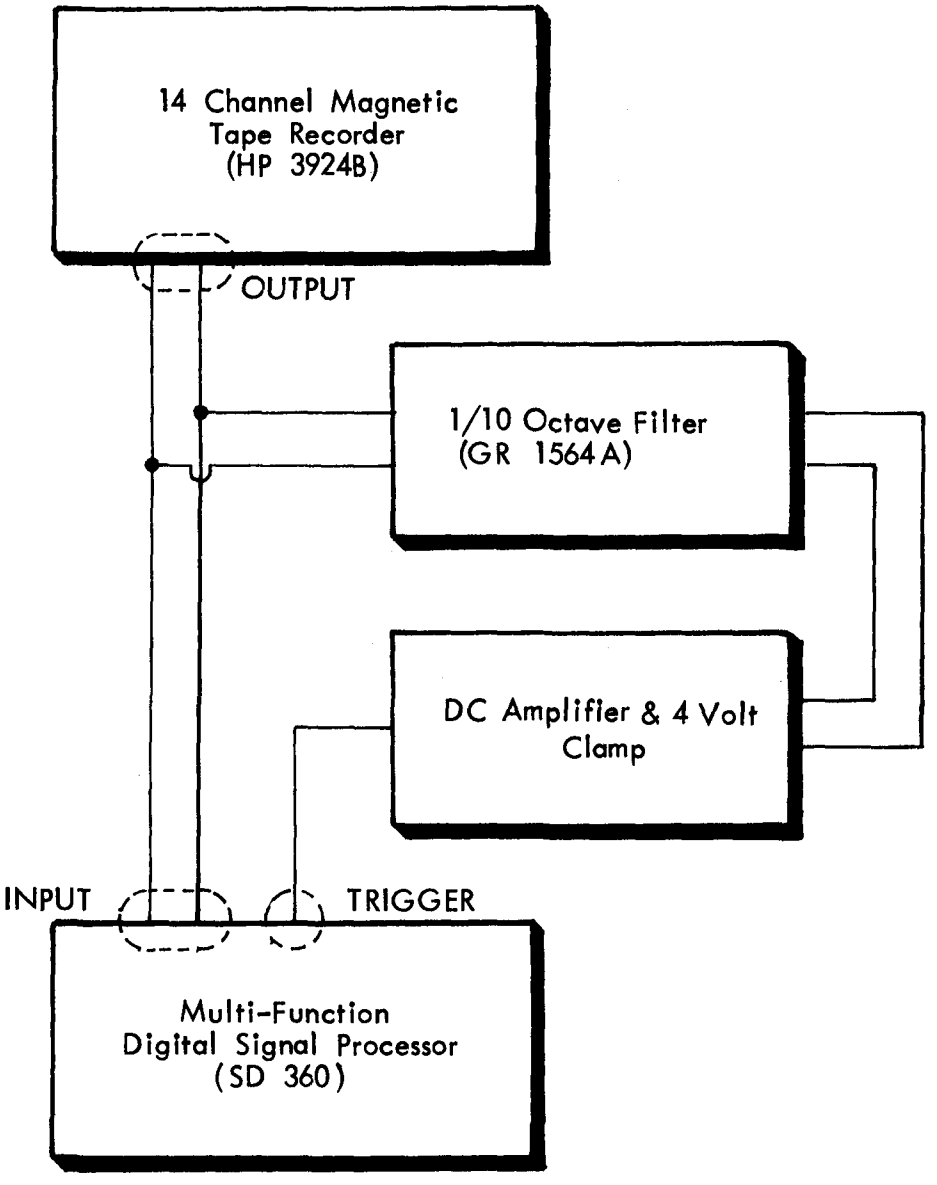

FIGURE 3. SCHEMATIC DIAGRAM OF SIGNAL ENHANCEMENT INSTRUMENTATION

errors in the resulting ensemble of records. These errors should not have a significant impact on the first few harmonics in the enhanced signal, but might tend to exaggerate the apparent noise in the magnitudes of higher harmonics.

Additional procedures used in the analysis of beats measured by the interior microphone(#11) are given in Appendix E, Section E.3.1.

3. DATA ANALYSIS PROCEDURES

The required data analyses broadly divide into four categories, as previously summarized in Section 1. For each type of analysis, certain preliminary steps were required to select appropriate analysis parameters and establish necessary calibrations.

3.1 Magnitude of Propeller Blade Passage Tones

This analysis was performed directly on the SD360 using Function 3 (2048 point forward transform) with a Kaiser-Bessel time window. To be consistent with the data previously analyzed for static operating conditions [2], the magnitude analysis was performed using a frequency resolution of B_e = 2 Hz over a frequency range from 0 to 2 kHz. The 2 kHz upper frequency cutoff was sufficiently high to include most of the significant blade passage tones. The 2 Hz resolution was sufficiently wide to cover the bandwidth of individual blade passage tones while still being narrow enough to isolate the blade passage tones from engine exhaust harmonics. An exception here was the seventh blade passage tone which cannot be separated from an exhaust harmonic that falls at almost identically the same frequency.

The calibration of the processor for this analysis was accomplished by analyzing the 124 dB calibration signals on the tape using exactly the same parameter settings as would be used later for the actual data analysis. The peak spectral value of the calibration signal on each channel was then fixed at 0 dB and all spectral values for the actual data were read off relative to this reference. It should be mentioned that because the digital processor calculates spectral values at discrete frequencies 2 Hz apart, the indicated magnitudes of the calibration signals,

as well as the data signals, are influenced by the exact ratio between the signal frequency and the A/D conversion rate of the processor. An effort was made to correct for this during calibration, but the resulting data should not be considered accurate to more than ± 1 dB relative to the calibration signal at the calibration frequency. Based upon the calibration of individual components in the data acquisition system by LRC personnel, the frequency response function of the acquisition system was assumed to be acceptably flat.

Having selected analysis parameters and calibrated the processor, the magnitudes of all significant propeller blade passage components at the seven locations of interest in Figure 1 were calculated for all test runs in Table 1. These data were then corrected for the various attenuator settings used for the recording and analysis.

3.2 Stability of Propeller Blade Passage Tones

The amplitude stability of significant propeller blade passage tones was evaluated in two ways;

(a) by signal enhancement of the recorded pressure time history signals, and

(b) by probability density analysis of the isolated blade passage tones.

3.2.1 Signal Enhancement Procedures

The signal enhancement was accomplished on the SD360 using Function 13 (signal average/1024 point forward transform) with

a minimum of n_d = 512 averages. The ensemble of sample records was generated on a common time base as previously illustrated in Figure 3. Each sample record in the ensemble was T = 0.5 seconds long and, hence, included about fifteen complete rotations of the propeller. The records were overlapped to maximize the number of records per unit time. The resulting enhanced time history was Fourier transformed to calculate a spectrum with a B_e = 2 Hz resolution over a frequency range from zero to 1000 Hz using a Kaiser-Bessel time window. Noting that the signal to noise ratio in the ensemble averaging operation increases as $\sqrt{n_d}$, the resulting increase in the signal (stable propeller blade passage tone) to noise ratio was over 27 dB in the enhanced spectrum. This was adequate not only to virtually eliminate the stochastic contributions in the blade passage tones, but also to strongly suppress the exhaust noise and other extraneous noise in the data. It should be kept in mind, however, that some of the signal at higher order harmonics was probably also suppressed due to the manner in which the time base was established for the signal enhancement operation, as discussed in Section 2.

The calibration of the processor for this analysis was accomplished exactly as described for the tone magnitude measurements in Section 3.1. The magnitudes of all significant propeller blade passage tones after signal enhancement at all exterior locations were then calculated for test runs No. 1,2,3, and 7 in Table 1 (static operation, and taxi speeds of 30, 40 and 70 knots).

3.2.2 Probability Density Procedures

The blade passage tone stability studies using probability density measurements were accomplished by procedures similar to those employed for the static test data [2]. Specifically, the output

of the tape recorder was passed through a narrow bandpass filter which could be tuned to isolate individual propeller blade passage tones without restricting their bandwidth. The output of the bandpass filter was then analyzed on the SD360 using Function 14 (probability density histogram), as previously illustrated in Figure 2. The bandpass operation was achieved using a 1/10 octave (7 percent) filter. The analyses were performed using a record length that was at least 50 times longer than the reciprocal of the isolation filter bandwidth ($T > 50/B$) to assure that the probability density calculation would truly reflect a representative sample of the narrow band data.

The instrumentation was calibrated for the tone stability studies by applying a sine wave from the oscillator in Figure 2 with the frequency fixed at the exact center frequency of the propeller blade passage tones summarized in Table 1. The narrow bandpass filter was tuned to have the sine wave at the center of its bandwidth. The actual data records were then passed through the filter, and the probability density functions of the isolated blade passage tones were computed. The resulting probability density plots were reduced to a ratio of the average magnitude of the side peaks to the magnitude of the minimum density at $x = 0$, called the probability density ratio (PDR). This ratio can be converted to a sine wave to noise power ratio in dB as shown in Figure 4. Such analyses were performed on the data from locations No. 1, 5 and 8 in Figure 1 for test runs No. 1, 2 and 7 (static operation, 30 kt taxi, and 70 kt taxi). This analysis was limited to the first five propeller blade passage tones because the exhaust noise contamination became too severe at higher frequencies for an effective analysis by the procedure.

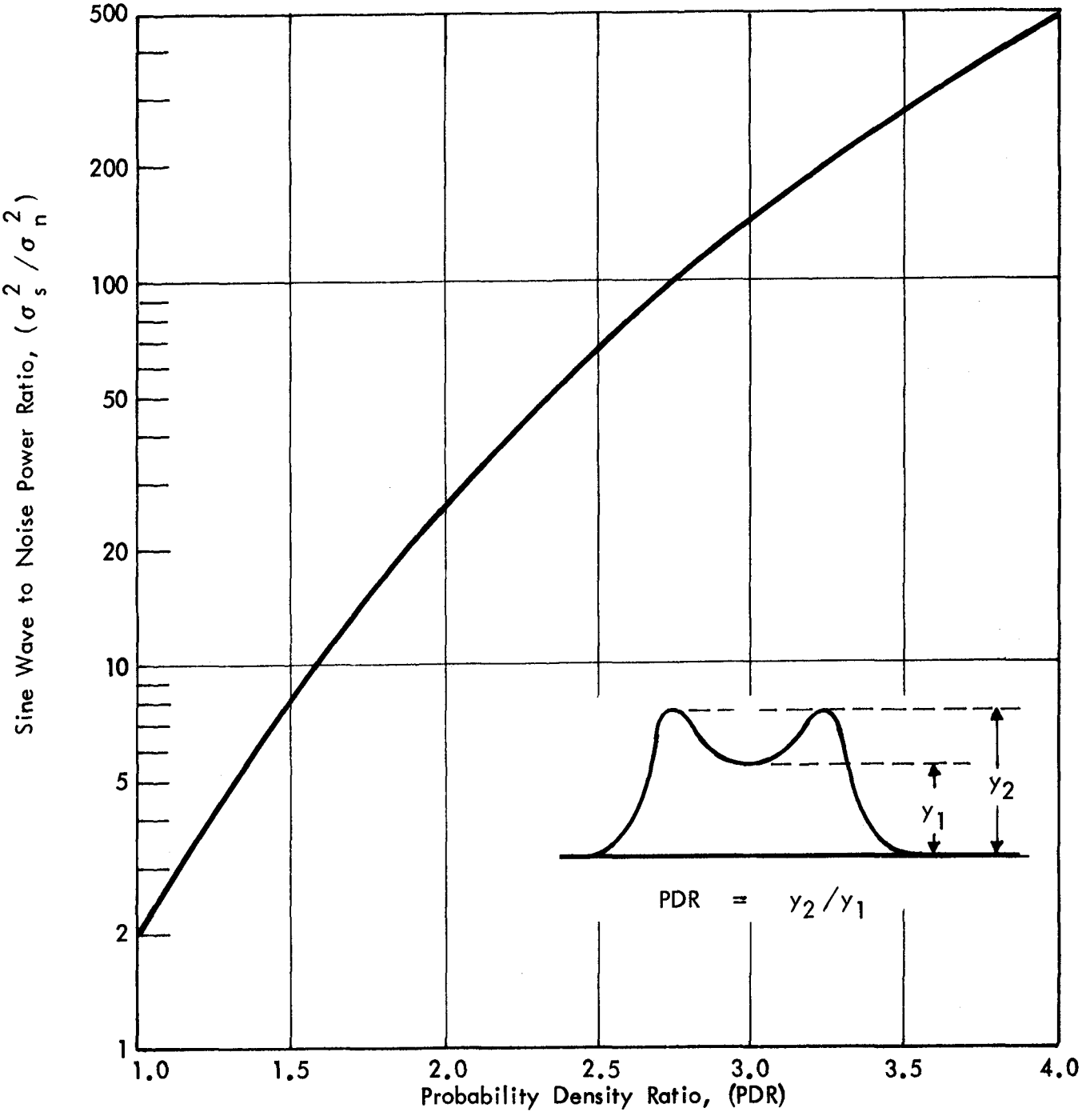

FIGURE 4. SINE WAVE TO NOISE RATIO VERSUS PROBABILITY DENSITY RATIO

3.3 Phase of Propeller Blade Passage Tones

The phase of the various propeller blade passage harmonics at a given location were determined by the following operations. First, the pressure time history was enhanced by ensemble averaging on the SD360 using Function 12 (signal average). A total of $n_d = 512$ overlapped records, each of T = 0.25 seconds duration, were averaged to suppress the random components in the data, as previously illustrated in Figure 3 and discussed in Section 3.2. Next, one full cycle of the resulting periodic data was digitized starting at the upward crossing of the mean value into approximately 50 values at equally spaced intervals and key punched on to cards. Finally, the digitized cycle of data was input to a Fourier series routine on a CDC 6600 computer and the magnitude and phase of the first 20 harmonic components were computed.

Since the phase data were the primary information desired from this analysis, no special calibration procedures were required. The phase of the first 20 harmonics were computed for the enhanced pressure signals at all exterior locations for test runs No. 1 and 4 in Table 1 (static operation), and at location 5 only for all test runs in Table 1.

3.4 Spatial Correlation of Propeller Blade Passage Tones

The spatial correlation characteristics of the propeller blade passage tones over the fuselage surface were determined by computing the coherence and phase between pairs of sound pressure signals on the SD360 using Function 6 (transfer function B/A). The analyses were made using a $B_e = 2$ Hz resolution over the frequency range from 0 to 1000 Hz. Since coherence is dimensionless and phase is relative, no special calibrations were required. The coherence and

The phase data measured at the exact frequencies of propeller blade passage tones are interpreted in terms of trace velocity $U_c(f)$ using the relationship.

$$\phi(f) = \frac{360\ fd}{U_c(f)} \qquad (1)$$

where f = frequency of tone

d = distance between measurement locations

$\phi(f)$ = frequency-dependent phase angle (in degrees) between locations

In some instances (such as case (a) of Section 4.5.1) where the phase angle follows different frequency relationships in different frequency ranges, the computation procedure described in [2] may result in the estimated phase angle $\phi_1(f)$ being displaced by a constant phase shift from the true value. Then

$$\phi_1(f) = \frac{360\ fd}{U_c(f)} + \phi_o \qquad (2)$$

From equations (1) and (2), if $\phi(f)$ or $\phi_1(f)$ are linear functions of frequency, then $U_c(f)$ is independent of frequency and is given by the slope of the straight line defined by either equation.

TABLE 2

Location Pairs for Coherence and Phase Analysis

Direction	Test Run Number	Taxi Speed (knots)	Location Numbers
Longitudinal	1	0	5 versus 1 5 versus 8 5 versus 9 8 versus 9
	2	30	5 versus 1 5 versus 8 5 versus 9 8 versus 9
	3	40	5 versus 1 5 versus 8 5 versus 9 8 versus 9
Circumferential	4	0	5 versus 3 5 versus 4 4 versus 3
	5	40	5 versus 3 5 versus 4 4 versus 3
	6	55	5 versus 3 5 versus 4 4 versus 3
	7	70	5 versus 3 5 versus 4 4 versus 3

4. RESULTS AND DISCUSSIONS

The results of the analyses are detailed in the appendices. These results are now summarized with discussions of their interpretations.

4.1 Magnitude of Propeller Blade Passage Tones

The magnitude of all significant propeller blade passage tones measured at all locations and for all test runs in Table 1 are detailed in Appendix A. The overall values of the propeller blade passage tones up through the 20th harmonic are summarized in Table 3. Also shown for comparison in this table are the overall values computed from previous data for static operation of this aircraft [2]. Note that the two sets of data for static operation obtained from the two independent experiments are in good agreement (generally within $\pm$ 1 dB).

Visual inspection of the data in Table 3 leads immediately to two conclusions. First, the propeller noise at all taxi speeds falls in both the longitudinal and circumferential directions with increasing distance from the closest location to the propeller tip (location 4), as would be expected. Secondly, the propeller noise at all locations falls with increasing taxi speed. In particular, the higher order harmonic components of the propeller noise fall dramatically with taxi speed at locations forward and aft of the propeller plane, as illustrated in Figures 5 through 7. The spectra of blade passage tones for various taxi speeds at locations 1 and 8, which are 0.62 m forward and aft of the propeller plane, respectively, are shown

Table 3

Overall Values of Propeller Blade Passage Tones

Location (Fig. 1)	Overall Level in dB by Taxi Speed (Test Run No.)						
	Static (1&4)	Static (Ref.2)	30 kts (2)	40 kts (5)	40 kts (3)	55 kts (6)	70 kts (7)
1	133.2	132.9	132.5	**	130.4	**	**
3	137.6	136.3	**	133.6	**	132.6	132.4
4	137.6	137.2	**	135.1	**	134.3	133.8
5	134.8	133.9	134.3	132.7	132.3	132.2	131.8
8	130.9	129.9	130.5	**	126.7	**	**
9	122.2	123.4	121.2	**	120.9	**	**
11	107.5	**	**	106.2	**	105.6	104.2
rpm*	2600	2600	2600	2710	2690	2770	2620
bpf*	81.8	81.8	81.8	85.4	84.6	87.2	82.6

*Engine speed in rpm and blade passage frequency in Hz.

**No data acquired.

in Figures 5 and 6. Note that most of the reduction in the higher order tones occurs at the lowest taxi speed for which measurements were obtained (30 kts). The results are quite different in Figure 7, which shows the spectra of blade passage tones at location 5 in the plane of the propellers. It is seen from these data that the higher order harmonics do not diminish significantly in magnitude even at the highest taxi speed for which measurements were obtained (70 kts). Also note in Figures 5 through 7 that the lower order harmonics (2 through 6) in the plane of the propeller (location 5) are substantially more intense than forward and aft of the propeller plane (locations 1 and 8) even during static operation.

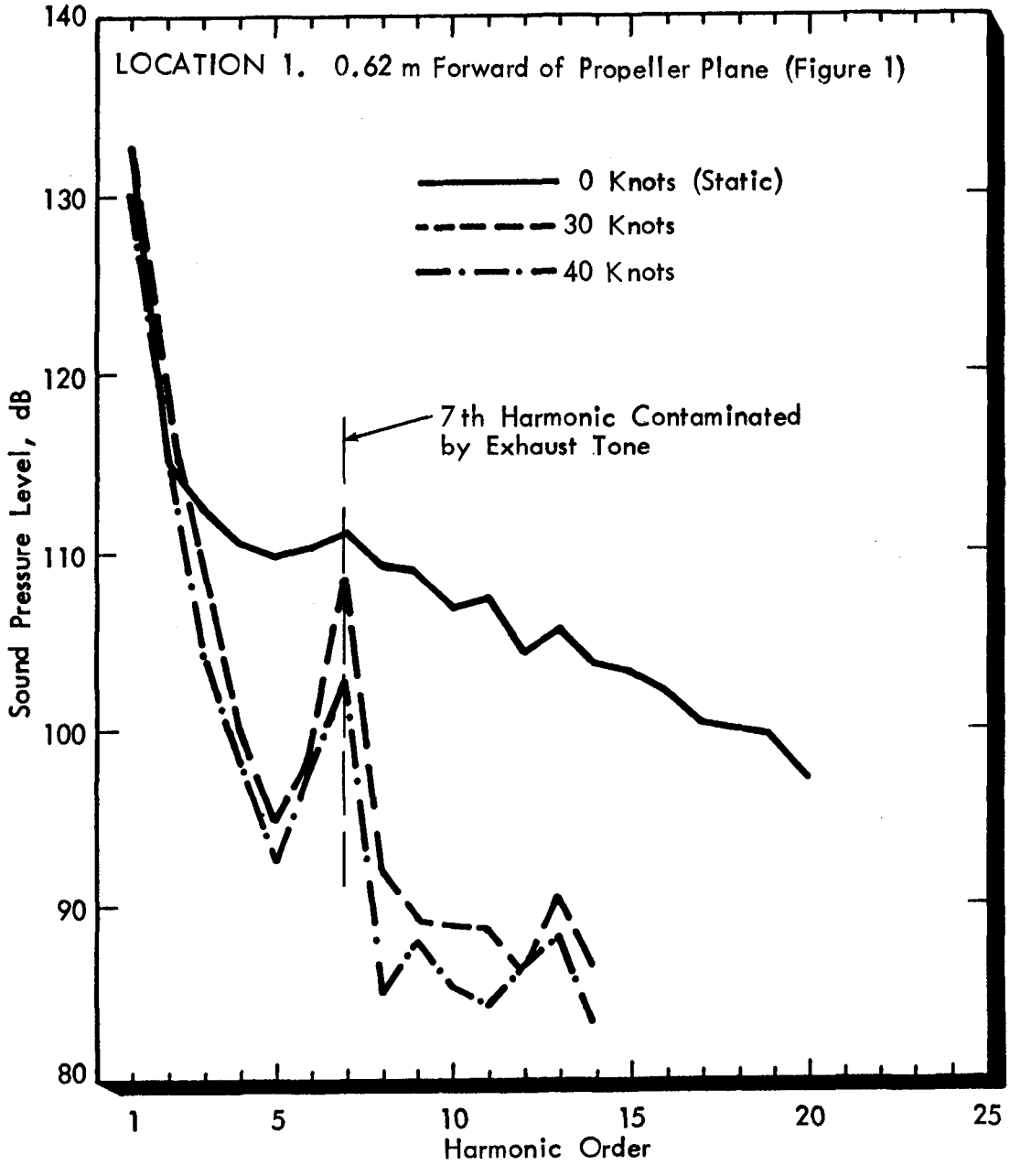

FIGURE 5. MAGNITUDE OF PROPELLER BLADE PASSAGE TONES VERSUS TAXI SPEED AT LOCATION 8

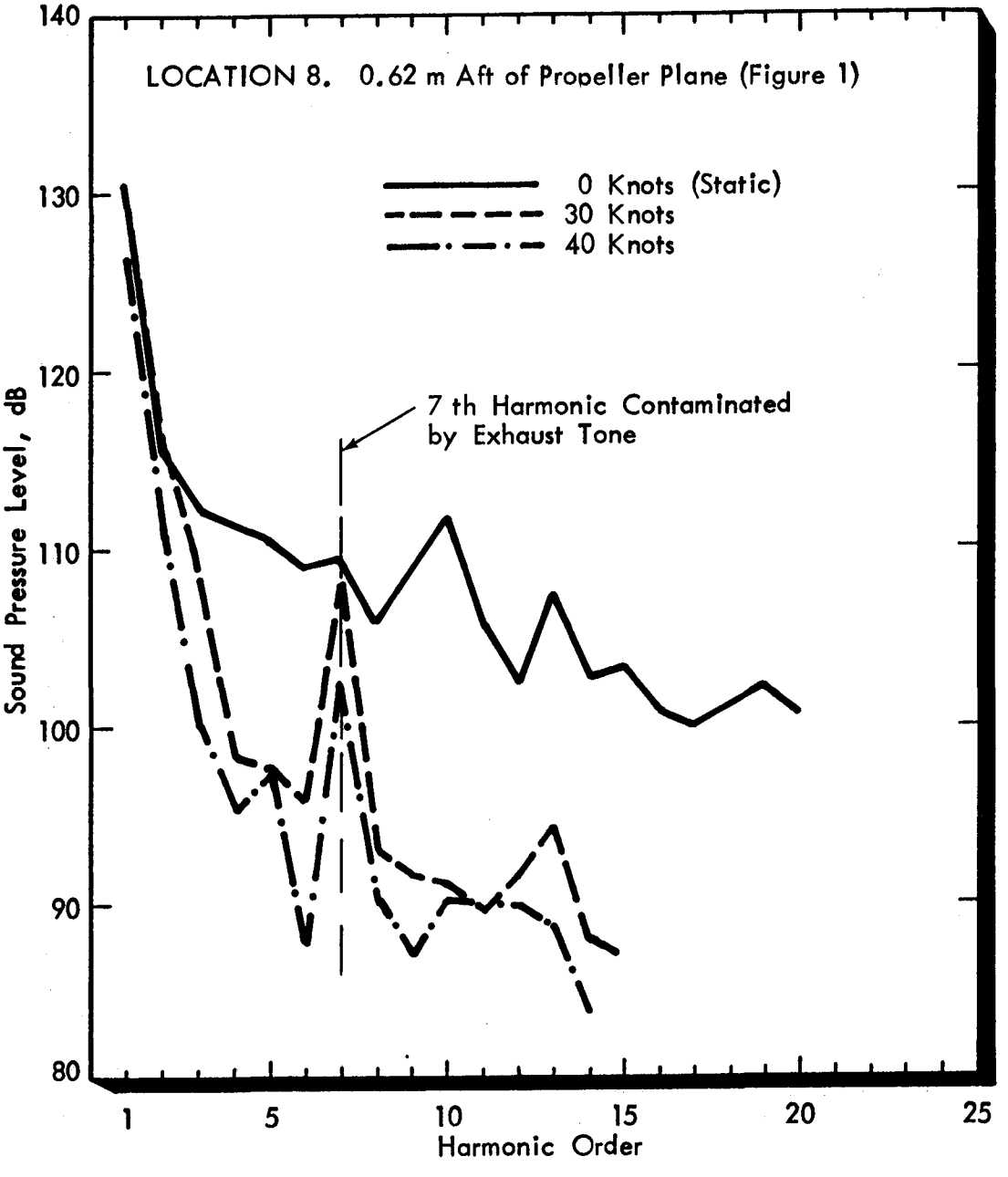

FIGURE 6. MAGNITUDE OF PROPELLER BLADE PASSAGE TONES VERSUS TAXI SPEED AT LOCATION 1

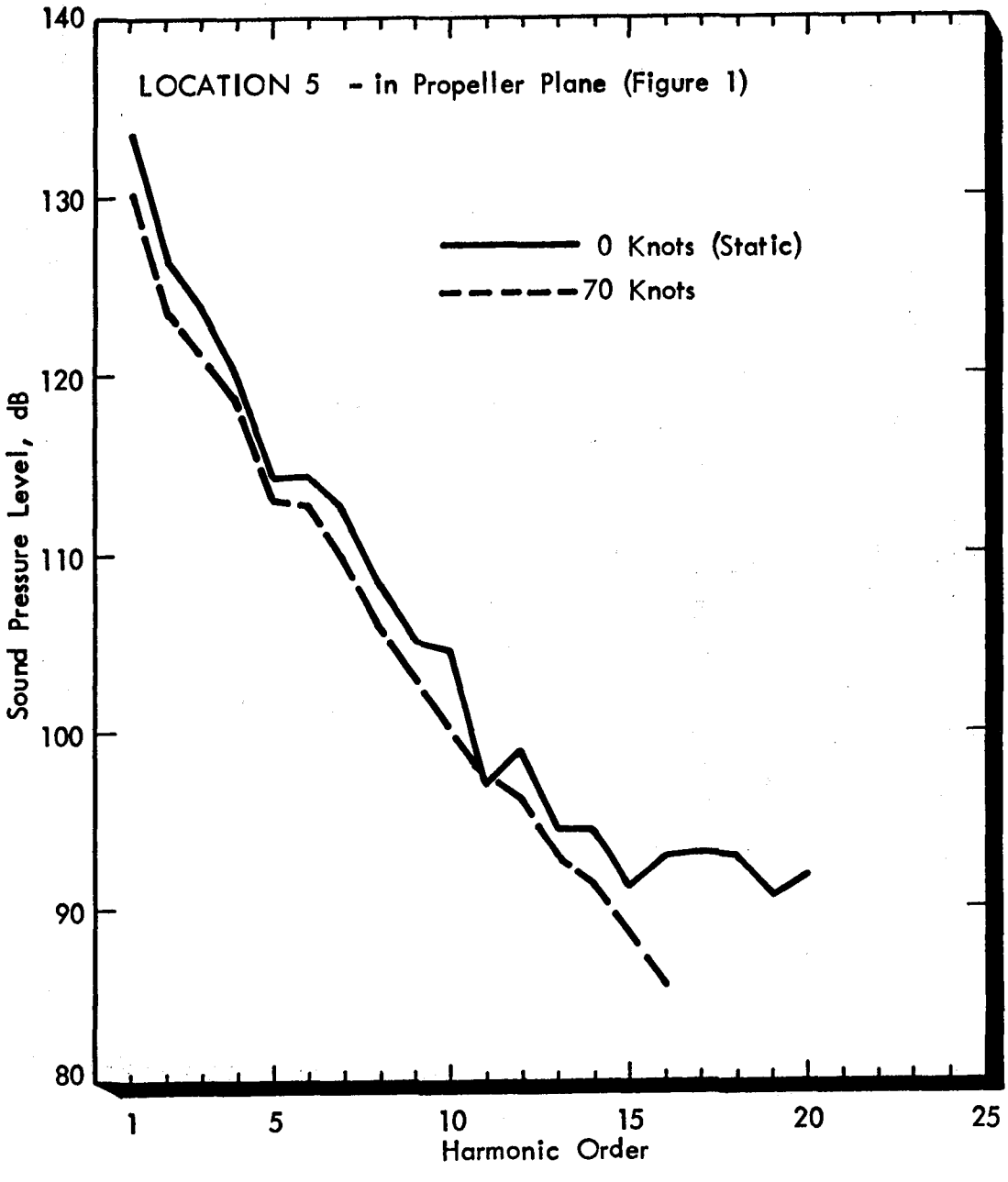

FIGURE 7. MAGNITUDE OF PROPELLER BLADE PASSAGE TONES VERSUS TAXI SPEED AT LOCATION 5

Measured harmonic levels for the static case were compared in [2] with predicted levels obtained from two near-field noise prediction methods [3,4]. The prediction methods use tip helical Mach number as the controlling parameter in calculating harmonic sound levels relative to the overall level. For the static case, helical and rotational tip Mach numbers are identical but this is not true when there is forward motion. Moreover, it has been observed in Figures 5 and 6 that the noise levels of the higher order harmonics show a significant decrease when there is forward motion of the airplane. Thus it is of interest to compare the two methods with data from the taxiing tests.

The microphone locations selected for the comparison are 1, 5 and 8, which refer respectively to locations forward of the plane of rotation, in the plane of rotation and aft of the plane. Results are shown first for the static case (Figure 8) where the tip helical (and rotational) Mach number is 0.592. This comparison is similar to that in Figure 8 of [2] and shows that at low harmonic order the predicted and measured noise levels decrease at similar rates as harmonic order increases. For harmonic orders greater than 5 the two prediction methods diverge with the SAE prediction method [3] following approximately the measured results for locations 1 and 8.

When forward motion of the airplane is introduced the comparison shows a significant change. Figure 9 contains data for a forward velocity of 50 knots and for the same propeller rpm as for Figure 8. The tip helical Mach number is now 0.617. The two prediction methods now show a slower decrease in harmonic level than is measured at locations 1 and 8, although the method of [4] seems to approach measured values for harmonic orders about 7.

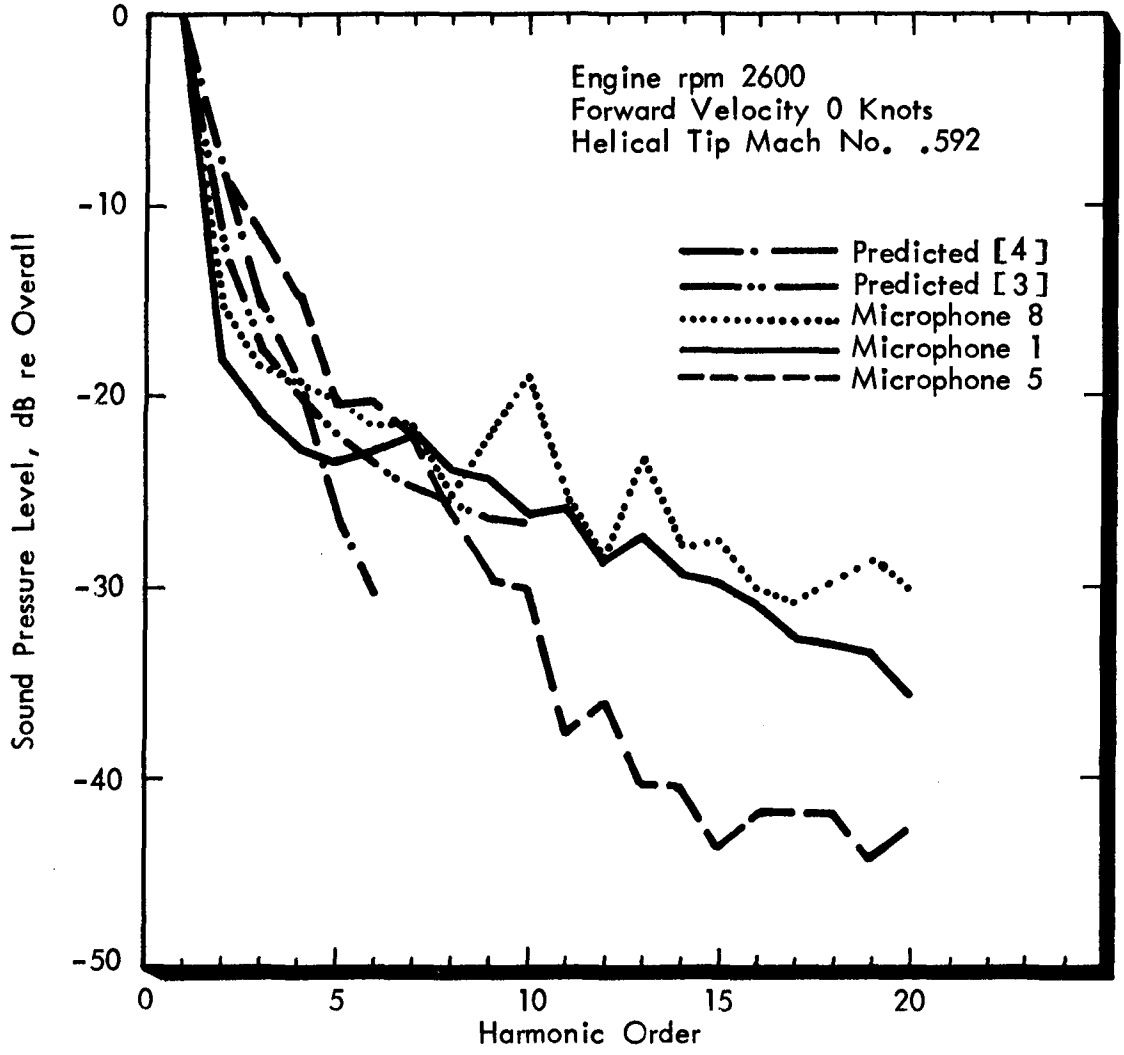

FIGURE 8. COMPARISON OF MEASURED AND PREDICTED PROPELLER HARMONIC LEVELS, STATIC RUN

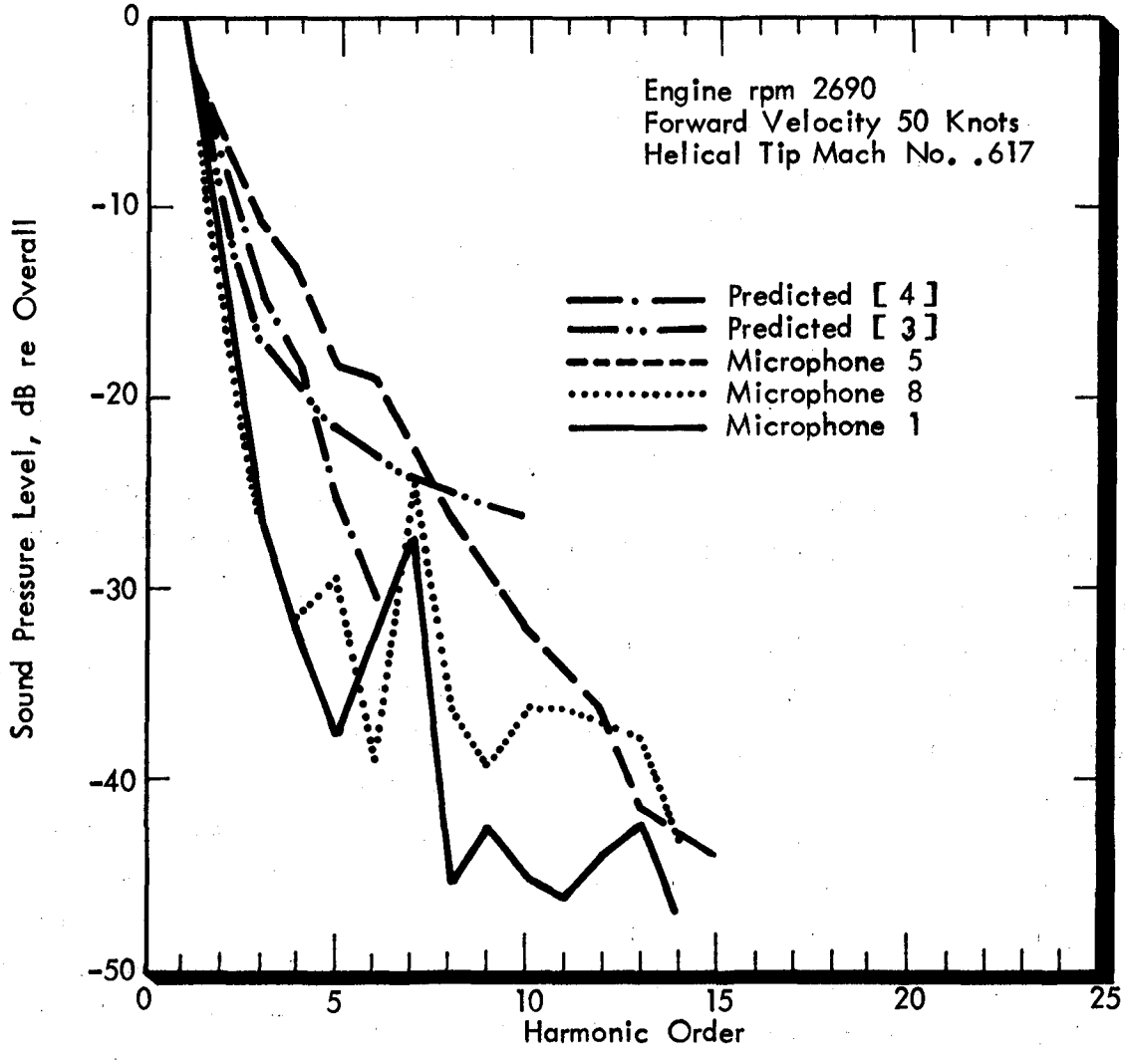

FIGURE 9. COMPARISON OF MEASURED AND PREDICTED PROPELLER HARMONIC LEVELS, 50 KNOTS TAXI RUN

At these higher-order harmonics, the SAE method [3] over-predicts the measured levels at locations 1 and 8 by 10 to 20 dB.

The comparison between predicted and measured levels can be continued a little further by considering the circumferential and longitudinal spatial variations. Such comparisons are limited in scope because of the small number of transducer locations in either the circumferential or longitudinal direction for the taxi tests, but the results can be supplemented by use of data from the static tests [2].

The analysis presented here for the circumferential direction utilizes tip clearance Y/D as the control parameter, and measured data for microphone locations 3 through 6 are expressed in terms of this parameter. The measured variation of overall sound level with tip clearance is then compared with correspondence predicted variations given in Figure 13 of [3]. (These curves are essentially the same as those in [4]). No attempt is made to compare sound levels, the comparison being solely in terms of rate of change or slope of the curves. In Figures 10(a) and (b) static data are presented for the four transducer locations and regression curves are fitted. These data are then superimposed on curves from Figure 13 of [3], the curves having been moved along the ordinate axis to provide slope comparisons. It is seen that the measured slopes tend to be similar to slopes predicted for somewhat high tip rotational Mach numbers. The comparison is, however, not as simple as is implied above, since the predicted effect of tip clearance assumes that the variation occurs in free space, whereas the measured levels were made on a curved surface.

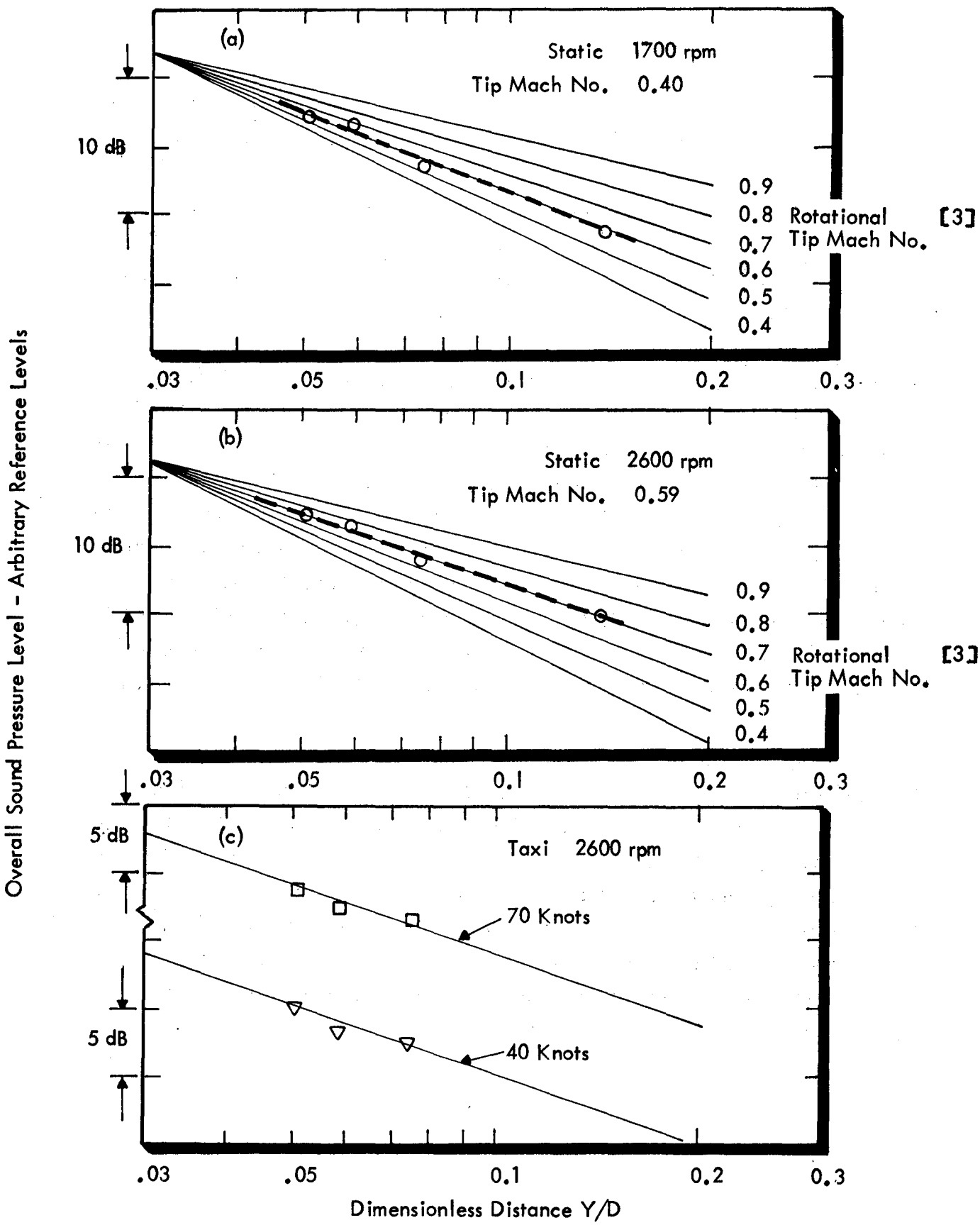

FIGURE 10. VARIATION OF SOUND PRESSURE LEVEL WITH TIP CLEARANCE, IN THE PROPELLER PLANE

Data for the taxi case are shown in Figure 10(c) where measurements are available for locations 3 through 5 only. Figure 10(c) contains data for taxi speeds of 40 and 70 knots and the curve drawn through the data points is the regression line from Figure 10(b). The regression line appears to fit the data fairly well, but without measured values for location 6 it is difficult to come to any firm conclusion.

In the longitudinal direction the situation is complicated because noise levels at the rearward locations are dominated by exhaust noise. Thus it is difficult to separate propeller noise components from exhaust noise. Prediction curves for the longitudinal spatial distribution given in [3] and [4] are essentially the same, and curves from [3] are reproduced on Figure 11. It is seen that the curves are symmetrical about the plane of rotation (X/D = 0). Test data for three airplane speeds (0, 30 and 40 knots) are superimposed on the prediction curves. The test data refer to a radial location Y/D = 0.075.

Several points of interest can be seen in the data. Firstly, the measured noise levels for a given X/D are higher at locations forward of the propeller than they are aft. Secondly, the data for locations just aft of the propeller ($-0.3 < X/D < 0$) are in general agreement with the prediction procedure. Thirdly, at larger separation distances aft of the propeller ($X/D \simeq -0.8$) the measured noise levels are much higher than predicted. (This difference may be due to contamination of the propeller noise data by the presence of exhaust noise.)

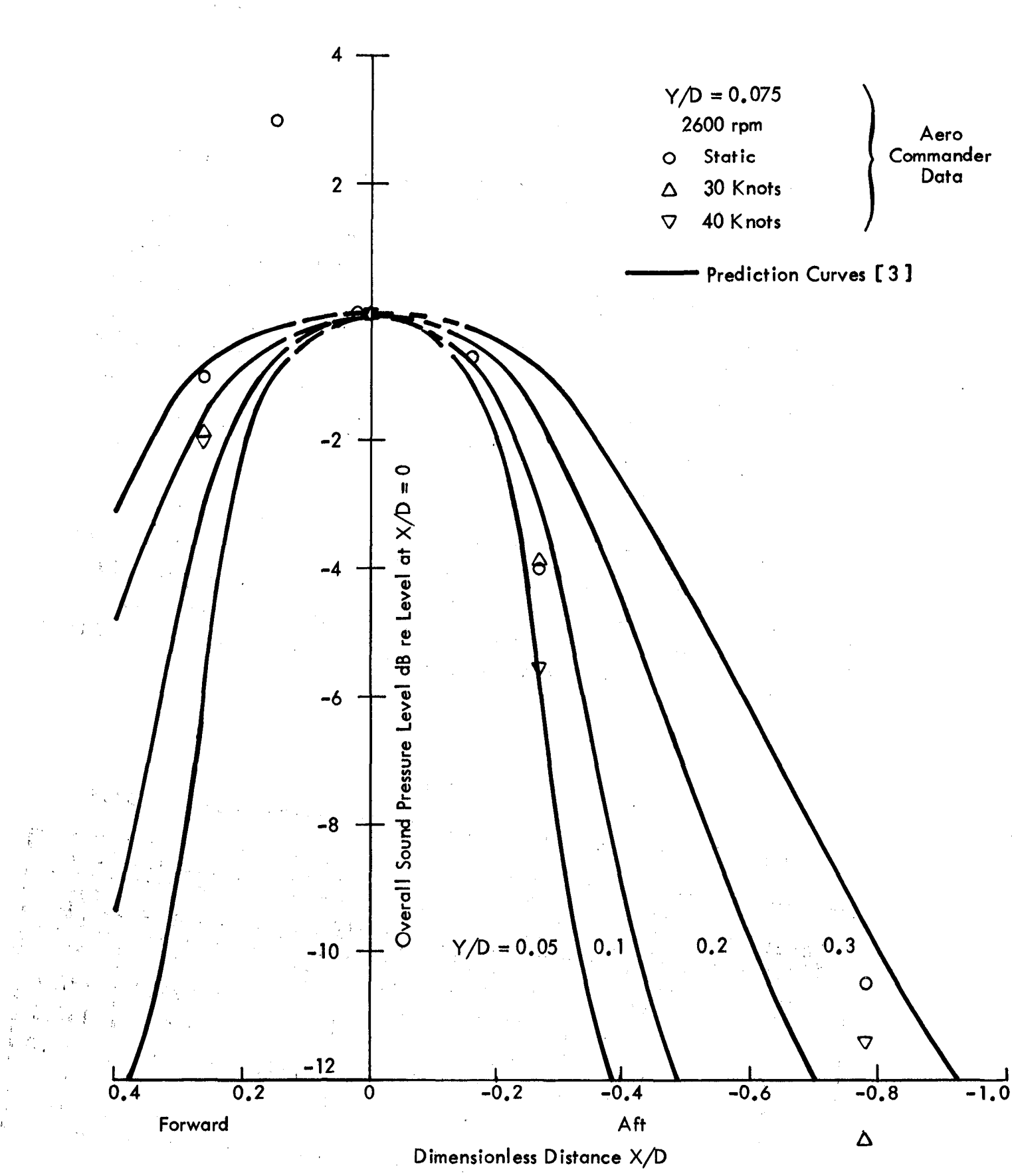

FIGURE 11. VARIATION OF SOUND PRESSURE LEVEL WITH DISTANCE IN THE LONGITUDINAL DIRECTION

4.2 Signal Enhancement of Propeller Blade Passage Tones

The magnitude of the first ten propeller blade passage tones after signal enhancement for the locations and test runs stated in Section 3.2.1 are detailed in Appendix B. The overall values of the enhanced data are presented in comparison to the overall values under the same conditions without enhancement in Table 4. The unenhanced values in this table represent the overall value for the first ten harmonics so as to be directly comparable to the enhanced values.

In most cases, the results in Table 4 do not reveal a major difference in the overall levels of the enhanced and unenhanced data, indicating the overall blade passage pressure signal is composed primarily of stable periodic components. However, a review of the detailed data in Appendix B indicates the stability

Table 4

Overall Values of Enhanced Propeller Blade Passage Tones

Location (Figure 1)	Overall Level in dB by Taxi Speed (Test Run No.)					
	Static (1&4)		30 kts (2)		70 kts (7)	
	e*	u*	e*	u*	e*	u*
1	132.9	133.1	132.5	132.5	**	**
3	136.4	137.5	**	**	130.3	132.4
4	137.3	137.6	**	**	131.9	133.7
5	134.0	134.8	133.9	134.3	130.8	131.8
8	130.2	130.8	129.8	130.5	**	**
9	117.6	121.9	119.0	121.2	**	**

*e - enhanced; u - unenhanced

** No data acquired

of the blade passage tones does fall with increasing harmonic order. Figure 12 shows a typical result of the signal enhancement calculations at location 1 during static operations. The spectra for the enhanced and unenhanced signals at this location are shown in Figure 13. Note that the enhancement operation was very effective in suppressing noise, including the intense exhaust harmonics which fall close to the 3rd, 4th, and 7th blade passage tones. Further note that the enhancement operation does reduce the magnitude of the higher order blade passage tones as well, indicating the blade passage tones become increasingly stochastic as the harmonic order increases. This reflects variations in the blade passage signal wave form from one cycle to the next. However, it must be remembered that it also may reflect in part the influence of time base errors in the signal enhancement operations, as discussed in Section 3.2.1.

The collapse of the higher order tones under signal enhancement increases as the location moves away from the closest point to the propeller tip (location 5). This is illustrated in Figure 14 which shows the reduction in tone magnitude after enhancement of the pressure signals at locations 1 (0.62 m forward of the propeller plane), 5 (in the propeller plane), and 9 (0.62 m aft of the propeller plane). The collapse of the higher order tones under signal enhancement also increases as the taxi speed of the aircraft increases. This is demonstrated in Figure 15 which presents the reduction in tone magnitude after enhancement at location 5 (in the propeller plane) for three different taxi speeds. Further discussion concerning this analysis is given in Sections 4.3 and 4.5.2 (page 56).

In summary, the most stable propeller noise signals occur in the plane of the propeller during static operation. The data

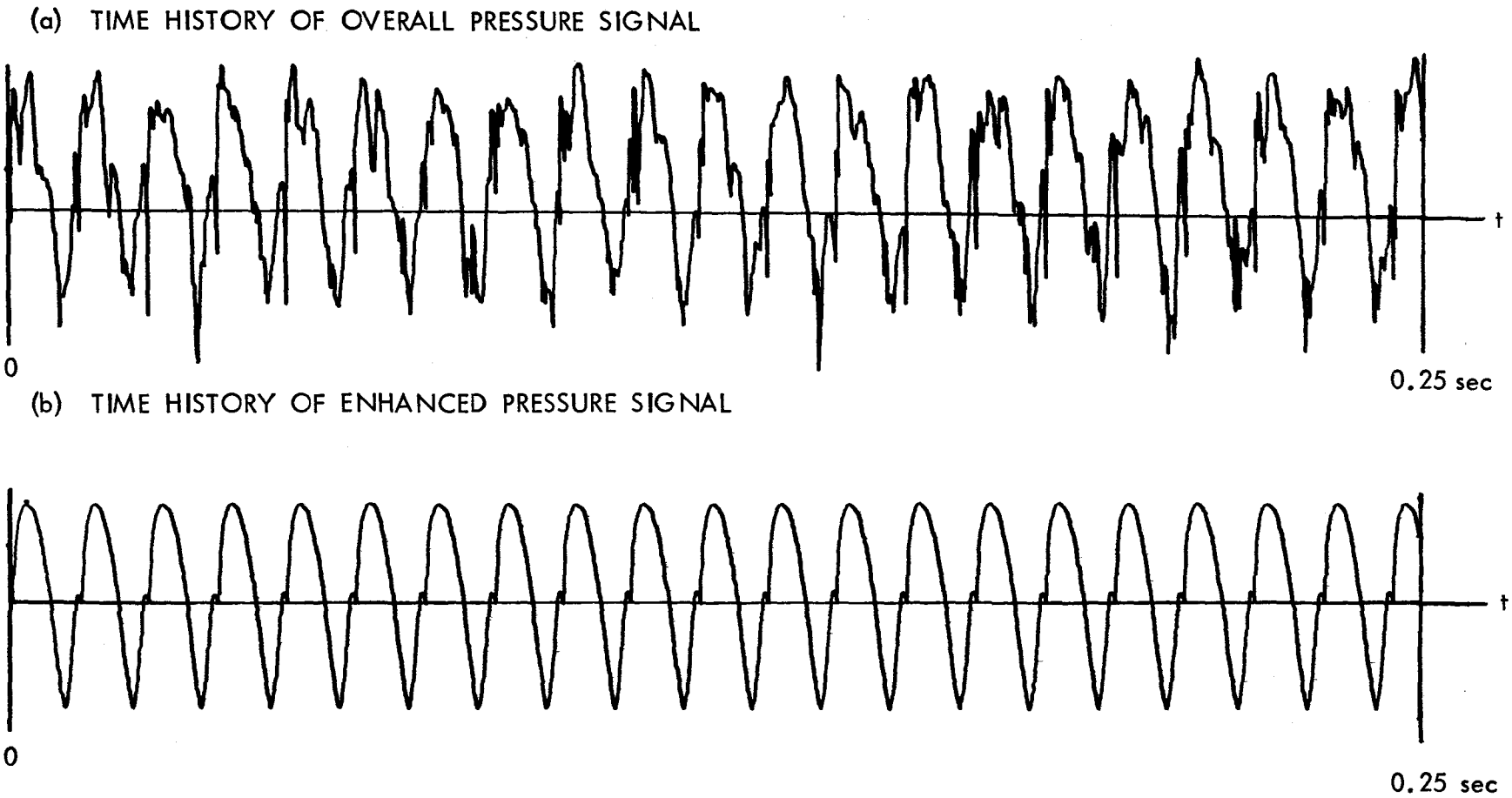

FIGURE 12. TIME HISTORIES OF ENHANCED AND UNENHANCED PRESSURE SIGNALS AT LOCATION 1 DURING STATIC OPERATION

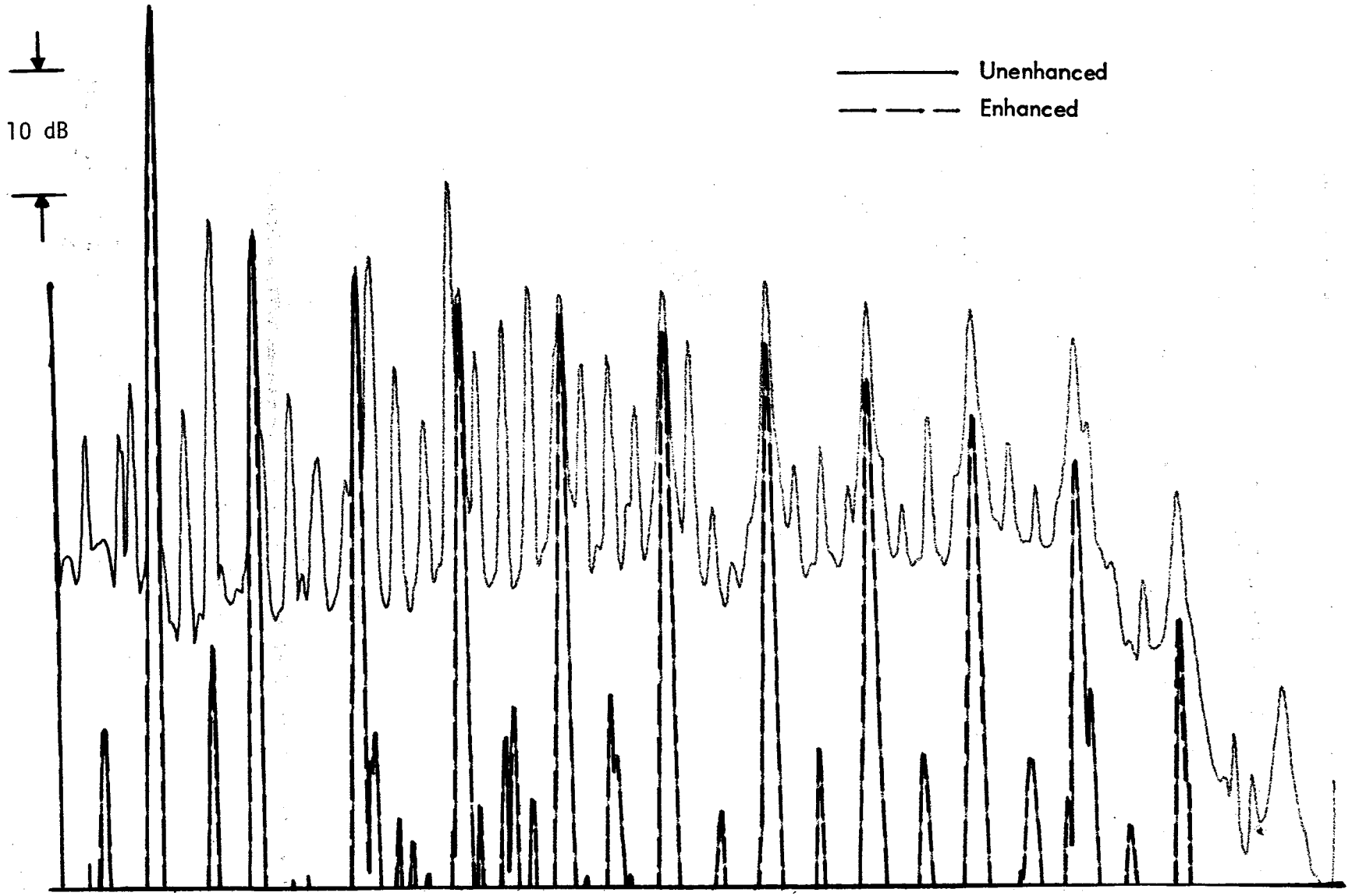

FIGURE 13. SPECTRA OF ENHANCED AND UNENHANCED PRESSURE SIGNALS AT LOCATION 1 DURING STATIC OPERATION

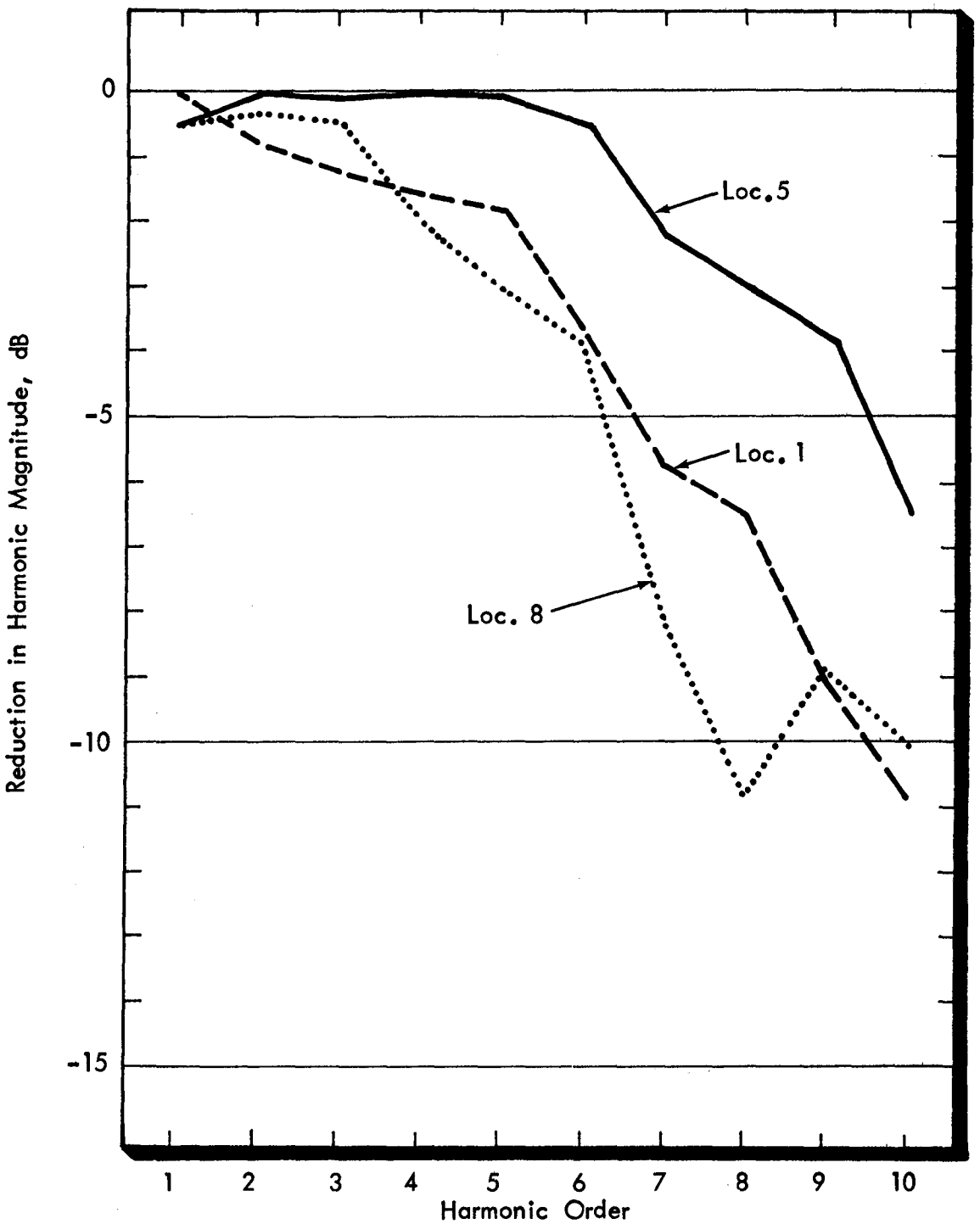

FIGURE 14. REDUCTION IN MAGNITUDE OF ENHANCED PROPELLER BLADE PASSAGE TONES AT VARIOUS LOCATIONS FOR STATIC OPERATION

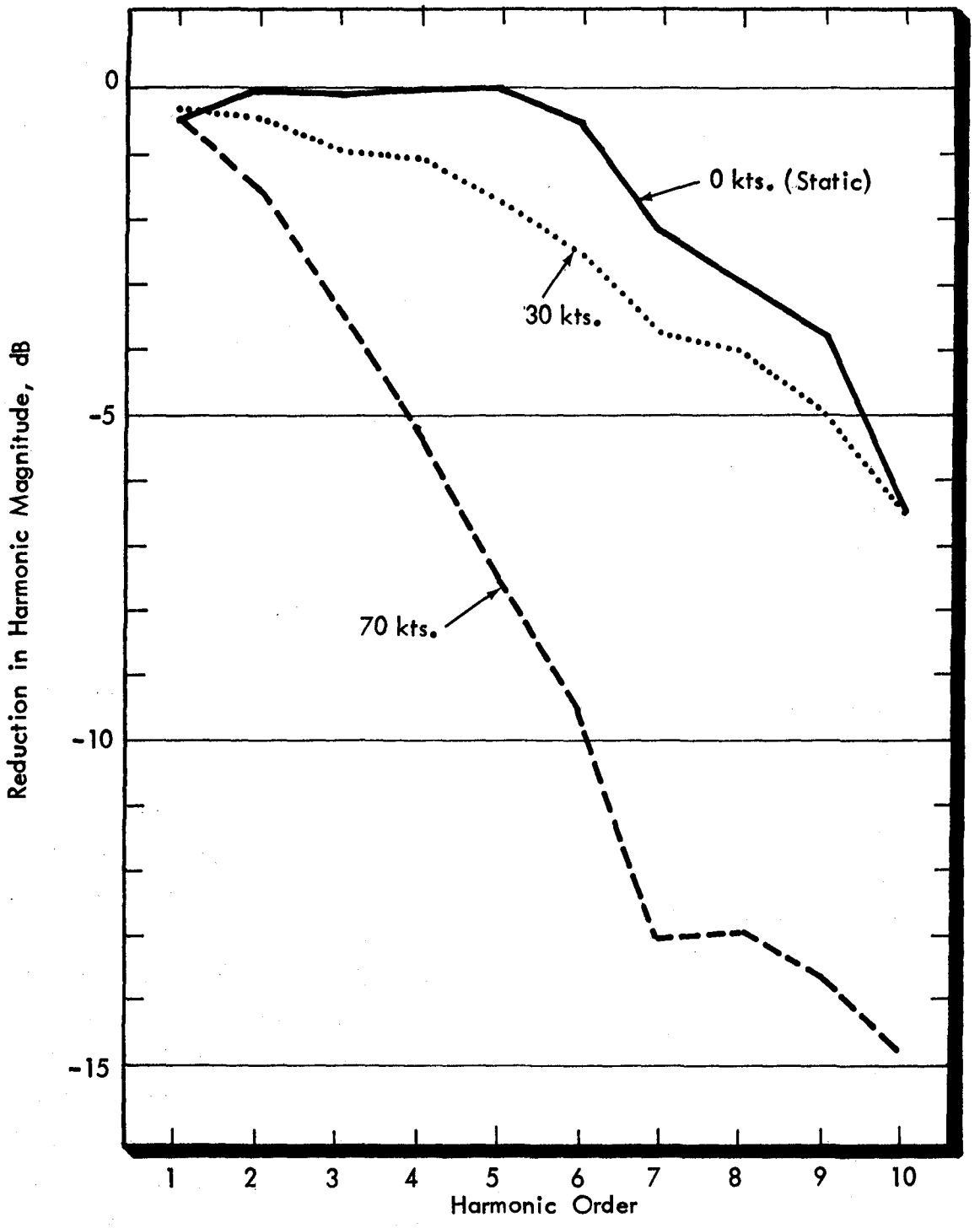

FIGURE 15. REDUCTION IN MAGNITUDE OF ENHANCED PROPELLER BLADE PASSAGE TONES AT LOCATION 5 FOR VARIOUS TAXI SPEEDS.

tend to become increasingly stochastic as the location moves away from the propeller tip and the taxi speed increases.

4.3 Probability Density of Propeller Blade Passage Tones

The sine wave to noise power ratio of the first five propeller blade passage tones determined by the probability density analysis procedures in Section 3.2.2 are shown for selected locations and taxi conditions in Table 5. Also shown in this table are the differences between the tone levels with and without noise calculated from the probability density data using the relationship

$$\Delta L_p = 10 \log \left[1 + \frac{1}{S/N}\right] \qquad (3)$$

and the equivalent results determined from the signal enhancement data in Appendix B (ΔL_e).

The comparison between the probability density and signal enhancement results is limited by the fact that the probability density analysis cannot accurately define S/N ratios of less than 2 corresponding to a reduction in tone level of $\Delta L = 1.8$. With this limitation in mind, the comparisons in Table 5 lead to the following general conclusions. The results of the probability density and signal enhancement analyses are in reasonable agreement in most cases for static operations. However, during the taxi runs, the probability density analysis suggests the tones have less noise (are more stable) than was indicated by the signal enhancement operations. This discrepancy is illustrated in Figure 16, which shows the reduction in level at location 5 during the 70 kt run as computed from the probability density and signal enhancement data.

Table 5. Probability Density Results For Propeller Blade Passage Tones

Location (Figure 1)	Harmonic Number	S/N Ratio and Reduction In Level Without Noise (ΔL) by Taxi Speed (Test Run Number)								
		Static Operation (1)			30 Knots (2)			70 Knots (7)		
		S/N	ΔL_p^*(dB)	ΔL_e^*(dB)	S/N	ΔL_p^*(dB)	ΔL_e^*(dB)	S/N	ΔL_p^*(dB)	ΔL_e^*(dB)
1	1	>500	0.0	0.1	>500	0.0	0.0	**	-	-
	2	30	0.1	0.8	65	0.1	0.3	**	-	-
	3	2	1.8	0.8	< 2	>1.8	0.8	**	-	-
	4	3	1.3	1.6	16	0.3	4.2	**	-	-
	5	< 2	>1.8	1.8	< 2	>1.8	6.7	**	-	-
5	1	290	0.0	0.5	500	0.0	0.3	250	0.0	0.4
	2	100	0.0	0.0	280	0.0	0.4	100	0.0	1.4
	3	17	0.2	0.1	10	0.4	0.9	17	0.2	3.3
	4	2	1.8	0.0	< 2	>1.8	1.1	< 2	>1.8	5.3
	5	< 2	>1.8	0.1	3	1.3	1.8	5	0.8	7.4
8	1	50	0.1	0.5	>500	0.0	0.7	**	-	-
	2	12	0.3	0.3	8	0.5	0.8	**	-	-
	3	2	1.8	0.5	5	0.8	1.1	**	-	-
	4	6	0.7	1.5	19	0.2	8.8	**	-	-
	5	< 2	>1.8	3.0	< 2	>1.8	4.1	**	-	-

* ΔL_p - computed probability density analysis; ΔL_e - computed from signal enhancement.
** - no data acquired.

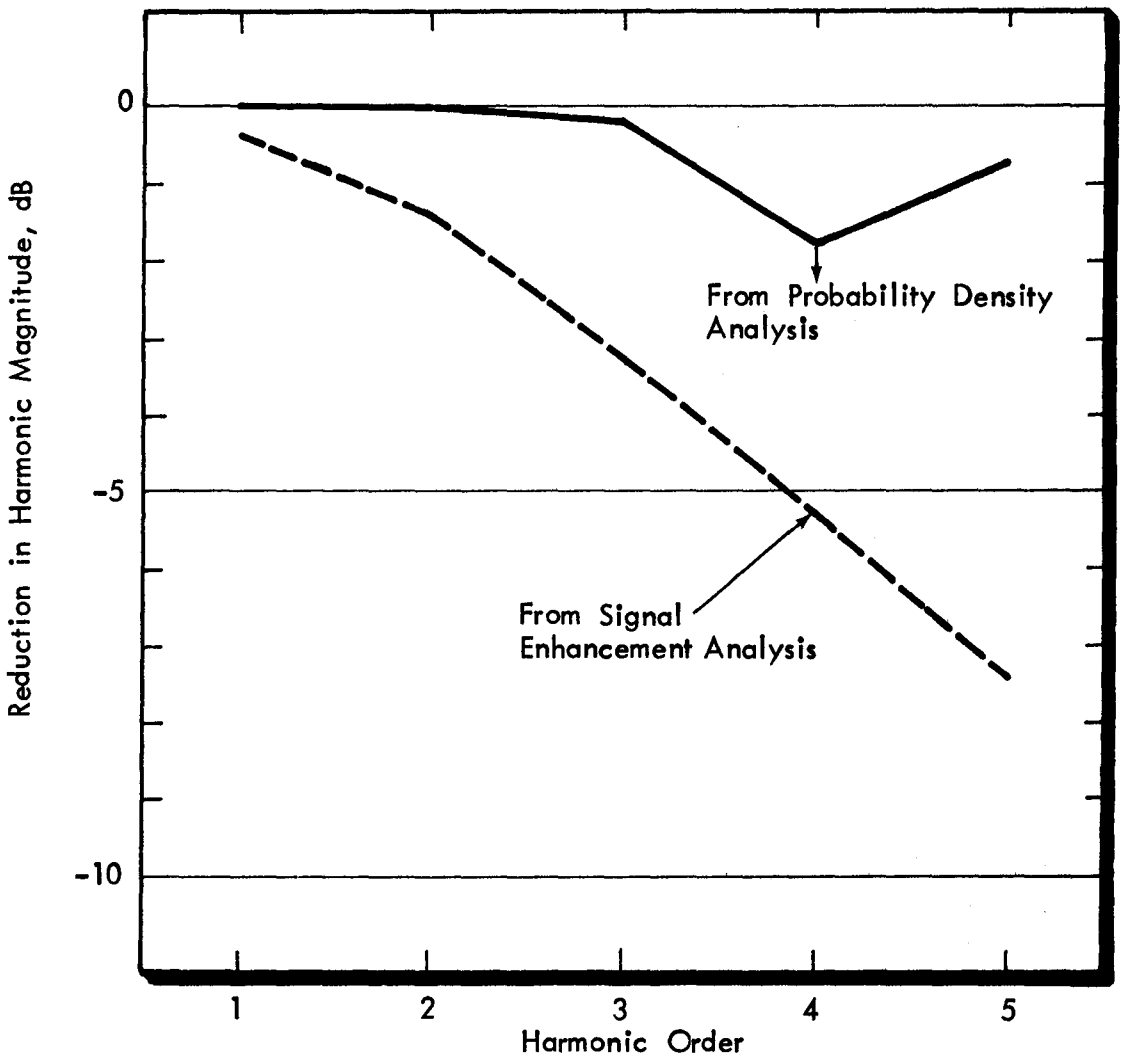

FIGURE 16. REDUCTION IN MAGNITUDE OF PROPELLER BLADE PASSAGE TONES AT LOCATION 5 FOR 70 KT. TAXI RUN

In summary, the probability density analysis does not reveal the reduction in stability of the propeller blade passage tones with increased distance from the propeller plane and increased taxi speed that was exhibited by the signal enhancement results in Figures 14 and 15. This discrepancy might be due in small part to the time base errors in the signal enhancement operations discussed in Section 3.2.1. However, such errors should not be significant in the first five harmonics. A more likely explanation is that the tonal instabilities revealed by the signal enhancement with increased distance from the propeller plane and/or taxi speed are due to random variations in the harmonic phasing rather than in the harmonic magnitudes. Phase variations of the tones appear as noise in the signal enhancement but will not affect the results of the probability density analysis (a probability density measurement of a sine wave is not influenced by phase or frequency change).

4.4 Relative Phase of Propeller Blade Passage Tones

The phases of the first 20 propeller blade passage tones for (a) all exterior locations during static operation and (b) location 5 during taxi runs at 0,30,40, and 70 knots are detailed in Appendix C. An inspection of the phase data at various locations during static operation reveals little consistency from one location to another, except for the first few harmonics at closely spaced locations in the plane of the propeller, for example, locations 3 and 4 in Table C-1. However, a strong similarity is apparent in the phasing of harmonics at a specific location for various taxi speeds. This is demonstrated by the data in Figure 17 which presents the relative phases of the first 5 harmonics of the propeller blade passage pressures measured at location 5 for various taxi speeds. Note that the

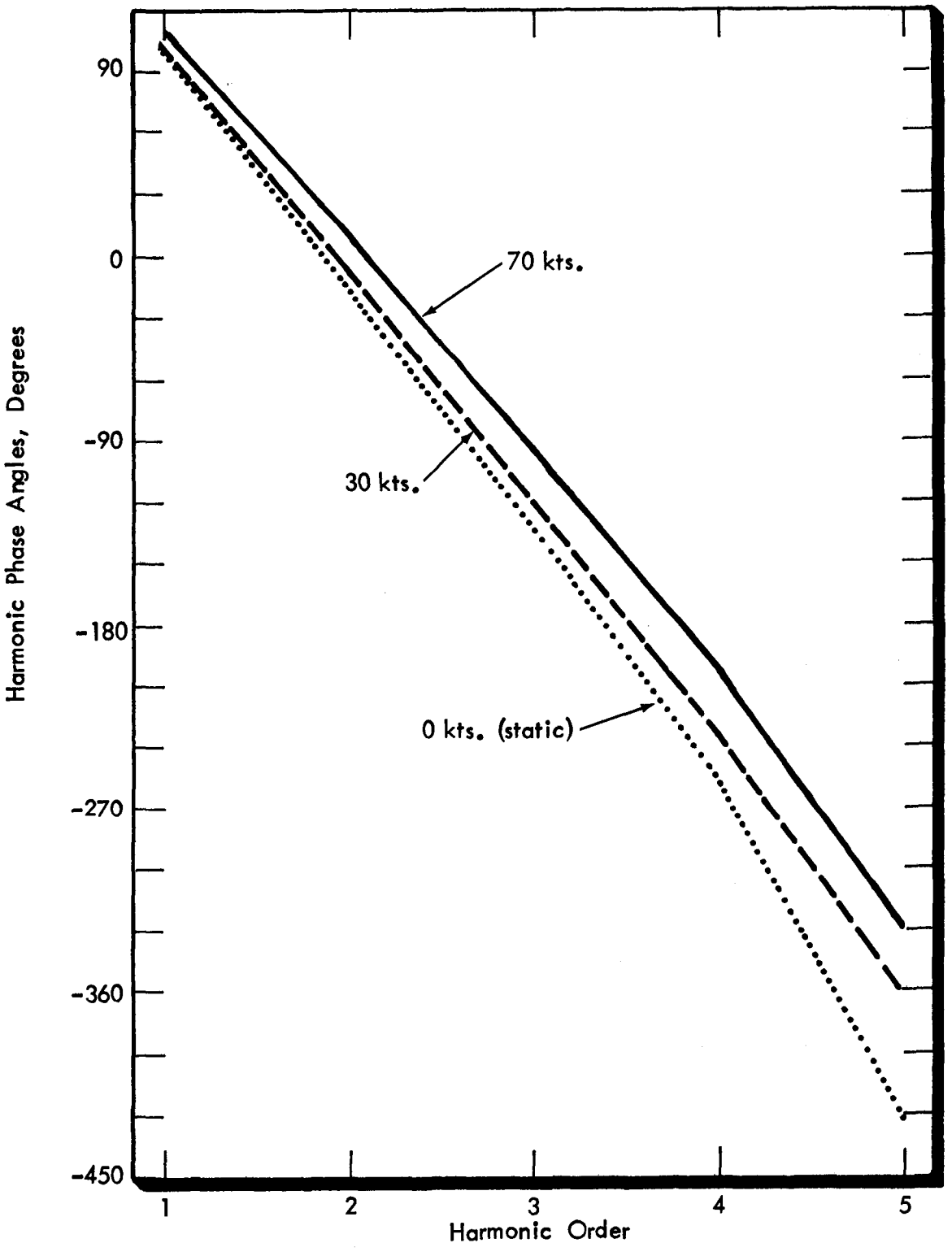

FIGURE 17. PHASE ANGLE OF PROPELLER BLADE PASSAGE TONES VERSUS TAXI SPEED AT LOCATION 5

phasing of the tones in Figure 17 are similar except perhaps for a trend towards smaller phase shifts from one harmonic to the next with increasing taxi speed.

4.5 Spatial Correlation of Propeller Blade Passage Tones

As indicated in Section 3.4, the spatial correlation of the propeller pressure field was reduced in terms of coherence and phase angle spectra for the measured pressure at selected pairs of locations. This format was employed because it presents the data in a manner which is readily usable for describing pressure forcing fields in the calculation of structural response and noise transmission.

Sample coherence and phase angle spectra obtained for the pressure field on the Aero Commander are presented in Appendix D. The appendix also contains tabulated coherence and phase angle data for the noise components at the propeller blade passage frequency and higher order harmonics.

An analysis of coherence and phase data for the static case is contained in [2] where phase results are interpreted in terms of phase or trace velocities, as indicated in equation (1), and coherence spectra are investigated for potential non-dimensional frequency parameters. A similar approach is followed in this discussion where the main objective is the identification of forward velocity effects. Analysis of the data is, however, limited because of the very small number of transducer locations used in the measurements. As in the previous analysis, interest is restricted to the discrete frequency noise components generated by the propeller. The coherence and phase data presented in the discussion will refer only to these discrete frequency

components. Problems of reflections and contamination by exhaust noise, which were encountered in the analysis described in [2], were also encountered in the present analysis.

4.5.1 Phase Analysis

In order to interpret the phase data in terms of trace velocities, it is necessary to plot the phase spectra as a continuously increasing or decreasing function, instead of a function bounded by $\pm \pi$ as shown in Appendix D. This conversion is discussed in [2]. Resulting phase spectra for the propeller noise components are plotted in Figures 18 - 20 for several pairs of transducers. Figure 18 refers to measurements in the circumferential direction and Figures 19 and 20 to the longitudinal direction.

Inspection of the data indicates that in Figures 18 and 20 the phase angle essentially decreases uniformly from zero at zero frequency. If a regression line is fitted to the data, it can be forced to pass through the origin. Such regression lines are shown in Figures 18 and 20 and, using equation (1), the slope of these lines can be interpreted in terms of a trace velocity which is independent of frequency. In Figure 19 the shape of the phase angle spectrum for propeller harmonics is somewhat different in that it can be divided into two frequency ranges. At low frequencies the phase angle is essentially independent of frequency. Then at higher frequencies the phase angle decreases as frequency increases. For this case, regression lines are fitted to the high frequency data only.

In most cases forward motion of the airplane, at least within the forward velocity range available in the tests, has little effect on the phase angle spectrum. The most noticeable

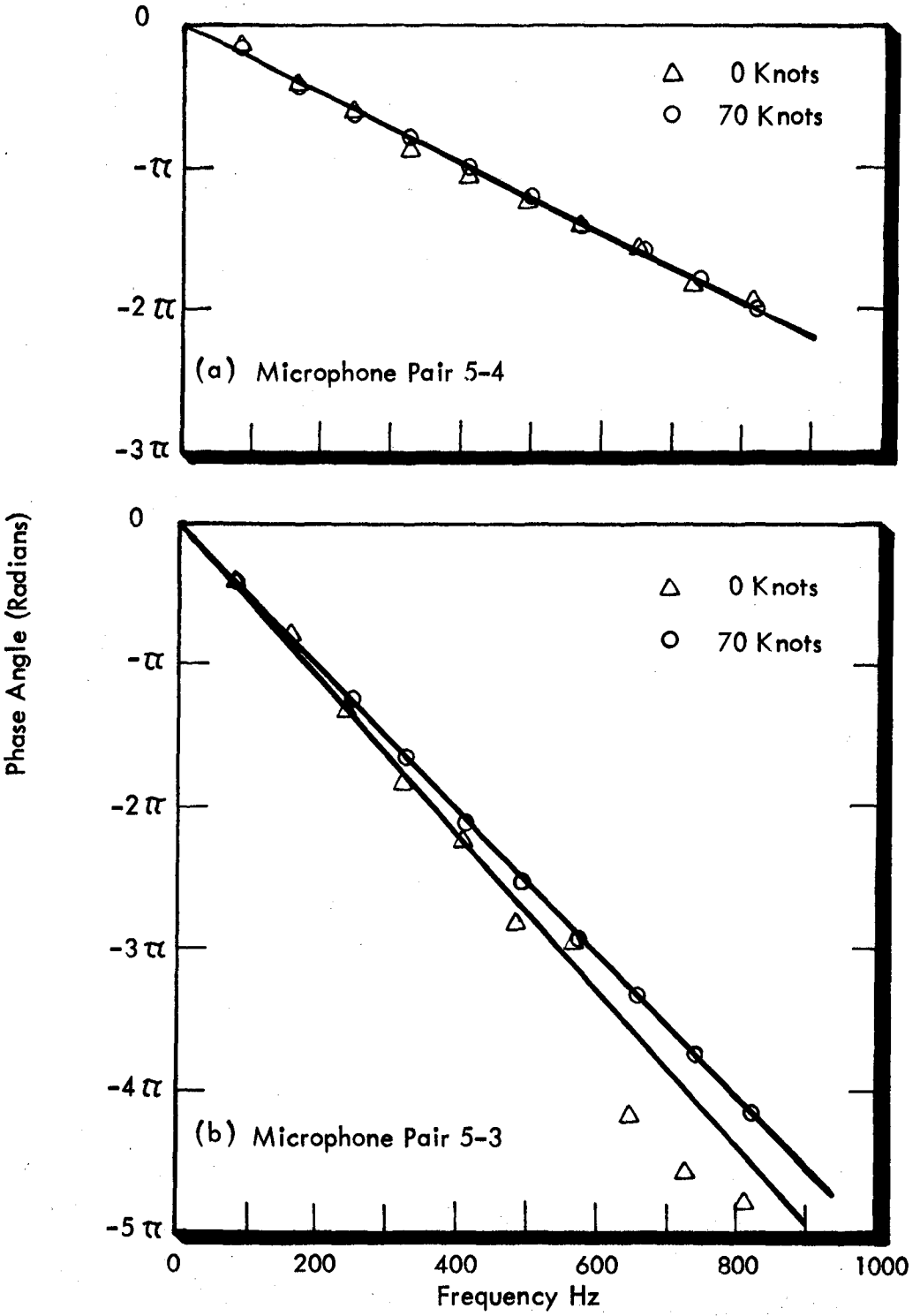

FIGURE 18. VARIATION OF PHASE ANGLE SPECTRA FOR PROPELLER NOISE COMPONENTS IN CIRCUMFERENTIAL DIRECTION

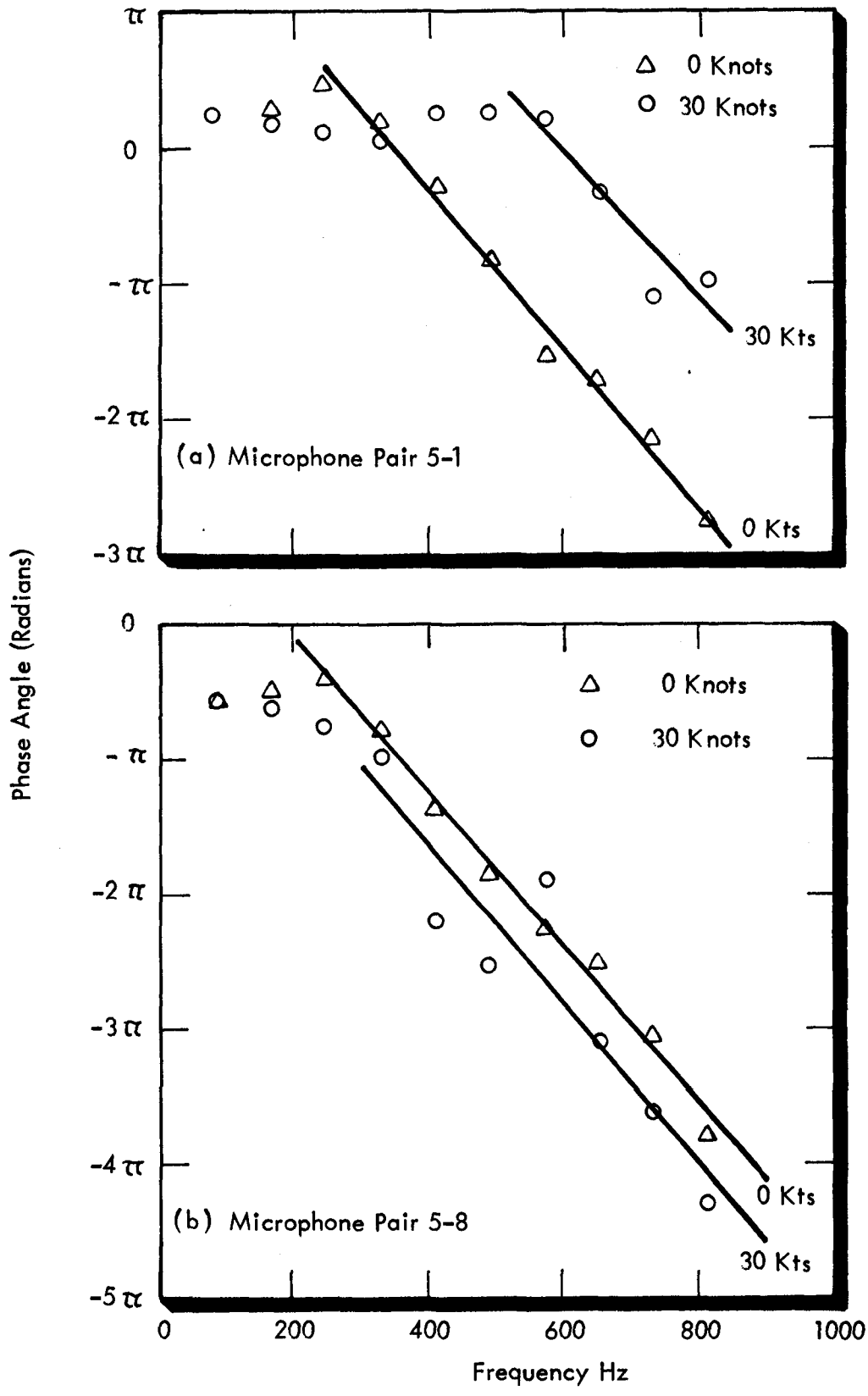

FIGURE 19. VARIATION OF PHASE ANGLE SPECTRA FOR PROPELLER NOISE COMPONENTS IN LONGITUDINAL DIRECTION

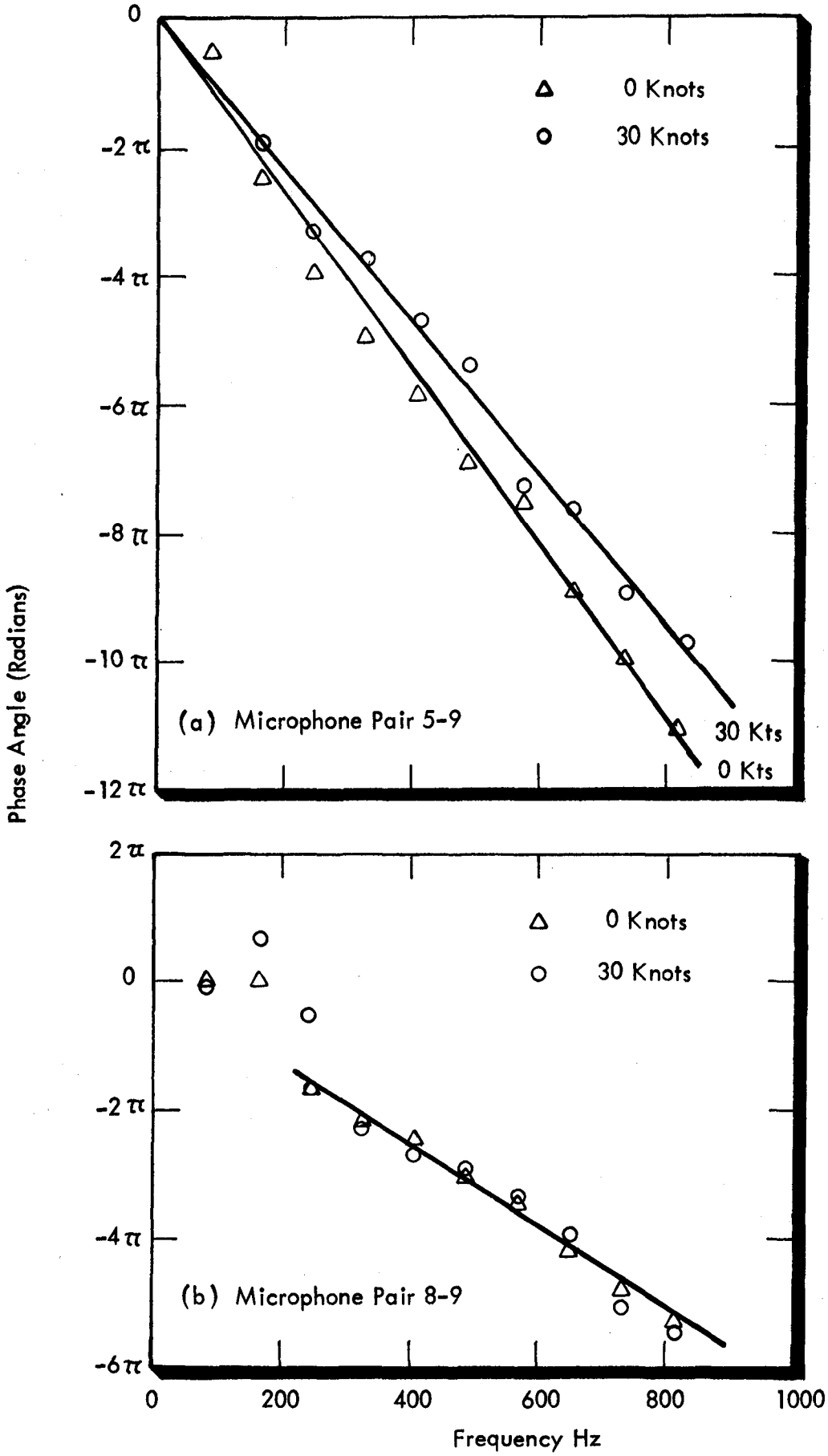

FIGURE 20. VARIATION OF PHASE ANGLE SPECTRA FOR PROPELLER NOISE COMPONENTS IN LONGITUDINAL DIRECTION

difference occurs for the microphone pair 5-1 (Figure 19) where the change from the frequency-independent to the frequency-dependent regime occurs at a higher frequency when forward motion is present.

Considering first the circumferential direction, trace velocities have been determined by means of equation (1) and the values are listed in Table 6. For comparison, corresponding trace velocities for the static case are reproduced from [2]. Although the data were measured at a nominal engine speed of 2600 rpm, differences in rpm were observed. Consequently, propeller rpm values are quoted for each test run, the values being determined from measured frequencies of the 10th harmonic of the propeller blade passage frequency.

Following the approach given in [2], pressure field trace velocities have been calculated on the basis of a "rigid body" pressure field rotating with the propeller blades. This theoretical trace velocity U_c' is given by

$$U_c' = 6 \frac{\Omega d}{\alpha} \qquad (4)$$

where Ω is the propeller rpm, and α is the angle subtended at the propeller hub by the distance d between a pair of microphones. Values of α were determined from measured distances provided by NASA Langley Research Center which are listed in Figure 1 or in Table 7.

Calculated values of the angular separations of the microphone pairs are given in Table 8.

TABLE 6

Estimated Circumferential Trace Velocities
(Nominal Engine Speed: 2600 rpm)

Test Run	Ref [2]	4	5	6	7
Aircraft Velocity (knots)	0	0	40	55	70
Propeller rpm*	1636	1628	1708	1744	1652
Microphone Pair	Trace Velocity** (m/s)				
4 - 3	217	203	241	246	232
5 - 3	217	214	239	244	231
5 - 4	209	229	237	243	231
	Velocity Ratio*** (U_c/U'_c)				
4 - 3	0.96	0.91	1.02	1.02	1.02
5 - 3	0.95	0.94	1.00	1.00	1.00
5 - 4	0.89	0.99	0.97	0.98	0.98

* Calculated from frequency of propeller 10th harmonic

** Positive in upward direction

*** U_c = measured circumferential trace velocity,
U'_c = trace velocity calculated from "rigid body" pressure field.

Table 7

Distances Between Propeller Hub and Microphone

Microphone Location	Distance (m)
3	1.33
4	1.31
5	1.36
6	1.52

Table 8

Calculated Angular Separation of Microphone Pairs

Microphone Pair	Angular Separation at Propeller Hub (degrees)
3 - 4	13.3
4 - 5	11.8
5 - 6	10.4

The measured, U_c, and theoretical, U_c', trace velocities were compared and the values for the ratio U_c/U_c' are shown in Table 6. It is seen that the values of the ratio are all close to unity, suggesting that the hypothesis of a rotating aerodynamic pressure field is a likely physical explanation of the observed phenomenon.

If average values of U_c/U_c' are calculated separately for static and taxi conditions, the averages are found to be 0.94 and 1.00, respectively. Thus the hypothesis appears to fit the data better in the forward velocity case. The significance of this

difference is not readily apparent.

The phase angle spectra for the longitudinal direction show several properties which can be summarized as follows:

(a) When one of the microphonesis in the plane of rotation of the propeller (i.e. at location 5) and the other microphone is fairly close to the plane of rotation (location 1 or 8, where X/D = 0.26), the phase angle is essentially constant at low frequency and then increases (or decreases) in an approximately linear manner at higher frequencies. This behavior is shown in Figure 19.

(b) When one of the microphones is in the plane of rotation (location 5) and the other is well separated from the plane of rotation (location 9, X/D = 0.78), the phase angle increases (or decreases) in an approximately linear manner with frequency. (Figure 20(a)).

(c) When neither microphone is located in the plane of rotation of the propeller (e.g. locations 8 and 9), the phase angle increases (or decreases) in an approximately linear manner. (Figure 20(b)).

In cases (b) and (c) regression lines passing through the origin are fitted to the data and the slope of the line can be interpreted in terms of a trace velocity. For case (a) the regression line at high frequencies is fitted to the data without constraining it to pass through the origin, and the slope is again interpreted in terms of a trace velocity (Section 3.4). The pressure field trace velocities measured for all microphone pairs in the longitudinal

direction are given in Table 9 which also includes data for the corresponding static case given in [2].

It is immediately apparent from Table 9 that there are large differences between the two sets of trace velocity data for the static case. Furthermore, there is no consistent relationship between trace velocity and forward velocity. For example, it might be predicted that a trace velocity in the forward direction (5 to 1) would decrease and in the aft direction increase. This trend is observed in some cases but not in others. In other words the changes seem to be random and of similar order of magnitude to the data repeatability.

Of course it is equally possible that forward velocity has no influence on the pressure field trace velocity because the local airflow velocity induced by the propeller remains independent of forward velocity at these low taxiing speeds. This interpretation seems to be the one supported by the data.

Table 9

Estimated Longitudinal Trace Velocities
(Nominal Engine Speed = 2600 rpm)

Test Run	Ref. [2]	1	2	3
Aircraft Velocity (knots)	0	0	30	50
Propeller rpm	1640	1636	1636	1692
Microphone Pair	Trace Velocity (m/s)			
5 - 1	-153	-212	-231	-150
5 - 8	129	218	213	223
5 - 9	334	269	309	293
8 - 9	417	384	378	436

The trace velocities listed in Table 9 for microphone pairs 5-1 and 5-8 are well subsonic for all forward speeds. For microphone pairs 5-9 the velocities are subsonic but approaching sonic values, and for microphone pairs 8-9 (which is aft of the plane of rotation of the propeller) the trace velocity is supersonic for all conditions. It would appear that when location 5 forms one of the microphone pairs, the subsonic aerodynamic pressure field influences the trace velocity. When both microphones are outside the local influence of the aerodynamic field, the trace velocity is supersonic, i.e., is a sound wave incident at some non-grazing angle of incidence.

4.5.2 Coherence

Interpretation of the coherence data for the propeller components in the noise field on the airplane fuselage presents a particular problem because of the wide variability in the data. This is caused at least in part by contamination of propeller noise signals by exhaust noise, and by interference effects from waves reflected from the lower wing surface on the ground. Also there appear to be large differences between the two sets of results for the static case, one set of data being reported in [2] and the other in this report. These differences may be associated with differences in ambient wind conditions for the two test series (see Section 2.1).

Coherence spectra for the circumferential direction are plotted in Figure 21 for the three separation distances 0.28m (5-4), 0.30m (6-5, 4-3) and 0.58m (6-4, 5-3). No data were obtained for microphone 6 during the present tests, but static test data are available from [2], as are data for the other microphone locations. It should be noted that, although different pairs of microphones have the same separation distances, they may be at different radii with respect to the propeller hub, and, therefore, subtend different angles at the hub.

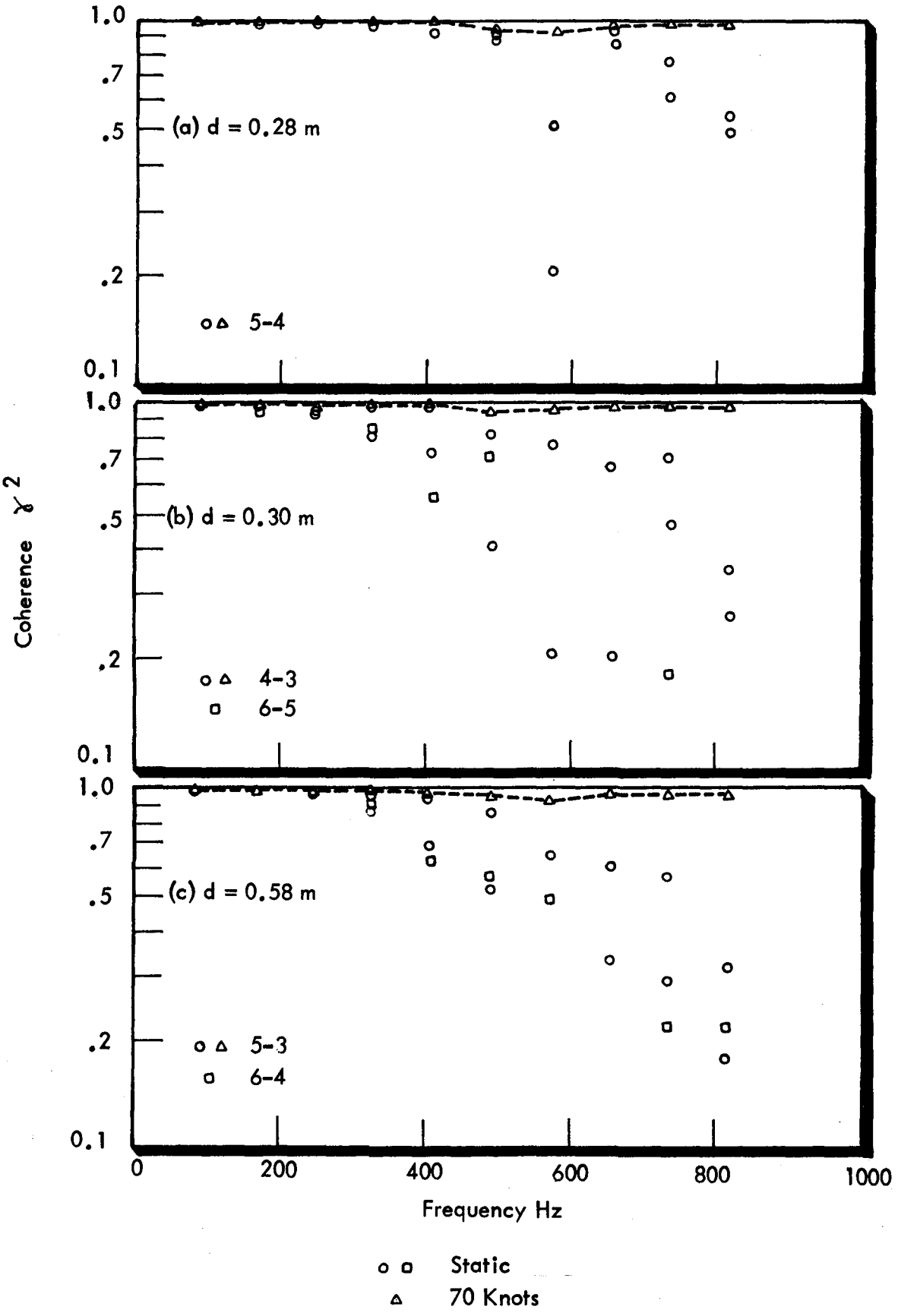

FIGURE 21. COHERENCE SPECTRA IN CIRCUMFERENTIAL DIRECTION FOR PROPELLER NOISE COMPONENTS (WITH AND WITHOUT FORWARD VELOCITY)

Two observations can be made from Figure 21. Firstly, the static test data show wide variation from run to run and frequency to frequency. Secondly, there is a marked difference between static and forward velocity conditions. Although Figure 21 shows taxi data for only the 70 knots case, these data have values which are very close to those for the 40-knot and 55-knot cases (as can be seen in Appendix D).

There was some discussion in [2] regarding possible non-dimensional frequency parameters which would collapse the coherence spectra onto a single curve. Two parameters were tried, one being the Strouhal number fd/U_c based on the microphone separation distance d and the measured trace velocity U_c. The other parameter was the harmonic order n. Neither parameter was successful, although it appears now that poor data repeatability may be part of the problem. Consequently, a second attempt is made in Figure 22 to collapse the data with Strouhal numbers. The wide variation in the data is again evident but there appears to be some clustering of the data, at least for Strouhal numbers less than 1.3.

It is probably appropriate to comment on the physical reasoning behind the choice of the Strouhal number fd/U_c as a non-dimensional frequency. This parameter is often used in describing aerodynamic pressure fields, such as turbulent boundary layers, where pressure "eddies" are formed and decay with some lifetime or spatial coherence. Since d/U_c is the time taken for the pressure disturbance to traverse the distance d, the coherence spectrum can be interpreted in terms of the travel time and the "eddy" lifetime for the frequency of interest. In the present case of a rotating propeller the lifetime of an "eddy" in the pressure signature of the blade could, for example, be related to the

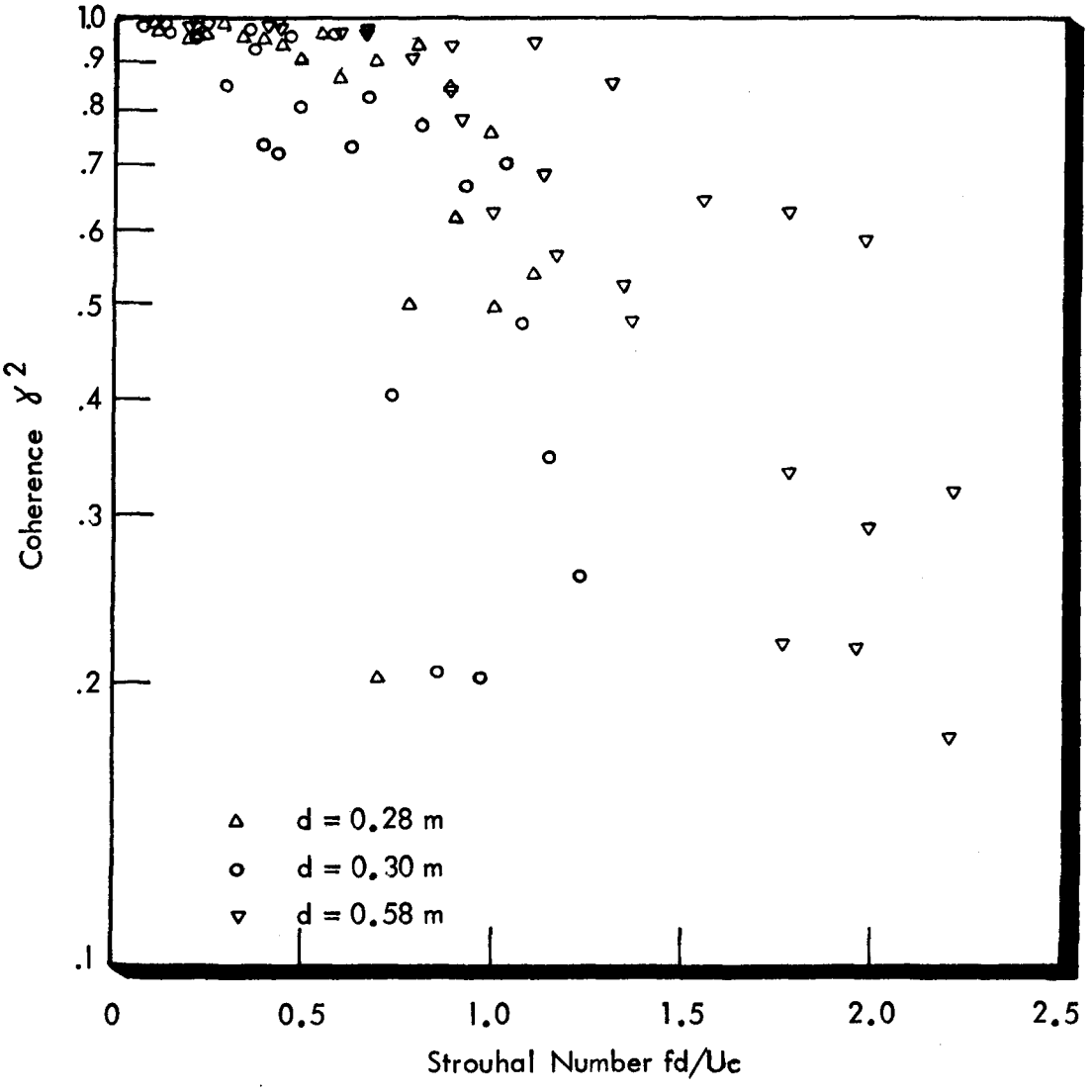

FIGURE 22. VARIATION OF COHERENCE IN CIRCUMFERENTIAL DIRECTION WITH STROUHAL NUMBER FOR PROPELLER NOISE COMPONENTS (STATIC RUNS)

spatial scale of turbulence in the air inflow to the propeller.

In the preceding discussion of Figure 21, it was observed that a given distance d could be associated with different radial distances from the propeller hub. This is taken care of in the parameter fd/U_c because, if U_c is replaced by U_c' from equation (4), it can be written in the equivalent form $f\alpha/\Omega$ which is independent of radial distance and depends solely on angular displacement between the two locations.

The coherence data for the circumferential direction are not plotted in terms of harmonic order in this report. As there is only one propeller rpm condition considered in the taxi data, use of harmonic order as non-dimensional frequency will result in a data presentation which is essentially the same as that when frequency is used directly, as in Figure 21.

At the present time physical explanations for the differences in coherence values for static and taxi conditions must be purely speculative because of the limitations of the data. Hypotheses may explain the observed effects but need not necessarily be the correct explanations. One possibility is that, during static operation, the turbulence in the inflowing air is elongated and thus becomes poorly correlated in the circumferential direction. As a consequence the pressure pulses generated by the blade at two measuring locations in the circumferential direction would be poorly correlated, particularly at the higher frequencies. When there is forward motion, the turbulence compondents are not elongated and the circumferential correlation is higher than for the static case.

An overall physical explanation for the effect of forward motion on circumferential coherence data has, however, to be consistent

with respect to other results of the analysis. For example, probability density and signal enhancement analyses are interpreted in Section 4.3 in terms of increased amplitude stability and decreased phase stability. Also forward motion has little influence on pressure levels measured in the plane of rotation of the propeller (see Figure 7), indicating that the pressures are associated with thickness rather than blade loading effects. An adequate explanation embracing all these observed phenomena is still wanting and may require aerodynamic (mean flow and turbulence) measurements.

Turning to the longitudinal direction, pressure coherence spectra for the propeller harmonic components are shown in Figure 23 for the microphone pairs 5-1 and 5-8. (Data for microphone pair 5-9 would show similar characteristics.) The figure compares static test data for the present tests and for the tests reported in [2] at the appropriate engine rpm (2600). These two sets of data show marked differences for some of the propeller harmonics. Also shown in the figure are coherence data associated with airplane speeds of 30 and 40 knots. The data for these two speeds are similar and tend to show coherence values at the higher order harmonics which are lower than those for the static case. For microphone pair 5-1 the divergence between static and taxi coherence occurs above the 5th harmonic and for microphone pair 5-8, above the 3rd harmonic.

The trend of decreased coherence when there is forward motion of the airplane is counter to that for the circumferential direction where the coherence increases when forward motion occurs. The physical reasons for these differences cannot be determined from the limited amount of available information, although certain inferences can be drawn. It has been shown in Figures 5, 6, and 7 that, when there is forward motion, the propeller harmonic

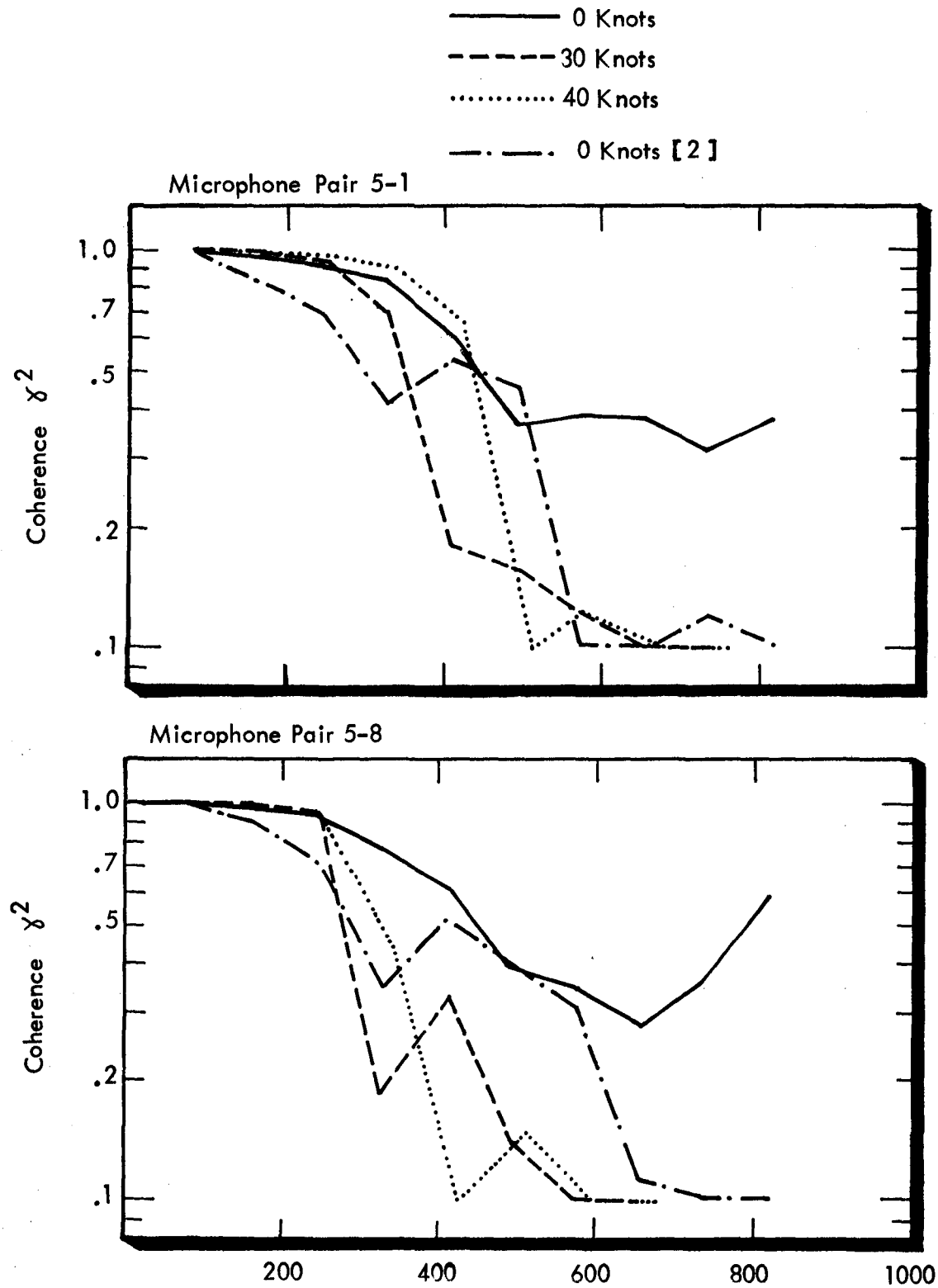

FIGURE 23. COHERENCE SPECTRA IN LONGITUDINAL DIRECTION FOR PROPELLER NOISE COMPONENTS (WITH AND WITHOUT FORWARD VELOCITY)

levels at microphone locations 1, 8 and 9 are lower than those for the static case, whereas at location 5 there is little difference between forward motion and static cases. At least two possible interpretations present themselves: (a) Because of low propeller noise levels the propeller noise signal at locations 1, 8, 9 could become contaminated by other signals such as engine exhaust when there is forward motion, thereby reducing the coherence, and (b) the aerodynamic pressure field which dominates the signal at location 5 propagates less to the other locations when there is forward motion of the airplanes.

The only microphone pair which lies outside the influence of the propeller near field is 8-9. Unfortunately, the coherence spectra for this pair show coherence values which vary so widely with harmonic order or with test condition that little or no useful conclusions can be drawn. This is disappointing as the phase angle data indicate that the pressure field is a propagating acoustic field. The irregular coherence data almost certainly results from the difficulties involved in accurately measuring propeller harmonic components when the noise spectrum is dominated by exhaust harmonic components. Although in theory the propeller harmonic could be isolated by sufficiently narrow filter band widths, this is not possible in practice because slight variations in propeller speed would move a propeller harmonic in and out of the filter band and because a very long sampling time would be required to get statistically reliable data.

The search for appropriate non-dimensional frequency parameters for the longitudinal coherence is still open. Physical arguments for the use of a Strouhal number fd/U_c are less convincing for the longitudinal direction than for the circumferential case, because there is less information regarding the pressure field.

However, a brief exploratory analysis was performed for microphone pairs 5-8 and 5-9 to see what the results would be. For this analysis the coherence data in Figure 23 were reduced in quantity by averaging the coherence values for the two static cases and for the two taxi cases, for each microphone pair. The resulting coherence spectra are shown in Figures 24 and 25 where both frequency and Strouhal number are used for the parameter on the abscissa. When Strouhal number is used for the microphone pair 5-8, the value of U_c used in fd/U_c is the value obtained for the higher order harmonics. If the value of U_c were taken to be that appropriate to the low order harmonics, the corresponding values of fd/U_c would be much smaller than those shown in the figures.

The data in Figure 24 for the static case show irregular shapes for the average coherence spectra and it is difficult to determine whether fd/U_c gives a better data collapse than does f alone. For the taxi case (Figure 25) the average spectra are much more regular in shape and there is an apparent improvement in data collapse when the Strouhal number is introduced. However, firm conclusions should not be drawn from this very limited comparison. Furthermore the Strouhal number based on d and U_c is probably not appropriate for microphone pairs such as 8-9 which appear to lie in a propagating acoustic field. Much more experimental testing is obviously required before firm conclusions can be drawn, and the testing should be designed to minimize signal contamination from the noise sources and interference from reflected acoustic waves.

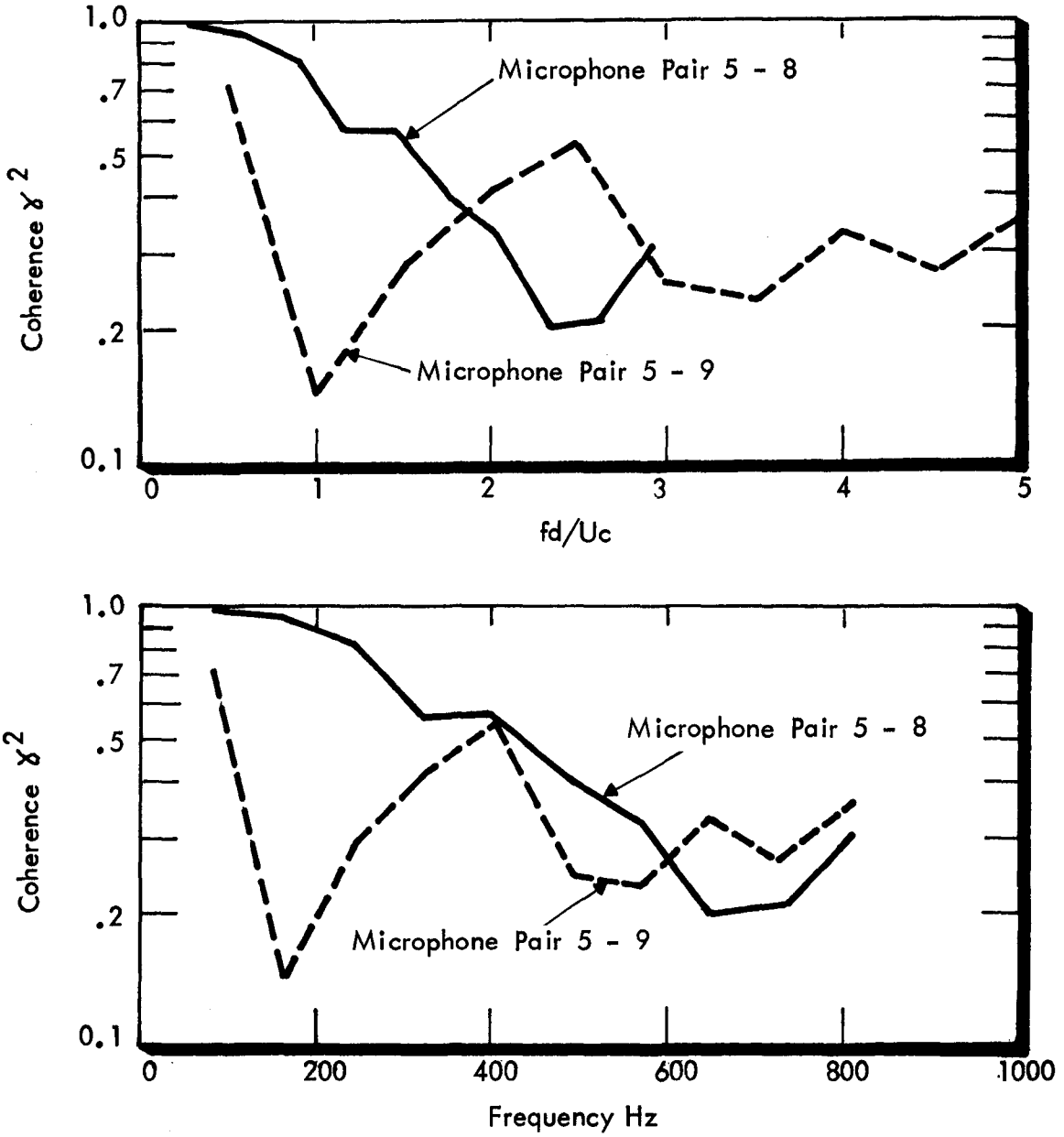

FIGURE 24. COMPARISONS OF AVERAGE COHERENCE SPECTRA IN LONGITUDINAL DIRECTION (AVERAGE OF TWO STATIC CASES)

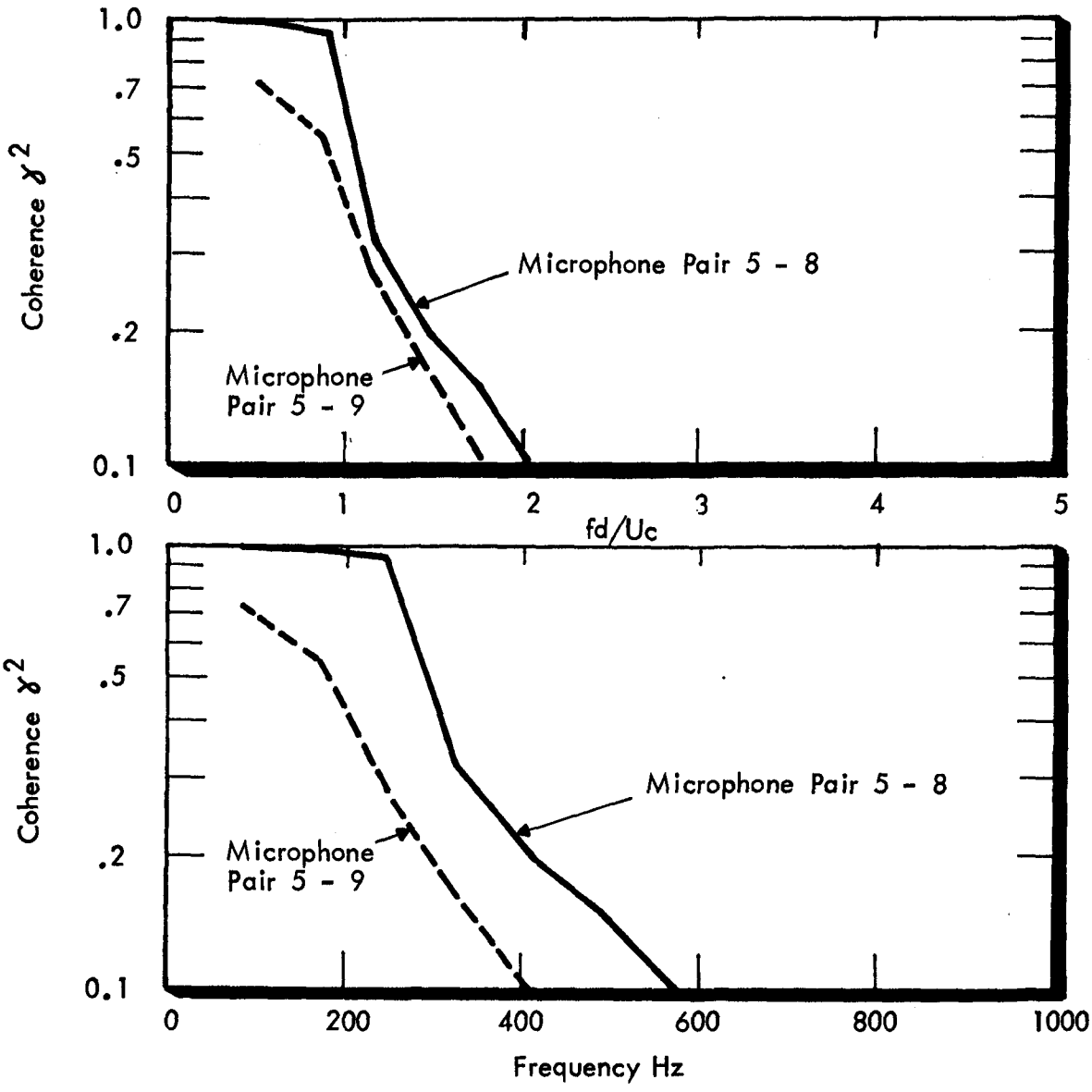

FIGURE 25. COMPARISONS OF AVERAGE COHERENCE SPECTRA IN LONGITUDINAL DIRECTION (AVERAGE OF 30 AND 40 KT TAXI CASES)

4.6 Interior Sound Levels

Sound levels were measured in the cabin of the Aero Commander at a single microphone location, #11, during tests discussed in this report, and during the tests reported in [2]. Discussion of interior sound levels has, however, been minimal as interest has been centered on the description of the exterior pressure field. To remedy the situation an analysis of the interior noise measurements is presented in this report as Appendix E. The discussion is given in an appendix as it refers not only to the taxi tests discussed in the main body of the text of this report, but includes also measurements from the static tests of [2].

REFERENCES

1. Mixson, J. S., Barton, C. K. and Vaicaitis, R., "Investigation of Interior Noise in a Twin-Engine Light Aircraft," Journal of Aircraft, Vol. 15, No. 4, pp 227-233, April 1978.

2. Piersol, A. G., and Wilby, E. G., and Wilby, J. F., Evaluation of Aero Commander Propeller Acoustic Data: Static Operations," NASA CR 158919, May 1978.

3. "Prediction Procedure for Near-Field and Far-Field Propeller Noise," SAE Aerospace Information Report AIR 1407, May 1977.

4. Ungar, E. E., et al, "A Guide for Estimation of Aero-acoustic Loads on Flight Vehicle Surfaces," AFFDL-TR-76-91, Vol. I, February 1977.

APPENDIX A

MAGNITUDES OF PROPELLER BLADE PASSAGE TONES

TABLE A-1. MAGNITUDE OF PROPELLER BLADE PASSAGE HARMONICS FOR STATIC OPERATION - TEST RUNS 1 AND 4.
(2 Hz Resolution)

Harmonic Order	Sound Pressure Level in dB by Location No.(Fig. 1)					
	1	3	4	5	8	9
1	132.9	134.9	135.4	133.4	130.4	118.7
2	115.1	131.8	130.6	126.5	115.6	106.7
3	112.2	128.1	127.6	123.5	112.3	106.0
4	110.4	122.8	124.8	119.8	111.3	106.2
5	109.7	117.7	120.7	114.1	110.6	102.2
6	110.3	115.7	119.2	114.3	109.0	114.4
7	111.2	114.9	116.2	112.5	109.4	114.2
8	109.2	112.5	115.5	108.3	105.8	104.4
9	108.8	114.4	111.6	105.0	108.8	104.9
10	106.9	115.8	110.3	104.6	111.9	107.3
11	107.3	114.4	106.9	96.9	105.8	104.2
12	104.3	113.0	104.8	98.8	102.5	105.1
13	105.6	111.9	103.7	94.4	107.5	101.9
14	103.7	110.2	101.5	94.4	102.9	100.2
15	103.3	107.6	97.6	91.1	103.3	97.7
16	102.2	106.0	97.1	92.8	100.9	103.0
17	100.4	105.0	96.0	93.0	100.0	99.1
18	100.1	103.0	94.5	92.8	101.2	95.1
19	99.8	100.8	94.4	90.4	102.2	101.1
20	97.3	98.8	-	91.9	100.7	-
Overall	133.2	137.6	137.6	134.8	130.9	122.2

TABLE A-2. MAGNITUDE OF PROPELLER BLADE PASSAGE HARMONICS FOR 30 KNOT AND 50 KNOT TAXI - TEST RUNS 2 AND 3
(2 Hz Resolution)

Harmonic Order	Sound Pressure Level in dB by Taxi Speed and Location No. (Figure 1)							
	30 Knot Taxi				40 Knot Taxi			
	1	5	8	9	1	5	8	9
1	132.3	132.6	130.3	119.7	130.2	130.4	126.5	118.4
2	119.0	126.5	115.8	109.7	116.6	125.2	111.3	115.6
3	109.6	123.4	108.5	100.9	104.5	121.5	100.5	106.0
4	100.0	120.9	98.3	98.2	97.8	119.0	95.1	98.1
5	94.9	115.8	97.7	93.9	92.5	114.2	97.3	100.4
6	98.4	115.8	95.7	107.0	98.0	113.5	87.7	107.4
7	108.6	112.4	108.0	113.0	103.2	110.0	102.2	105.2
8	92.1	108.7	93.0	97.7	84.9	106.0	90.6	94.9
9	89.1	105.8	91.6	90.3	88.0	103.0	87.1	92.4
10	88.9	103.3	91.1	90.9	85.3	100.2	90.2	93.3
11	88.7	100.5	89.7	89.7	84.3	97.7	90.1	97.0
12	86.2	98.4	91.6	94.7	86.5	95.8	89.8	93.5
13	90.5	96.8	94.4	96.7	88.3	90.7	88.7	91.5
14	86.6	89.6	87.9	90.4	83.3	89.4	83.6	89.4
15	-	91.9	86.9	88.9	-	88.1	-	86.9
16	-	89.3	-	86.5	-	-	-	-
Overall	132.5	134.3	130.5	121.2	130.4	132.3	126.7	120.9

TABLE A-3. MAGNITUDE OF PROPELLER BLADE PASSAGE HARMONICS FOR 40 KNOT, 55 KNOT, AND 70 KNOT TAXI - TEST RUNS 5, 6, AND 7
(2 Hz Resolution)

Harmonic Order	Sound Pressure Level in dB by Taxi Speed and Location Number (Figure 1)											
	40 Knot Taxi				55 Knot Taxi				70 Knot Taxi			
	3	4	5	11	3	4	5	11	3	4	5	11
1	129.4	131.9	130.9	104.6	128.8	131.0	130.2	104.1	128.5	130.7	130.2	102.6
2	127.2	127.8	124.6	99.8	126.2	127.4	124.5	99.5	126.2	126.7	123.5	98.2
3	125.8	125.7	122.4	93.1	124.6	124.7	121.6	90.5	124.7	124.4	121.0	89.4
4	123.6	124.2	119.4	84.5	121.8	123.2	118.6	83.5	121.9	122.8	118.2	80.7
5	120.2	121.5	115.8	85.2	119.5	121.7	116.7	84.0	118.6	120.4	112.9	81.7
6	118.7	120.3	115.2	77.9	116.6	119.2	114.2	74.5	116.5	118.0	112.7	79.6
7	116.6	118.4	111.9	79.5	115.2	117.8	111.1	80.4	114.1	116.2	109.8	74.9
8	113.4	115.8	108.0	66.1	111.9	115.1	107.7	65.7	111.5	113.8	105.8	69.1
9	111.3	114.2	105.7	61.3	110.2	113.4	105.2	59.2	108.3	111.4	102.8	63.9
10	109.2	112.1	103.1	67.1	107.6	111.1	102.1	67.9	106.2	109.3	99.9	57.4
11	106.9	109.7	99.9	63.1	105.5	109.0	100.0	60.8	103.7	106.9	97.2	61.7
12	103.8	107.1	97.4	62.1	102.5	106.7	96.5	61.2	101.4	104.6	96.1	58.0
13	101.9	105.6	92.6	60.8	100.7	104.9	94.3	57.9	99.0	102.3	92.7	57.6
14	98.7	103.6	93.1	56.4	98.5	101.9	92.3	55.5	96.5	100.5	91.3	58.3
15	97.4	100.5	90.4	52.5	97.1	99.2	91.4	52.4	94.3	98.0	88.4	56.7
16	93.7	98.4	86.9	-	93.1	97.4	89.6	53.3	91.2	95.0	85.3	-
17	91.4	96.6	86.2	-	92.2	96.7	85.7	-	90.0	93.5	-	-
18	90.3	94.2	85.0	-	90.7	93.4	-	-	91.3	92.8	-	-
19	-	91.5	-	-	-	90.4	-	-	89.8	90.2	-	-
Overall	133.6	135.1	132.7	106.2	132.6	134.3	132.2	105.6	132.4	133.8	131.8	104.2

APPENDIX B

MAGNITUDES OF PROPELLER BLADE PASSAGE TONES AFTER SIGNAL ENHANCEMENT PROCEDURES

TABLE B-1. MAGNITUDE OF ENHANCED PROPELLER BLADE PASSAGE TONES FOR STATIC OPERATIONS - TEST RUNS 1 AND 4

Harmonic Order	Sound Pressure Level in dB by Location No. (Figure 1)					
	1	3	4	5	8	9
1	132.8	134.2	135.4	132.9	129.9	117.3
2	114.3	131.0	130.3	126.5	115.3	99.5
3	111.0	126.0	127.0	123.4	111.8	98.7
4	108.8	119.0	123.7	119.8	109.2	95.0
5	107.9	111.9	118.9	114.0	107.6	90.1
6	106.6	106.1	115.5	113.7	105.1	99.5
7	105.5	102.5	111.1	110.3	101.3	100.1
8	102.7	99.4	109.6	105.4	95.1	88.3
9	99.7	101.0	104.3	101.3	99.9	82.9
10	96.1	99.9	101.4	98.1	101.9	84.7
Enhanced Overall	132.9	136.4	137.3	134.4	130.2	117.6
Unenhanced Overall*	133.1	137.5	137.6	134.8	130.8	121.9

*Computed using first 10 harmonics only.

TABLE B-2. MAGNITUDE OF ENHANCED PROPELLER BLADE PASSAGE TONES FOR 30 KNOT AND 70 KNOT TAXI - RUNS NO. 2 AND 7

Harmonic Order	Sound Pressure Level in dB by Taxi Speed and Location Number (Figure 1)						
	30 Knots				70 Knots		
	1	5	8	9	3	4	5
1	132.3	132.3	129.6	118.5	128.1	130.4	129.8
2	118.7	126.1	115.0	108.7	124.2	124.8	121.9
3	108.8	122.5	107.4	94.7	120.6	120.2	117.7
4	95.8	119.8	89.5	95.0	115.7	115.6	112.9
5	88.1	114.0	93.6	85.6	110.9	110.8	105.5
6	90.1	113.3	85.9	84.8	106.5	106.1	103.1
7	86.8	108.7	86.0	95.5	100.9	102.6	96.7
8	84.4	104.6	82.6	80.9	98.4	97.6	92.9
9	76.8	100.9	80.8	75.9	92.6	93.6	89.2
10	74.7	96.8	77.6	81.1	87.8	87.5	85.1
Enhanced Overall	132.5	133.9	129.8	119.0	130.3	131.9	130.8
Unenhanced Overall*	132.5	134.3	130.5	121.2	132.4	133.7	131.8

*Computed using first 10 harmonics only.

APPENDIX C

PHASE ANGLES OF PROPELLER BLADE PASSAGE TONES COMPUTED FROM ENHANCED DATA

TABLE C-1. HARMONIC PHASE ANGLES AT VARIOUS LOCATIONS FOR STATIC OPERATION

Harmonic Number	Phase Angle in Degrees at Various Locations (Figure 1)					
	1	3	4	5	8	9
1	79.7	109.7	108.0	97.8	82.3	78.2
2	- 24.1	.9	4.5	- 14.7	-170.4	163.5
3	-147.4	-119.7	-115.5	-132.7	- 72.3	-157.0
4	168.9	122.0	120.8	105.2	105.7	149.6
5	159.9	2.6	4.2	- 39.3	- 45.2	10.3
6	148.7	-114.6	-114.6	-146.2	158.7	- 29.3
7	140.5	134.3	132.1	73.3	15.0	-107.4
8	120.1	20.0	20.8	- 79.6	153.2	155.5
9	151.3	-112.3	-100.6	153.0	7.5	62.1
10	- 13.8	126.9	147.7	12.1	-127.1	- 5.5
11	- 19.2	13.5	25.6	-105.5	133.1	- 59.1
12	- 66.3	-110.6	- 92.8	151.8	100.2	-105.4
13	- 90.8	124.6	142.5	56.3	45.5	-151.8
14	-109.1	- 6.9	10.6	-101.1	96.2	155.3
15	- 86.6	-129.9	-103.5	-143.6	-154.6	56.4
16	-101.4	81.2	143.9	-167.4	-133.2	100.8
17	-124.0	- 33.6	21.2	- 41.1	- 24.0	33.8
18	-136.0	-172.4	-120.4	-113.7	100.3	- 7.8
19	-153.4	75.6	154.6	-169.3	- 6.1	- 35.0
20	-136.5	- 81.4	42.0	156.9	-143.7	140.8

TABLE C-2. HARMONIC PHASE ANGLES AT LOCATION 5 FOR VARIOUS TAXI SPEEDS

Harmonic Number	Phase Angle in Degrees at Various Speeds			
	0 Knots	30 Knots	40 Knots	70 Knots
1	97.8	102.5	103.3	108.1
2	- 14.7	- 7.5	- 7.6	10.5
3	-132.7	-120.1	-123.0	- 94.8
4	105.2	128.4	111.3	154.5
5	- 39.3	- 2.0	- 68.5	31.4
6	-146.2	-105.2	171.9	- 85.1
7	73.3	141.9	70.0	123.3
8	- 79.6	20.2	- 18.6	4.2
9	153.0	-103.5	-106.5	- 96.9
10	12.1	129.4	157.1	156.2
11	-105.5	- 16.9	55.9	76.2
12	151.8	-136.4	-116.1	70.9
13	56.3	111.1	150.1	- 44.6
14	-101.1	- 25.5	72.8	-125.5
15	-143.6	-129.6	- 51.0	159.2
16	-167.4	141.8	-165.7	113.9
17	- 41.1	27.7	155.3	-111.8
18	-113.7	- 87.8	23.4	- 2.2
19	-169.3	-174.8	133.3	-151.8
20	156.9	81.9	93.4	81.7

APPENDIX D

SPATIAL COHERENCE AND PHASE OF PROPELLER BLADE PASSAGE TONES

This appendix presents measured values of coherence and phase angle for several pairs of microphones and several test conditions.

Sample spectral plots are given for two microphone pairs. Figures D1-D4 contain coherence and phase angle spectra for microphone pair 4-3 for the static run and for the 70 knot taxi run. Figures D5-D8 contain the spectra for microphone pair 8-9 for the static run and for the 40 knot taxi run. The coherence by definition, has a value in the range $0 \leq \gamma^2 \leq 1$, and the phase angle is presented such that $-\pi \leq \phi \leq \pi$. Consequently, when ϕ reaches $\pm\pi$ the plot switches over to $\mp\pi$, respectively, showing a full scale sweep on the figure.

Values for coherence and phase angle at the propeller harmonic frequencies were read directly from the digital meter on the SD360 analyzer, and the resulting values are listed in a series of tables presented in this appendix. The output of the SD360 for a microphone pair A-B will give a negative slope for the phase angle spectra when the wave travels from A to B.

COHERENCE AND PHASE ANGLE - 2600 RPM

Harmonic Order	0 Knots		30 Knots		40 Knots	
	Co-herence	Phase (degrees)	Co-herence	Phase (degrees)	Co-herence	Phase (degrees)
Microphones 5 and 1						
1	1.00	45	1.00	44	1.00	31
2	.95	52	.99	32	.99	17
3	.89	88	.95	20	.97	23
4	.82	34	.71	10	.91	-17
5	.61	-53	.18	45	.67	-38
6	.36	-146	.16	46	.04	4
7	.39	87	.12	38	.12	-12
8	.38	50	.10	-59	.02	0
9	.32	-59	.04	161	.05	168
10	.38	-138	.01	-179	.01	106
Microphones 5 and 8						
1	.99	-107	1.00	-105	.99	-106
2	.98	-89	.99	-112	.98	-123
3	.92	-73	.95	-136	.90	-152
4	.77	-142	.18	-178	.46	-145
5	.61	118	.32	-34	.07	-41
6	.39	25	.14	-96	.15	-67
7	.34	-52	.05	22	.09	-111
8	.28	-90	.06	158	.03	-25
9	.36	162	.04	70	.03	-154
10	.57	40	.07	-53	.03	-38

COHERENCE AND PHASE ANGLE - 2600 RPM

Harmonic Order	0 Knots		30 Knots		40 Knots	
	Co-herence	Phase (degrees)	Co-herence	Phase (degrees)	Co-herence	Phase (degrees)
Microphones 5 and 9						
1	.79	-99	.92	-108	.51	-177
2	.06	-77	.79	9	.31	- 67
3	.33	7	.20	124	.33	23
4	.57	-177	.30	43	.02	- 12
5	.56	34	.03	-125	.01	103
6	.36	-168	.02	107	.03	-135
7	.23	96	.08	137	.09	165
8	.49	-161	.02	62	.01	- 45
9	.51	6	.02	-174	.05	- 9
10	.68	170	.04	43	.01	- 54
Microphone 8 and 9						
1	.84	6	.93	- 4	.53	- 68
2	.09	4	.72	122	.27	51
3	.37	63	.24	- 95	.34	179
4	.81	-33	.11	- 58	.03	88
5	.62	-81	.07	-126	.54	-139
6	.55	172	.49	-168	.06	- 81
7	.65	98	.92	108	.90	- 97
8	.34	-39	.23	10	.40	65
9	.73	-145	.15	163	.10	-156
10	.84	133	.15	89	.04	135

COHERENCE AND PHASE ANGLE - 2600 RPM

Harmonic Order	0 Knots		40 Knots		55 Knots		70 Knots	
	Coher-ence	Phase (deg.)	Coher-ence	Phase (deg.)	Coher-ence	Phase (deg.)	Coher-ence	Phase (deg.)
Microphones 5 and 3								
1	.99	-75	.99	-70	.99	-65	.99	-70
2	.99	-144	1.00	-156	1.00	-157	1.00	-154
3	.98	123	1.00	131	1.00	130	1.00	133
4	.85	32	1.00	62	1.00	62	1.00	63
5	.69	-43	1.00	-30	.99	-28	.99	-19
6	.53	-146	.98	-92	.98	-90	.97	-94
7	.00	-171	.98	-167	.97	-166	.94	-168
8	.34	-36	.99	119	.99	120	.98	120
9	.30	-104	.99	47	.99	47	.96	49
10	.18	-140	.99	-28	.95	-28	.96	-28
Microphones 5 and 4								
1	.99	-22	1.00	-30	1.00	-28	1.00	-29
2	.96	-69	1.00	-78	1.00	-78	1.00	-74
3	.99	-105	1.00	-114	1.00	-114	1.00	-112
4	.96	-157	1.00	-142	1.00	-141	1.00	-140
5	.91	173	1.00	166	.99	166	.99	178
6	.87	141	.99	143	.96	145	.94	141
7	.20	111	.95	109	.95	110	.93	108
8	.94	84	.99	72	.99	72	.97	74
9	.62	30	.99	36	.99	37	.96	38
10	.50	10	.99	0	.97	0	.96	2

COHERENCE AND PHASE ANGLE - 2600 RPM

Harmonic Order	0 Knots		40 Knots		55 Knots		70 Knots	
	Coher-ence	Phase (deg.)	Coher-ence	Phase (deg.)	Coher-ence	Phase (deg.)	Coher-ence	Phase (deg.)
Microphones 4 and 3								
1	.99	-53	1.00	-40	.99	-37	1.00	-41
2	1.00	-79	1.00	-78	1.00	-60	1.00	-80
3	.94	-132	1.00	-115	1.00	-117	1.00	-115
4	.80	-177	1.00	-157	1.00	-158	1.00	-157
5	.73	139	1.00	164	1.00	165	1.00	163
6	.41	65	.98	124	.98	124	.96	123
7	.21	-5	.93	85	.75	85	.97	85
8	.20	-88	.98	48	.99	49	.98	46
9	.47	-94	1.00	12	1.00	12	.99	11
10	.26	-179	1.00	-26	.99	-26	.98	-27

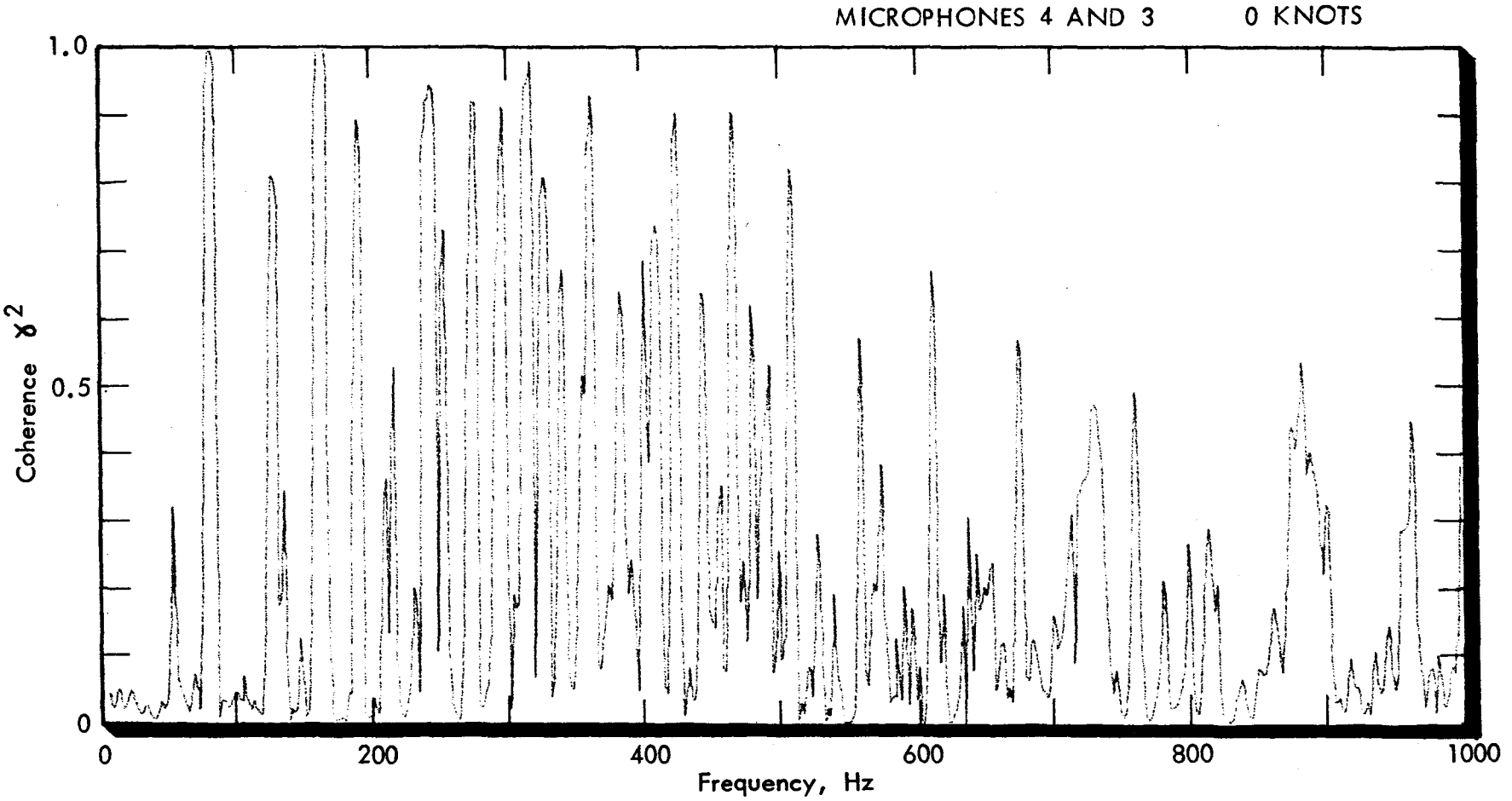

FIGURE D1. COHERENCE SPECTRUM FOR MICROPHONES 4 AND 3. STATIC RUN

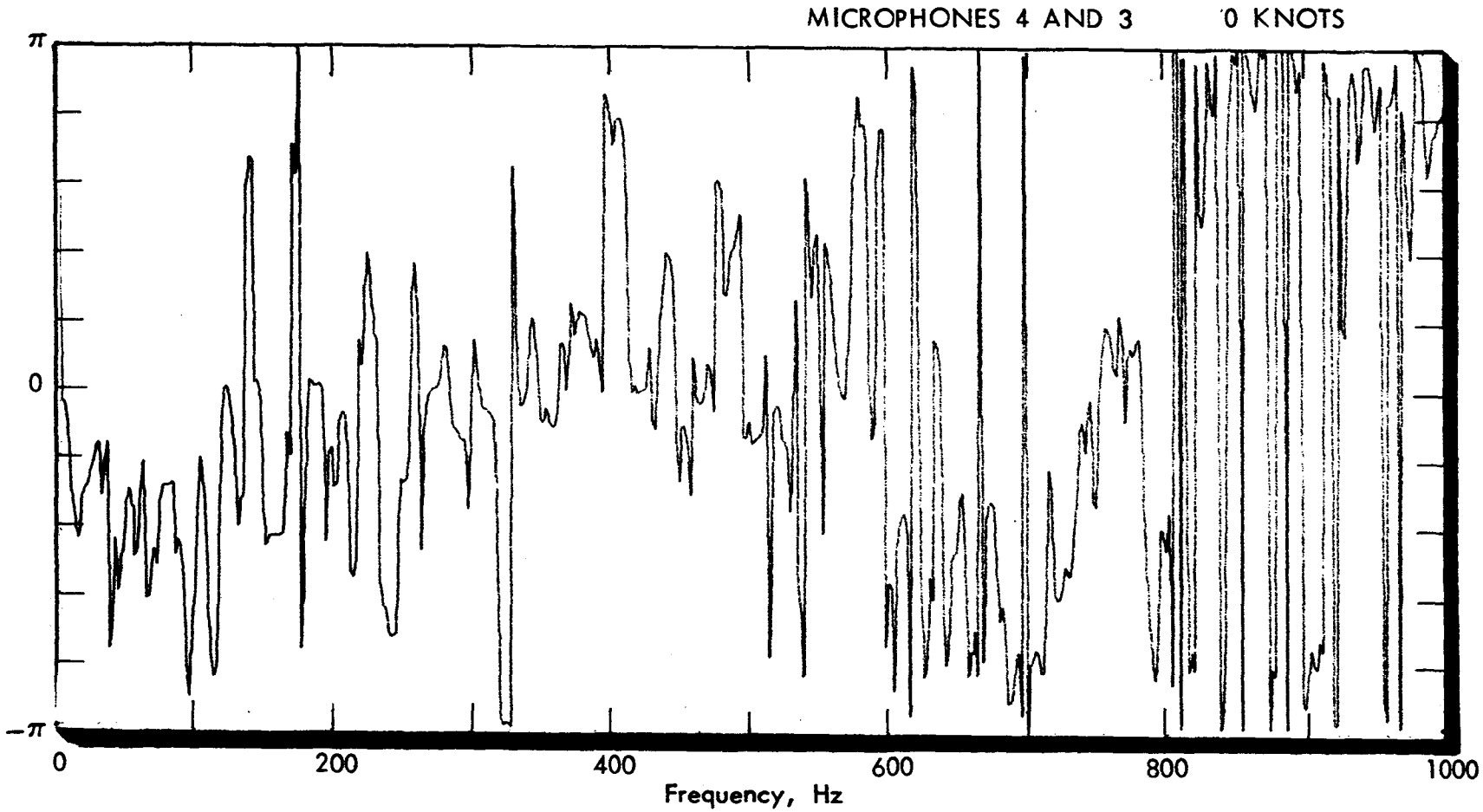

FIGURE D2. PHASE SPECTRUM FOR MICROPHONES 4 AND 3. STATIC RUN

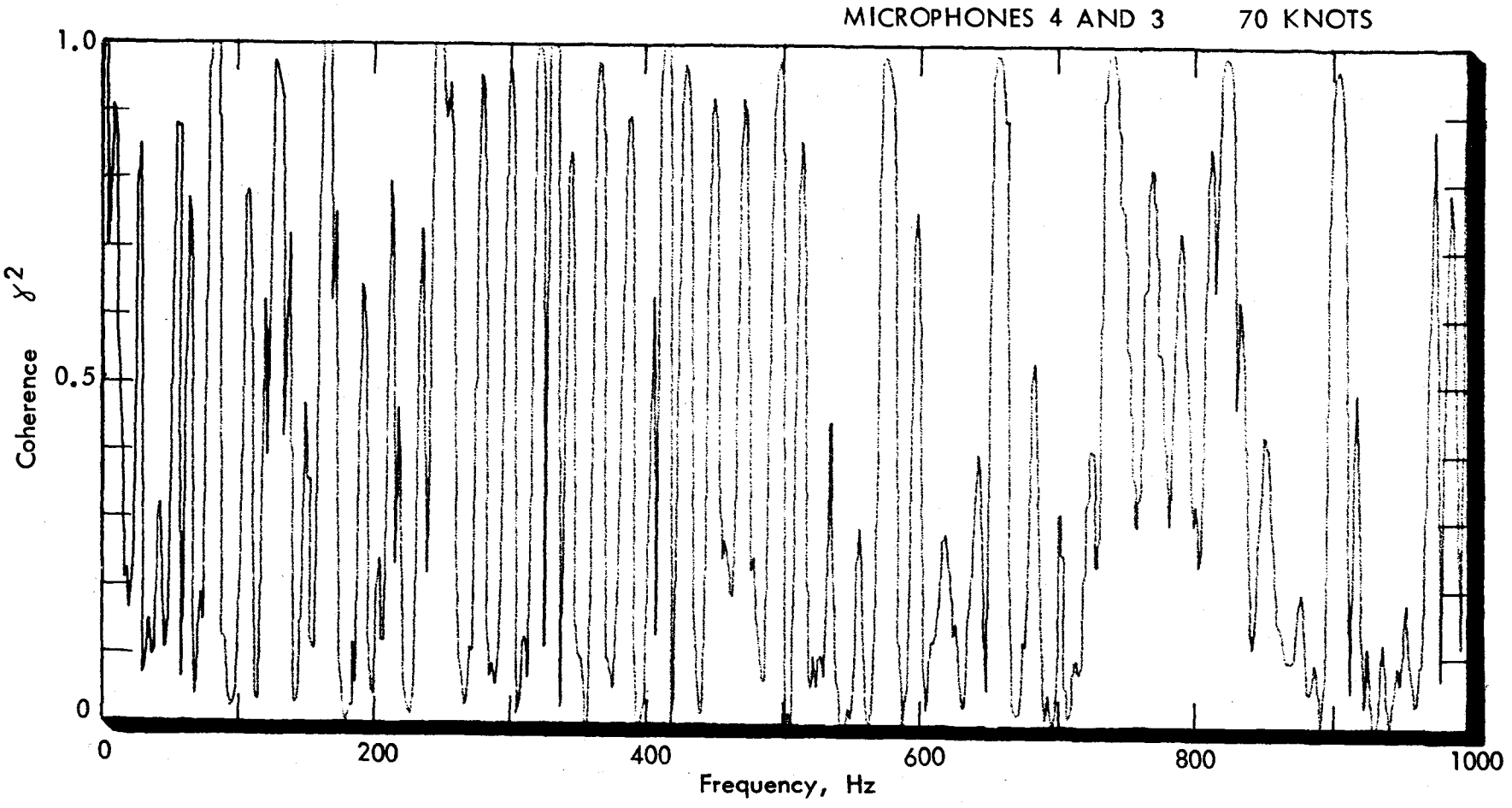

FIGURE D3. COHERENCE SPECTRUM FOR MICROPHONES 4 AND 3. 70 KNOTS TAXI RUN

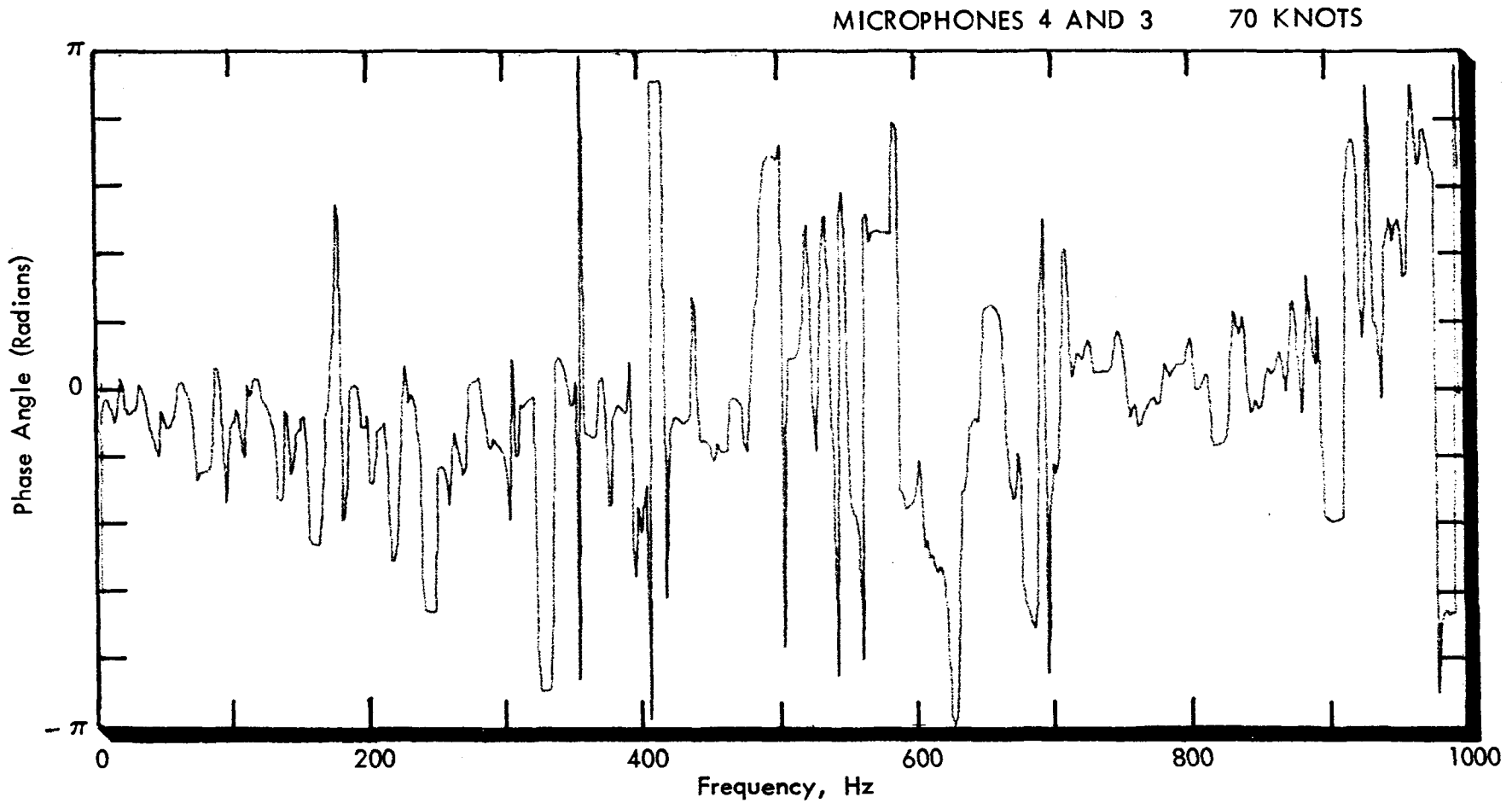

FIGURE D4. PHASE SPECTRUM FOR MICROPHONES 4 AND 3. 70 KNOTS TAXI RUN

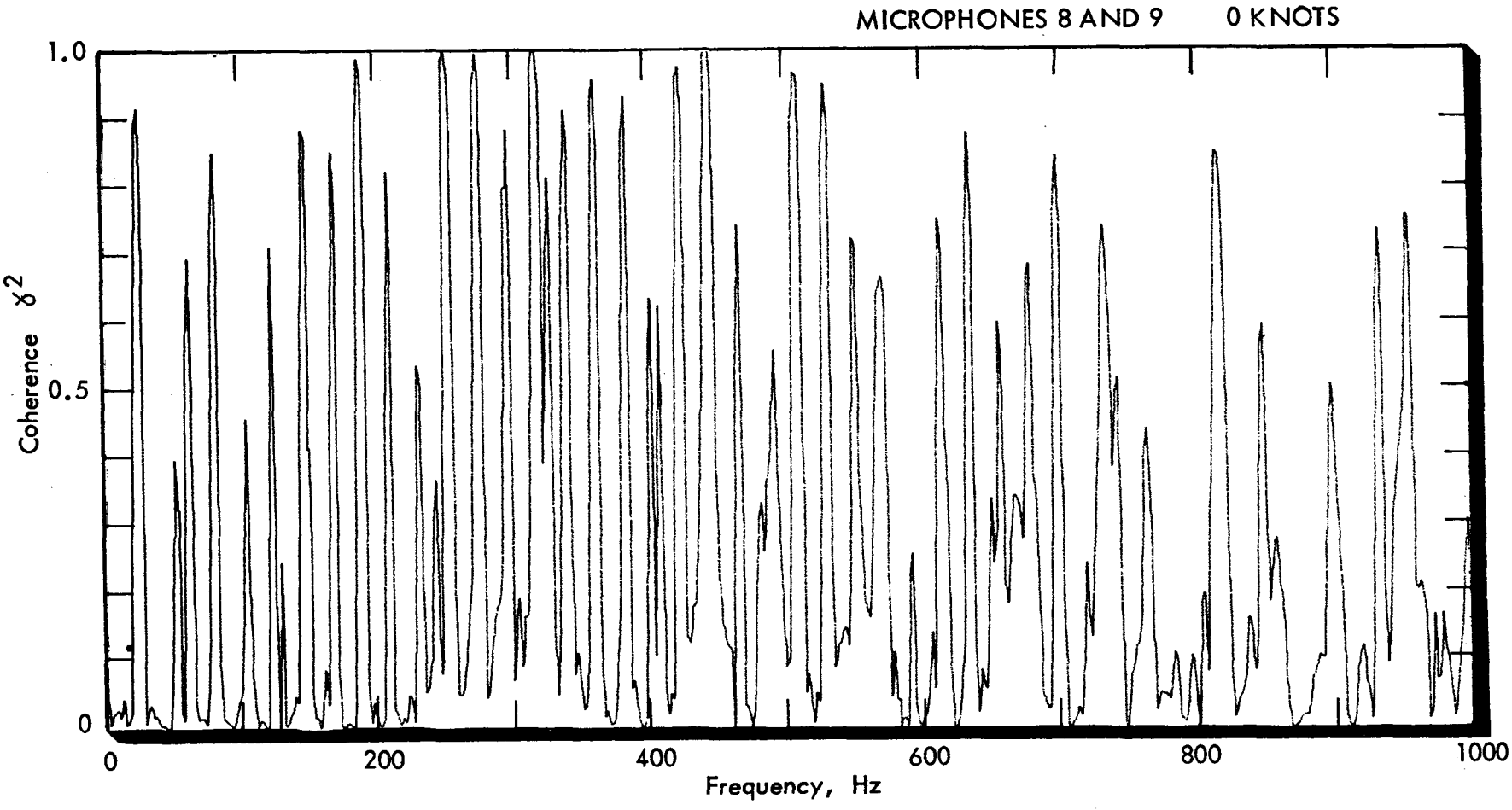

FIGURE D5. COHERENCE SPECTRUM FOR MICROPHONES 8 AND 9. STATIC RUN

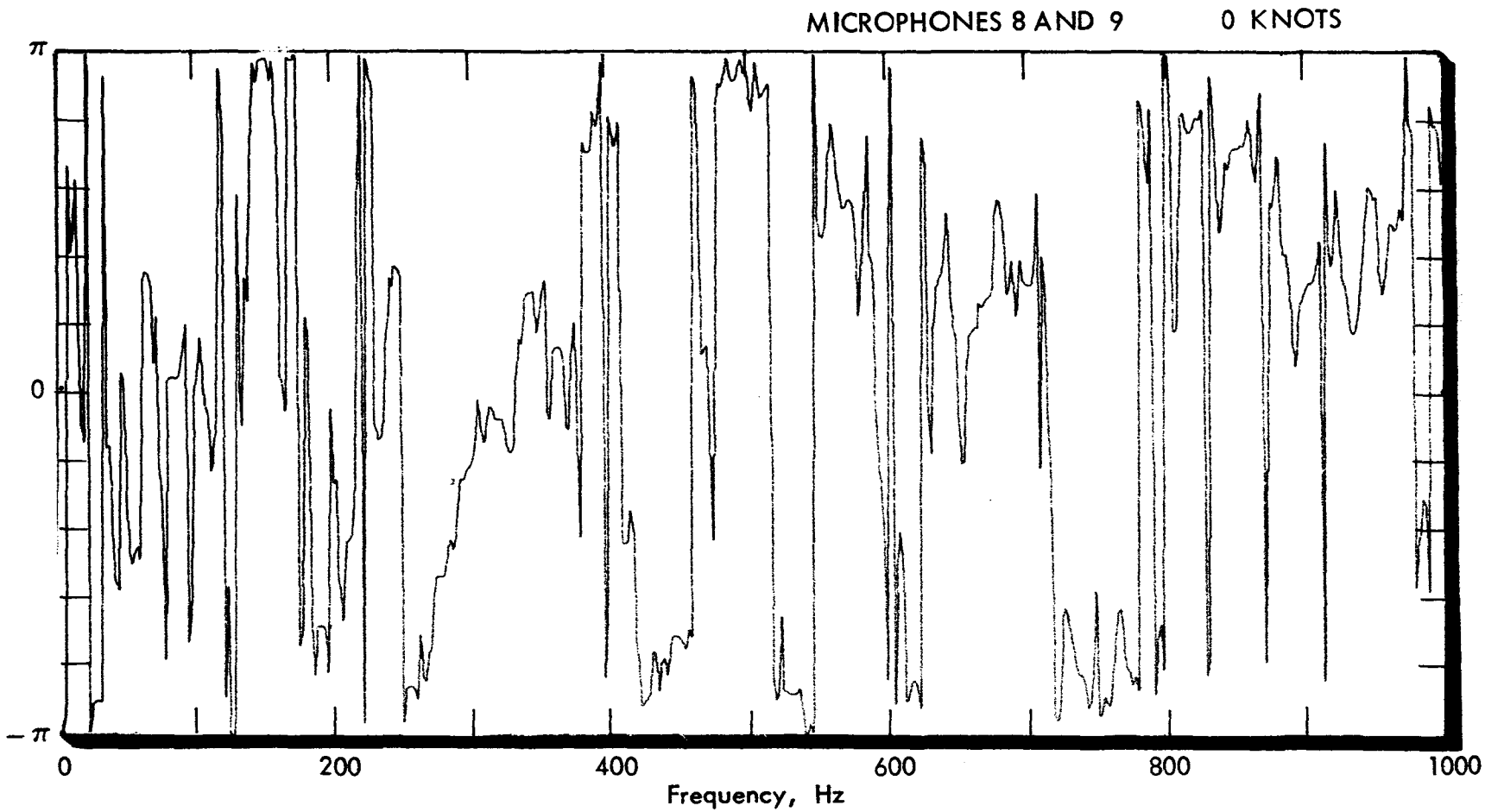

FIGURE D6. PHASE SPECTRUM FOR MICROPHONES 8 AND 9. STATIC RUN

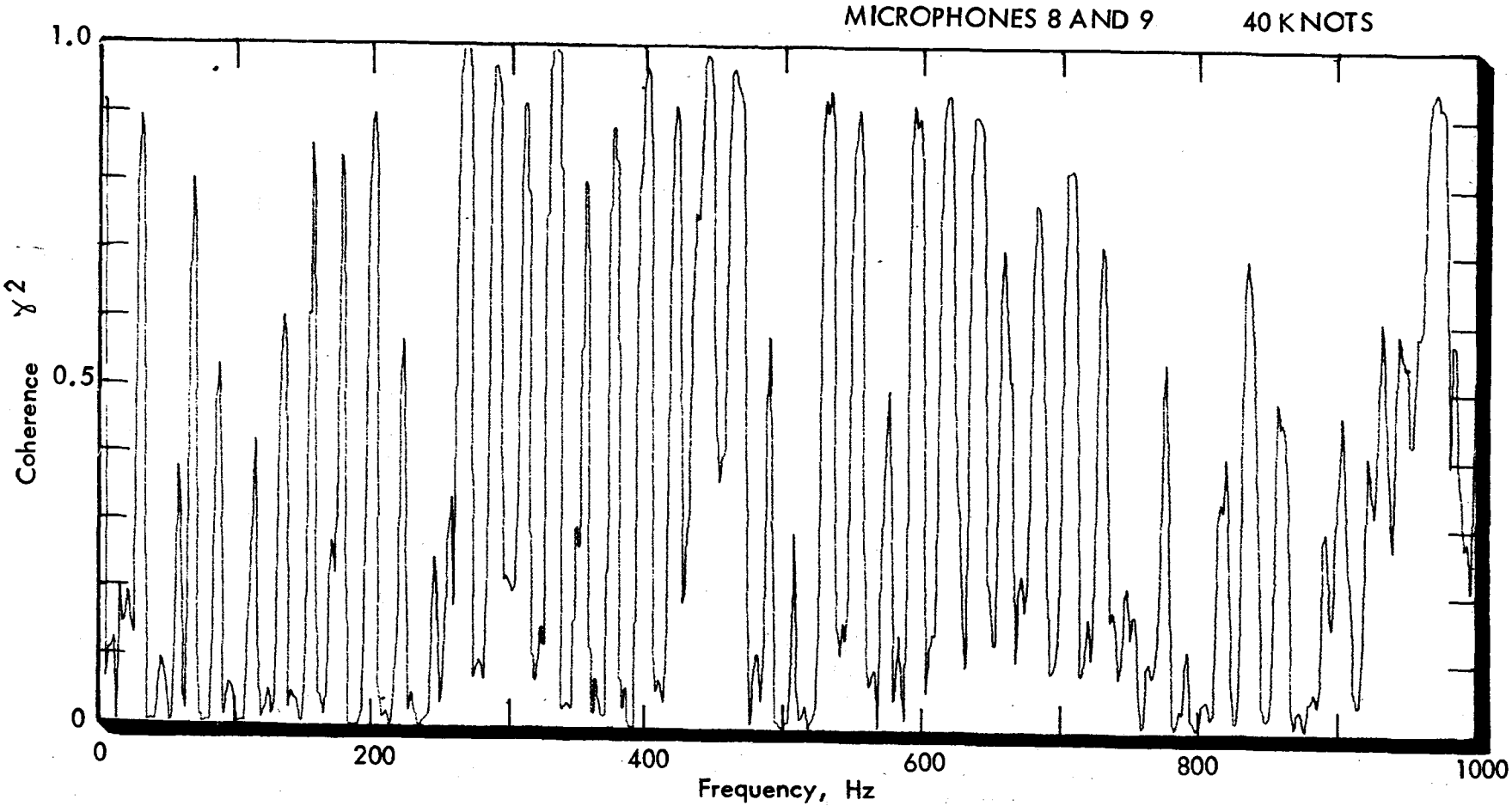

FIGURE D7. COHERENCE SPECTRUM FOR MICROPHONES 8 AND 9. 40 KNOTS TAXI RUN

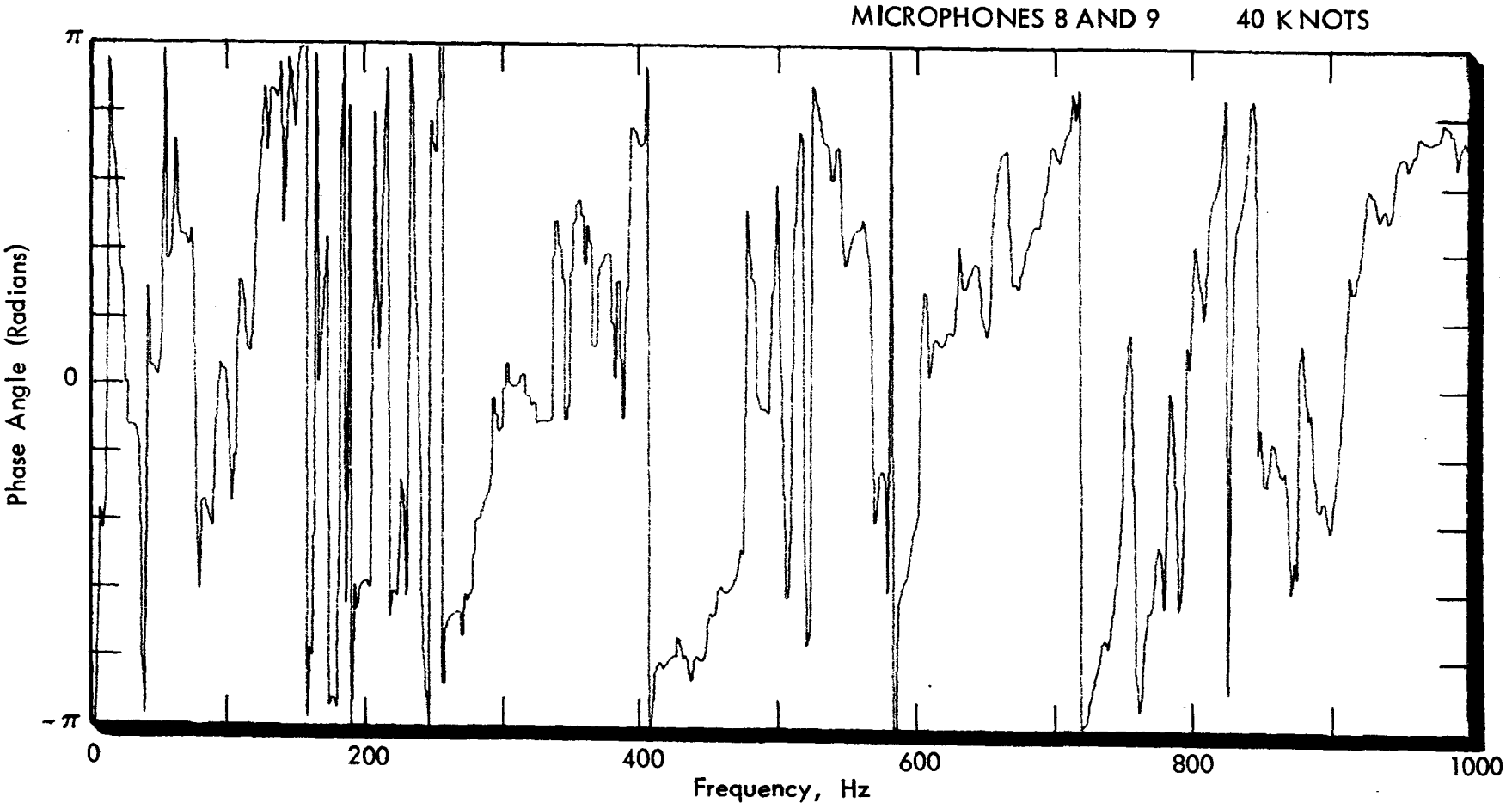

FIGURE D8. PHASE SPECTRUM FOR MICROPHONES 8 AND 9. 40 KNOTS TAXI RUN

APPENDIX E

CABIN INTERIOR SOUND LEVELS

E.1 Introduction

This report and reference 2 present an evaluation of propeller noise levels measured during two test series on an Aero Commander airplane. The main emphasis of the tests and of the data presentation has been the evaluation of sound levels measured on the exterior of the fuselage on the right-hand side of the airplane. The tests did, however, include one microphone location inside the cabin, and it is the purpose of this appendix to present an evaluation of the interior sound levels measured during the two test series.

For convenience in the discussion that follows, the first test series, discussed in [2], will be referred to in this appendix as Test Series I; and the second test series, discussed in the main body of this report, as Test Series II. Measurements in Test Series I were all associated with static operation of the airplane, whereas Test Series II contained both static and taxi operations. Interest in Test Series II is, however, directed toward the taxi data because the static results are investigated in much greater detail in Test Series I and because test conditions, particularly with respect to wind velocity, may have caused significant variations in the static test data for Test Series II--as will be discussed later.

Noise levels measured inside a twin-engined airplane, with both engines operating, are highly susceptible to beat effects, and the data for the Aero Commander are no exception. Thus, this appendix considers the interior sound levels from two points of view. First, the time-averaged harmonic sound levels are obtained following the data analysis procedures outlined in Section 3.1. A frequency resolution of 2 Hz was used over the

frequency range from zero to 2 kHz. Secondly, time histories were obtained for the sound levels of several of the propeller harmonics so that the beat frequencies and peak-to-trough ratios could be measured.

E.2 Magnitude of Propeller Blade Passage Tones

Some of the data for the time-averaged interior sound levels of the propeller blade passage tones have been presented in [2] for a frequency resolution of 4 Hz and in Table A-3 of this report. However, the opportunity is taken in this appendix to collect together all the time-averaged interior sound level data with a common frequency resolution of 2 Hz. Thus, Table E-1 presents interior sound levels measured under static conditions (Test Series I) for several engine operating conditions. Similarly, Table E-2 contains corresponding data for Test Series II, where now the engine operating condition is a constant 2600 rpm but the airplane taxi speed is varied. (Three repeat static runs are also available in Test Series II.)

Special notes in Tables E-1 and E-2 identify propeller harmonic levels that are influenced by engine exhaust noise. The harmonics are those that have frequencies very close to engine exhaust harmonic frequencies associated with high noise levels. (Roughly these occur at multiples of 3 of the cylinder firing frequency.) Figure E.1 presents a typical narrowband spectrum of the interior noise levels measured at microphone location 11 and shows the relative locations of engine and propeller harmonic contributions.

Consider first the sound levels listed in Tables E-1 and E-2 for the static, 2600 rpm conditions. It is readily apparent that there are differences between the data for the two test series.

TABLE E.1 SOUND LEVELS OF PROPELLER HARMONICS MEASURED AT INTERIOR MICROPHONE LOCATION #11: TEST SERIES I (STATIC OPERATION) (2Hz Resolution)

Harmonic Order	Sound Pressure Level dB re $20\mu N/m^2$								
Engine RPM	1700 rpm		2100 rpm				2400	2600 rpm	
Run No.	7	8	1	4†	5	6	2	3	4
Engine	Stbd	Stbd	Both	Port	Stbd	Stbd	Both	Both	Both
1	91.3	90.6	101.4	101.3	93.9	93.8	104.4	105.1	106.0
2	85.8	86.9	98.0	87.9	98.3	96.9	98.4	100.1	100.2
3	88.3*	88.1*	88.3	81.0	88.2	89.3	92.2	92.8	93.0
4*	81.5	80.6	84.8	81.5	76.4	81.9	89.9	86.1	88.7
5	75.4	71.6	89.1	73.8	85.4	84.0	82.3	93.6	94.2
6	85.1	81.8	88.4	71.4	85.0	83.5	86.5	88.6	88.8
7*	75.0	75.2	84.4	73.3	82.2	81.6	80.1	88.1	88.4
8	76.1	76.9	78.7	60.8	74.2	75.1	82.0	80.5	81.6
9	73.0	71.7	78.7	62.0	75.8	76.7	73.2	76.2	76.6
10*	69.6	65.5	71.5	60.3	67.0	71.8	72.9	73.4	74.9
11*	68.5	69.9	71.6	65.2	69.4	71.7	70.3	74.5	74.5
12	66.1	66.4	69.2	63.2	63.0	68.7	70.2	70.5	73.2
13	60.2	56.6	65.9	60.6	66.4	69.4	67.2	67.7	70.1
14*	60.3	58.9	62.7	63.0	63.7	67.3	64.7	66.6	68.1
15	56.5	58.8	60.7	56.2	56.6	60.3	62.4	70.5	68.2
16	60.6	55.5		54.8	56.6	59.8	61.6	70.6	70.6
17*	58.2	55.2		53.8	55.0	59.4	63.7	64.2	65.8
18	50.9	52.1		55.9	55.2	56.2	60.7	61.1	63.8
19	50.8	50.0			56.1	57.3	60.3	65.1	64.6
20	48.4	51.2			57.7	58.7	61.9	61.4	62.2
Overall	94.8	94.3	103.6	101.6	100.3	99.6	105.8	106.9	107.6

*These data points are contaminated by exhaust noise. Contamination may occur at other harmonics, particularly those of higher order.
†This is Run 4 in the LRC numbering sequence (see Table 1 [2]).

TABLE E.2 SOUND LEVELS OF PROPELLER HARMONICS MEASURED AT INTERIOR MICROPHONE LOCATION #11: TEST SERIES II (2600 RPM, STATIC AND TAXI OPERATION)(2 Hz Resolution)

Harmonic Order	Sound Pressure Level dB re $20\mu N/m^2$					
Run	5**	6**	7**	5	6	7
Taxi Speed	0	0	0	40	55	70
1	105.0	104.9	105.7	104.6	104.1	102.6
2	101.6	103.4	100.0	99.8	99.5	98.2
3	96.3	96.4	89.3	93.1	90.5	89.4
4*	84.2	85.9	96.4	84.5	83.5	80.7
5	84.4	88.1	93.7	85.2	84.0	81.7
6	82.3	79.8	89.8	77.9	74.5	79.6
7*	81.7	81.1	83.9	79.5	80.4	74.9
8	73.6	72.8	79.6	66.1	65.7	69.1
9	72.6	69.8	73.0	61.3	59.2	63.9
10*	71.7	69.3	69.4	67.1	67.9	57.4
11*	73.4	72.2	72.2	63.1	60.8	61.7
12	73.0	70.1	68.5	62.1	61.2	58.0
13	72.0	70.0	68.7	60.8	57.9	57.6
14*	69.1	67.7	69.3	56.4	55.5	58.3
15	66.3	62.3	68.8	52.5	52.4	56.7
Overall	107.1	107.7	107.5	106.2	105.6	104.2

*These data points are contaminated by exhaust noise. Contamination may occur at other harmonics, particularly those of higher order.

**This static run precedes the taxi run of the same numerical designation.

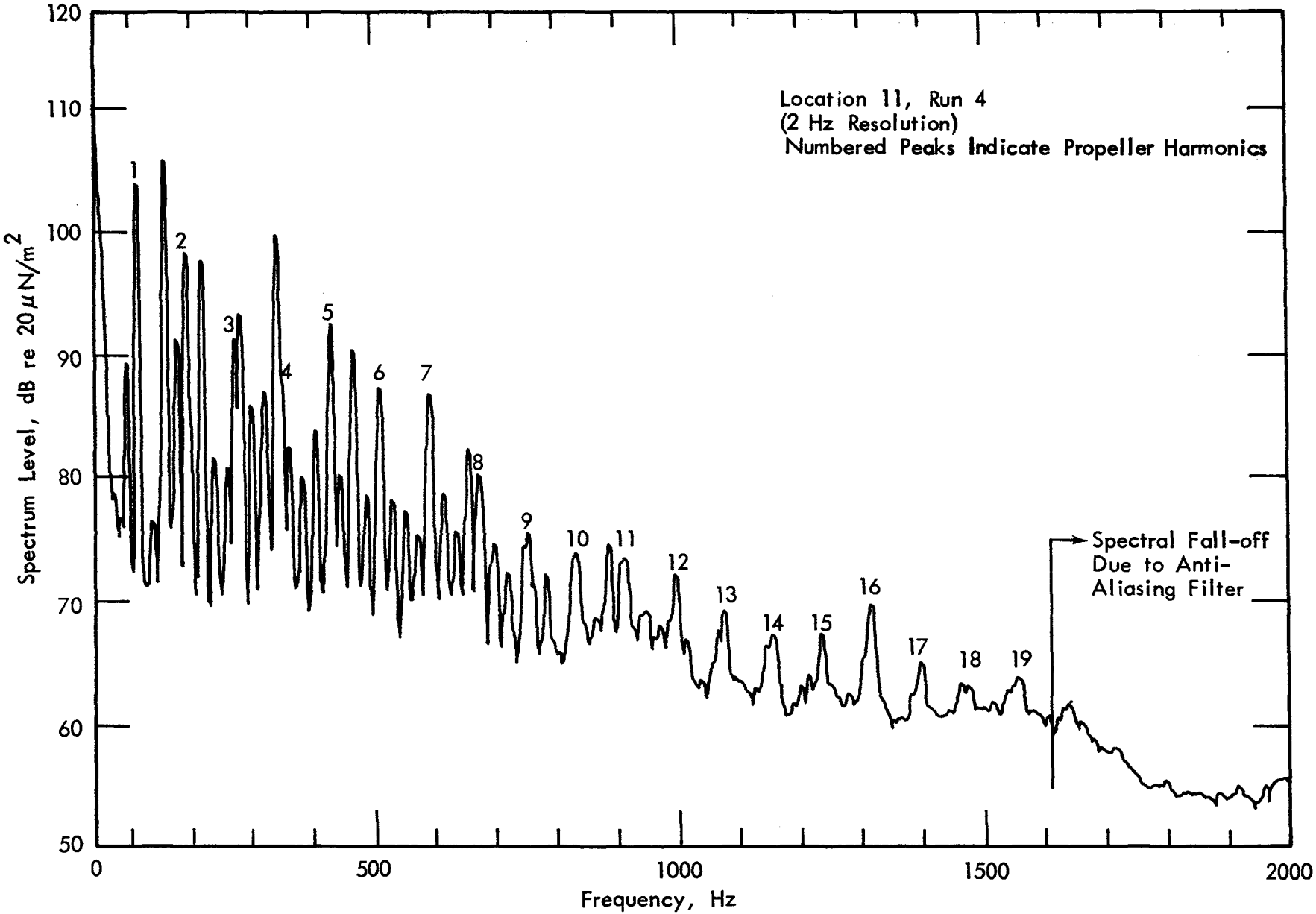

FIGURE E1. NARROWBAND PRESSURE SPECTRUM AT MICROPHONE LOCATION 11, TEST RUN 4

For example, Table E-3 compares average harmonic levels for the two test series, and it is seen that there are differences of up to 6 dB between the two sets of data. Furthermore, inspection of Tables E-1 and E-2 shows that in some cases harmonic levels vary by ±5 dB or more during Test Series II, but the variations are no more than ±1 dB for Test Series I. It is reported by private communication that during Test Series I the local wind speeds were less than 2.6 m/s (5 kts), but that wind speeds of up to 10.3 m/s (20 kts) were measured during Test Series II. Also, during the later tests the orientation of the airplane relative to the wind direction varied from run to run for the static tests as the measurements were made at convenient time periods prior to each taxi run. As inflow turbulence is a significant factor in determining propeller noise levels during static tests, the variability in static test data for Test Series II is not surprising.

Interior noise levels measured during the taxi test show some variability, but this is generally in the form of a decrease in level as taxi speed increases as is shown in Figure E.2. Inflow turbulence effects have much less importance when there is forward motion of the airplane, and, consequently, the wind should have a small influence on sound levels during taxi conditions.

Figure E.2 also contains data for microphone location 5 which was used as a reference measurement for the microphone array on the exterior of the fuselage. For the lowest-order harmonics, the interior and exterior sound levels follow approximately the same trend with forward speed, but at higher orders the sound levels measured by the interior microphone fall off much more rapidly than do exterior levels at microphone location 5 as forward velocity increases. As has been shown in Figure 7, the harmonic noise levels at location 5 show only a small reduction with forward

TABLE E-3. AVERAGE PROPELLER HARMONIC SOUND LEVELS FOR INTERIOR MICROPHONE LOCATION #11: STATIC CONDITION, 2600 RPM (2 Hz Resolution)

Harmonic Number	Average Harmonic Sound Level (dB)	
	Test Series I	Test Series II
1	105.6	105.2
2	100.2	101.7
3	92.9	94.0
4*	87.4	88.8
5	93.9	88.7
6	88.7	84.0
7*	88.3	82.2
8	81.1	75.3
9	76.4	71.8
10*	74.2	70.1
11*	74.5	72.6
12	71.9	70.5
13	68.9	70.2
14*	67.4	68.7
15	69.4	65.8

*These data points are contaminated by exhaust noise. Contamination may also occur at other harmonics, particularly those of higher order.

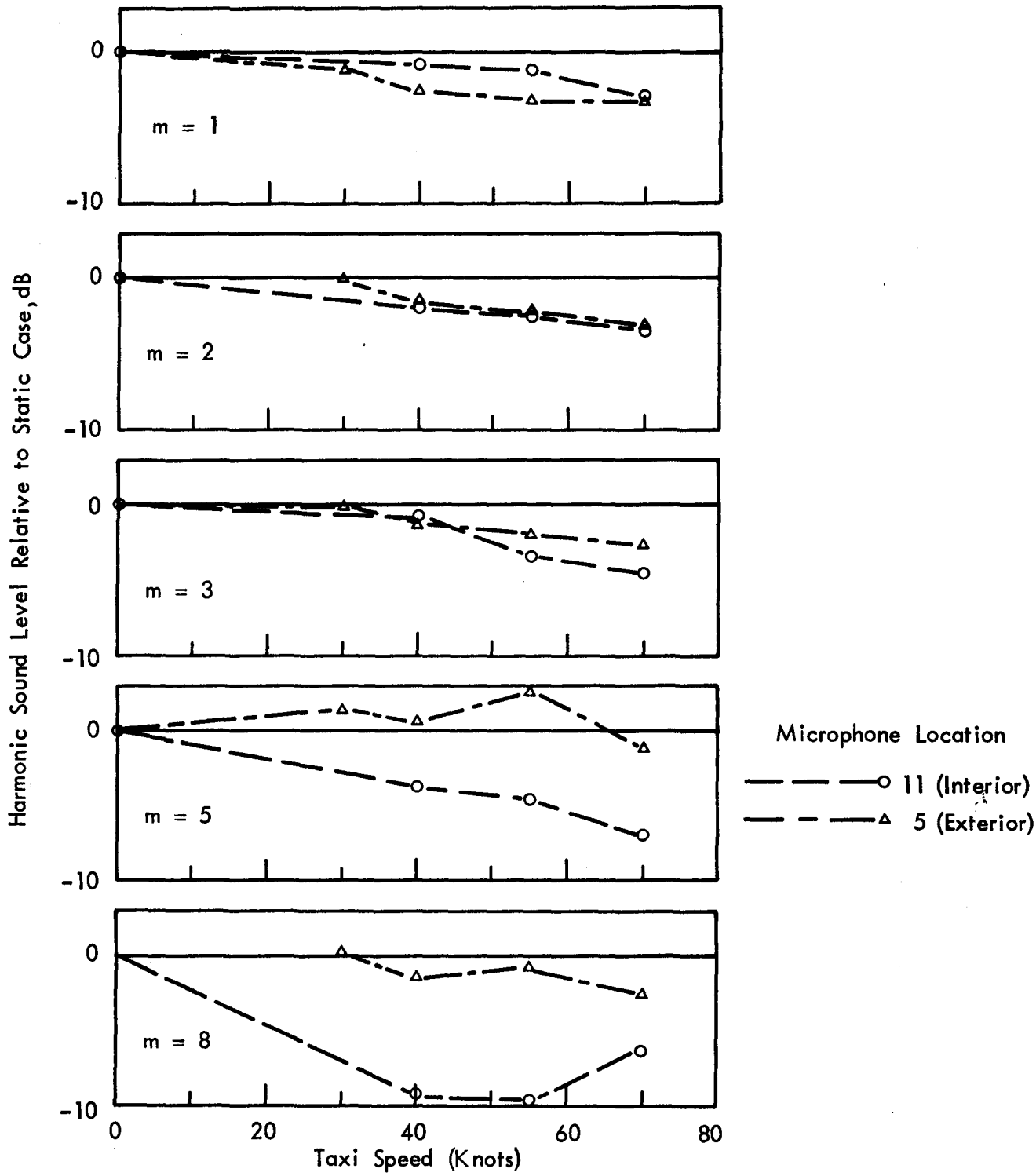

FIGURE E2. VARIATION OF PROPELLER HARMONIC SOUND LEVELS (INTERIOR AND EXTERIOR) WITH TAXI SPEED

motion. In contrast, Figures 5 and 6 show that exterior noise levels measured at locations fore and aft of the propeller plane of rotation decrease markedly as forward speed increases. Thus, the data trend in Figure E.2 suggests that the interior sound levels at location 11 are not determined solely by the high exterior sound levels that occur in the plane of rotation of the propeller.

Although the concept of noise reduction across the fuselage sidewall is difficult to apply in the present circumstances, it is interesting to consider the difference between the sound levels measured at exterior microphone location 5 and interior microphone location 11. Data in this form are shown in Table E-4 where it is seen that the difference appears to be essentially independent of harmonic order (or frequency). There is a general trend, which is to be expected, in that the difference in levels is smaller when both engines are operating than it is when only the starboard engine is running. This is discussed further in Section E.4.

E.3 Beats

E.3.1 Data Analysis Procedures

The general procedure followed in determining the time histories of the sound levels at several propeller blade passage frequency harmonics was similar to that used in determining the time-averaged levels, with the exception that the SD 360 Digital Signal Processor was not operated in a time-averaging mode. Instead, the time-varying level of a given harmonic was plotted using a Bruel and Kjaer Type 2306 level recorder operated in the DC-linear setting. Time history plots were obtained using a paper speed of 3 mm/s and a writing speed of 250 mm/s. This combination of paper and writing speeds was adequate to follow the data signals for the beat frequencies encountered in the data reduction.

TABLE E-4. DIFFERENCE BETWEEN EXTERIOR SOUND LEVELS (LOCATION #5) AND INTERIOR SOUND LEVELS (LOCATION #11) FOR PROPELLER HARMONICS MEASURED IN TEST SERIES I (2 Hz Resolution)

Harmonic	ΔSPL = (Exterior Level - (Interior Level) dB								
Engine RPM	1700 rpm		2100 rpm				2400	2600	
Run No.	7	8	1	4†	5	6	2	3	4
Engine(s)	Stbd	Stbd	Both	Port	Stbd	Stbd	Both	Both	Both
1	30.5	30.5	26.3		33.2	33.0	26.2	28.0	26.8
2	29.4	28.0	22.0		22.0	23.1	24.4	24.6	24.4
3	23.4*	22.3*	28.0		28.6	26.8	27.5	29.4	28.6
4*	26.1	26.4	30.0		36.1	30.5	25.8	33.4	29.8
5	29.1	31.1	21.7		24.3	24.7	30.1	22.9	21.5
6	18.3	20.4	18.2		20.9	22.0	22.9	25.6	24.2
7*	22.2	21.0	20.8		21.6	22.9	27.5	23.1	22.5
8	22.0	18.4	21.8		25.9	25.6	20.1	27.3	25.8
9	17.9	20.5	18.4		22.5	21.1	27.8	28.6	28.1
10*	20.5	22.7	23.7		27.9	25.0	25.6	27.1	25.5
11*	16.4	17.5	22.0		25.0	24.9	24.0	25.7	25.6
12	19.4	20.2	21.5		30.4	25.8	24.3	26.1	24.9
13	23.7	27.0	24.0		24.4	21.9	27.0	29.0	26.4
14*	22.3	26.3	25.6		26.6	24.7	26.2	25.9	25.1
15	23.7	24.5	27.4		33.2	31.4	28.1	22.3	25.1

*These data points are contaminated by engine exhaust noise. Contamination may also occur at some of the other higher order harmonics.

†This is Run 4 in the LRC numbering sequence (see Table 1 [2]) No data are presented because the Starboard engine was not operating.

Initial data reduction for a particular run was performed using 2 Hz frequency resolution on the SD 360. This enabled the beat frequencies for the run to be estimated for the different harmonics of interest. The frequency resolution was then adjusted as necessary in order to keep the effective filter bandwidth greater than the beat frequency. Failure to maintain this criterion would result in the attenuation of one or both signals causing the beat, thereby altering the beat characteristics. Usually, application of the criterion resulted in the frequency resolution being changed to 4 Hz or 8 Hz. This increase in effective filter bandwidth, however, posed two other problems. First, as bandwidth was increased signal contamination due to engine exhaust noise could also increase, thereby decreasing the effective signal-to-noise ratio and possibly introducing beating effects between engine exhaust and propeller harmonics. Second, since the filter center frequency is dictated by the SD 360 and cannot be controlled independently, the harmonic frequency of interest did not always fall close to the center of the wider filter bandwidth. This resulted in data reduction conditions that were not optimum.

Figures E.3 and E.4 contain time histories obtained for Run 2 of Test Series I, using different frequency resolution settings on the SD 360. Figure E.3 presents four time histories for the first-order harmonic and Figure E.4 for the second-order harmonic. The figures show that when the beat frequencies are relatively high, the difference between the peak and trough levels increases as filter bandwidth increases. This is particularly clear in Figure E.4. At lower beat frequencies there is no significant change in peak and trough levels. The two lowest traces in Figure E.3 are both associated with a frequency resolution of 8 Hz, but because of the predetermined center frequencies one

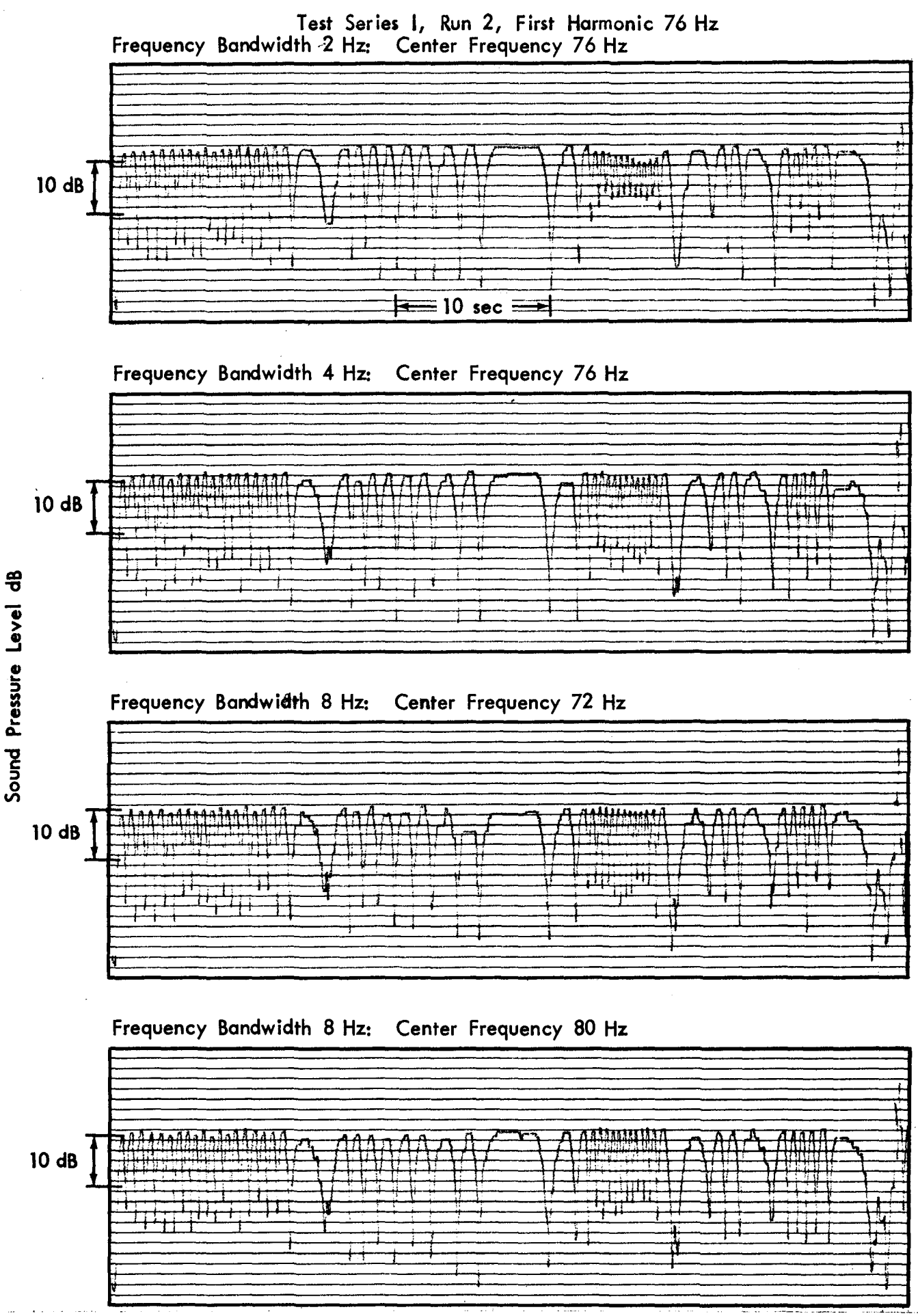

FIGURE E3. EFFECT OF FILTER BANDWIDTH ON TIME HISTORY OF INTERIOR SOUND LEVEL (FIRST HARMONIC)

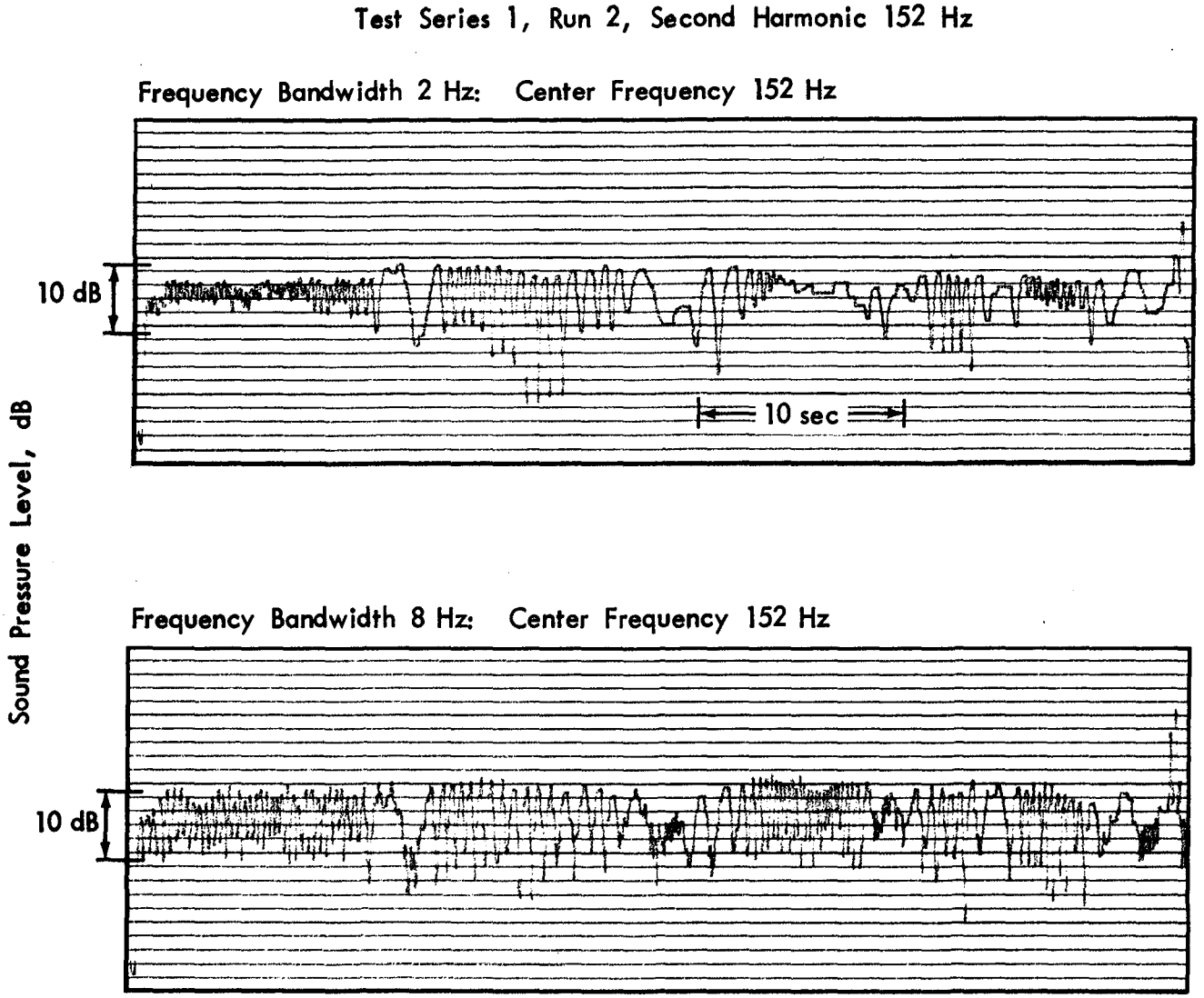

FIGURE E4. EFFECT OF FILTER BANDWIDTH ON TIME HISTORY OF INTERIOR SOUND LEVEL (SECOND HARMONIC)

filter bandwidth is centered at 72 Hz and the other at 80 Hz. The optimum center frequency is 76 Hz. Comparing the two lower traces with the two upper traces shows that the non-optimum center frequencies result in slight attenuation of some of the beat peak levels.

E.3.2 Data Presentation

Before considering the time histories in detail, it can be demonstrated that the variations in harmonic sound level observed in the time histories are due to beating between the sound pressures generated by the two propellers. Figure E.5 compares sound level time histories recorded at the interior microphone location for twin-engine operation and for conditions where only one engine (port or starboard) was operating. During two-engine operation, the sound level shows almost periodic fluctuations whereas for one-engine operation the sound level is almost constant.

The frequency of the beats observed at the cabin microphone location is quite arbitrary since it depends on the accuracy to which the rotational speeds of the engines can be synchronized and on the relative stability of the engine rotational speeds. Figure E.6 compares time histories of the first-order harmonic for four runs of Test Series I. In all cases the traces show the presence of beats, but in only one case does the beat frequency stay almost constant throughout the 30-second recording period. In the other three cases the beat frequencies stabilize for periods up to 10 seconds but then shift to a lower or higher frequency before changing yet again.

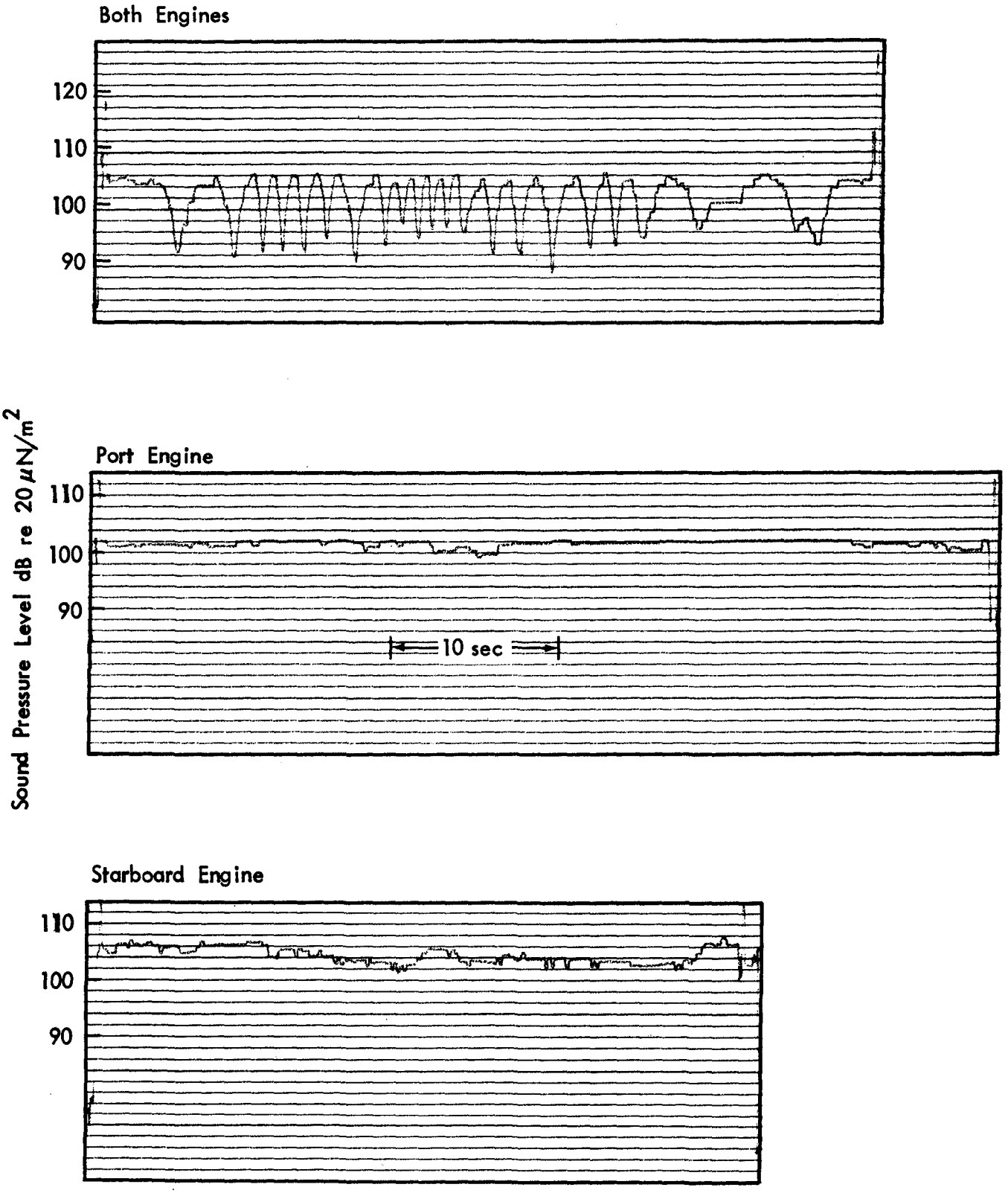

FIGURE E5. COMPARISON OF CABIN NOISE TIME HISTORIES FOR SINGLE AND TWIN-ENGINE OPERATION (PROPELLER FIRST HARMONIC, TEST SERIES I, 2100 RPM)

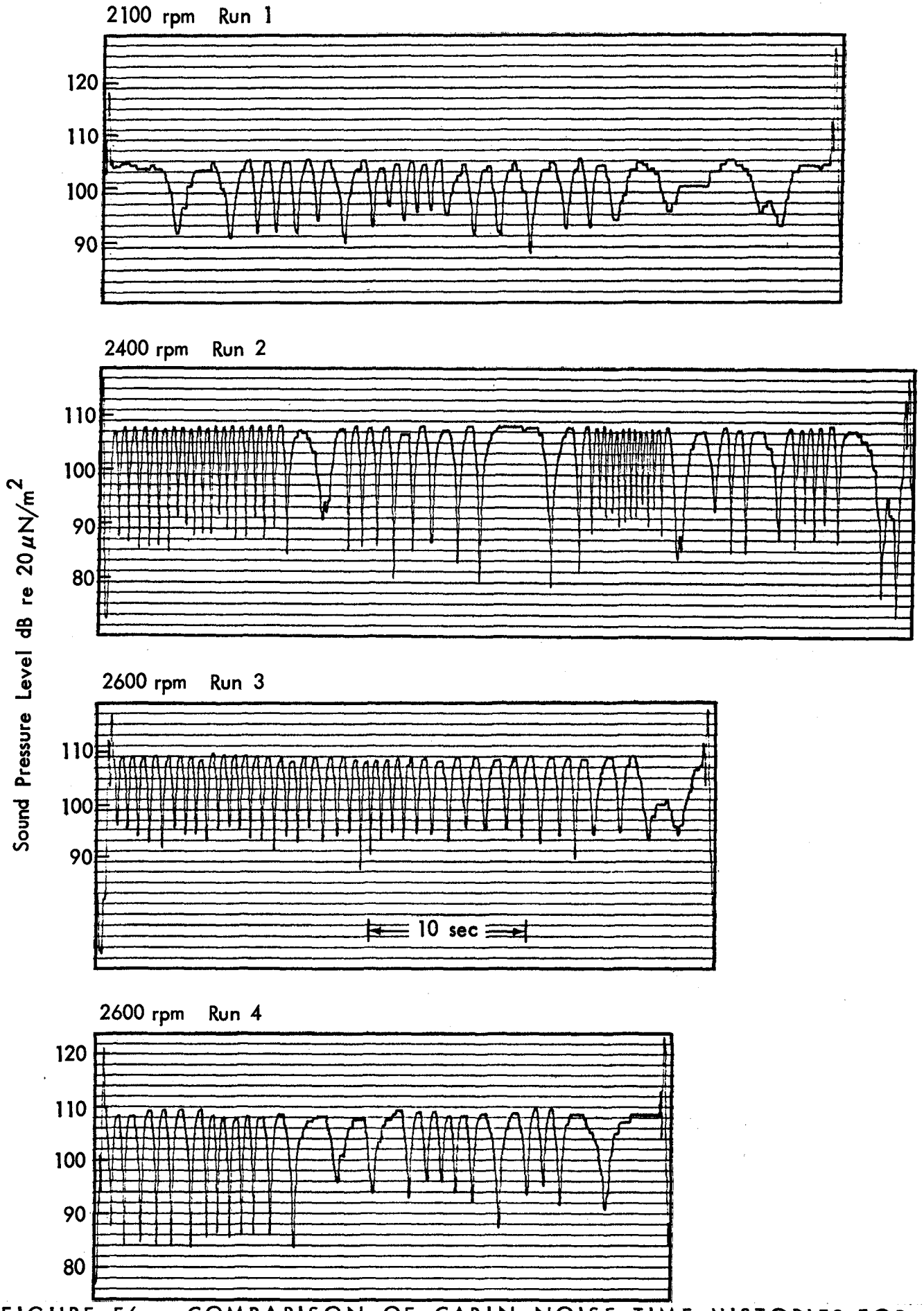

FIGURE E6. COMPARISON OF CABIN NOISE TIME HISTORIES FOR PROPELLER FIRST HARMONIC AT DIFFERENT ENGINE RPM (TEST SERIES I)

Similar patterns are observed for the second harmonic and sometimes for higher-order harmonics (Figure E.7) with the exception that the beat frequency increases in proportion to harmonic order. Figure E.7 also shows the general randomness of the time history as harmonic order increases. The ability to detect a significant beat frequency rapidly diminishes as harmonic order increases, as is to be expected with the rapid decrease in sine-wave-to-noise ratio. Values of this ratio were not measured for the interior microphone location because of the presence of the beats. However, data for exterior microphone locations can be used as a guide. Data in Table 5 of this report and [2] show that for static conditions large values (greater than 3, say) of the sine-wave-to-noise ratio generally occur only for the three lowest-order harmonics. When there is forward motion, harmonics m = 4 and 5 may be included within this category. However, data for harmonic of order 4 suffer from the closeness of an exhaust harmonic with a high noise level, and the data have thus been excluded from the present discussion. Thus, time histories are presented in this appendix for harmonics of order 1, 2, 3, and 5 only.

The selected time histories were inspected to determine the maximum beat frequency for each run and the maximum and minimum sound levels associated with the beat. It is apparent from Figure E.7 that sound levels show some variation from cycle to cycle in a given sequence of beats. This is particularly true for the troughs in the time histories because of the sensitivity of the logarithmic plot to small changes in sound levels of the two constituent signals. For present purposes it was deemed adequate to perform visual averaging of the peak and trough sound levels. The resulting sound levels are listed in Table E-5, which in addition includes time-averaged values obtained from Tables E-1

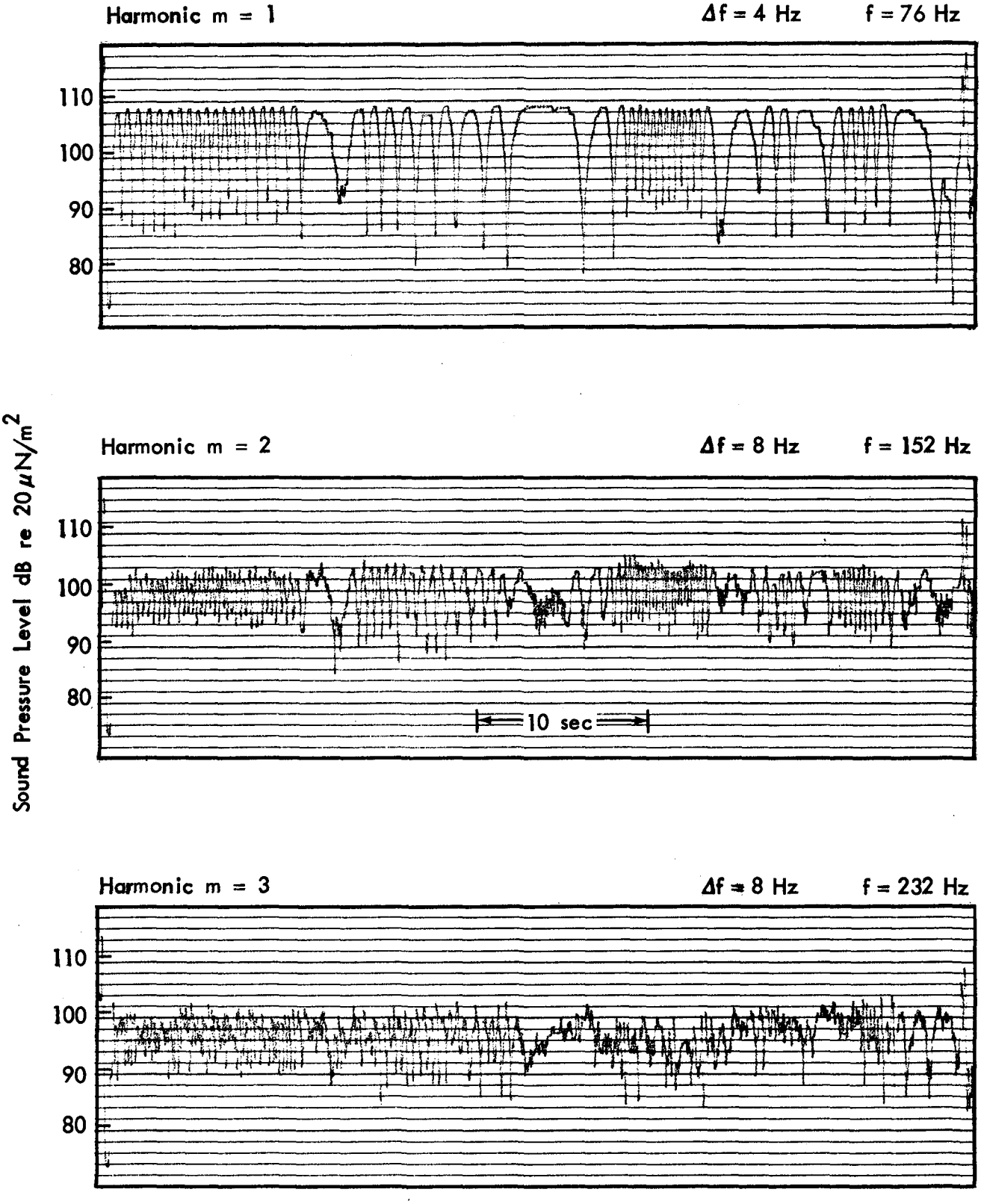

FIGURE E7. TIME HISTORIES OF PROPELLER HARMONIC LEVELS: TEST SERIES I, RUN 2, 2100 RPM

TABLE E-5. BEAT MAXIMUM, MINIMUM, AND AVERAGE SOUND LEVELS

Harmonic Order				1	2	3	5
Test Series Run	Engine rpm	Taxi Speed kts	Measured Parameter	Harmonic Sound Level (dB)			
I/1	2100	0	Average	101.4	98.0	88.3	89.1
			Maximum	105	102	95	-
			Minimum	91	94	85	-
I/2	2400	0	Average	104.4	98.4	92.2	82.3
			Maximum	108	103	101	-
			Minimum	85	92	89	-
I/3	2600	0	Average	105.1	100.1	92.8	93.6
			Maximum	109	105	99*	-
			Minimum	93	90	89*	-
I/4	2600	0	Average	106.0	100.2	93.0	94.2
			Maximum	109	104	97*	-
			Minimum	90	88	84*	-
II(40)	2600	0	Average	105.0	101.6	96.3	84.4
			Maximum	108.5	105	-	-
			Minimum	88	93	-	-
II(55)	2600	0	Average	104.9	103.4	96.4	88.1
			Maximum	108.5	106	-	-
			Average	84	96	-	-
II(70)	2600	0	Average	105.7	100.0	89.3	93.7
			Maximum	109	104	-	98*
			Minimum	94	92	-	90*
II/5	2600	40	Average	103.9	100.5	93.9	85.3
			Maximum	106	103	96	-
			Minimum	76	94	90	-
II/6	2600	55	Average	103.6	99.8	90.7	84.6
			Maximum	106	104	-	90
			Minimum	93	96	-	82
II/7	2600	70	Average	102.4	98.1	89.8	82.2
			Maximum	105	101	93	-
			Minimum	83	88	82	-

*These data may be contaminated by exhaust noise.
( )Number in parentheses indicates taxi speed for test immediately following the static test.

and E-2. Even with the critical review of the time histories described above for the selection of valid beat data, some results in Table E-5 are considered to be of borderline value and an indication is made to this effect.

The maximum beat frequency observed for the first harmonic was measured for each static and taxiing run, and the values are given in Table E-6. It is interesting to note that the maximum beat frequencies are consistently lower for the taxiing case (average maximum frequency = 0.49 Hz) than for the static cases (1.51 Hz).

E.3.3 Discussion

Simple analysis of the beat phenomenon for two sinusoidal signals with close frequencies is instructive in the interpretation of the Aero Commander data. Assume that the two signals p_1, p_2 with different amplitudes P_1, P_2 are given by

$$p_1 = P_1 \sin \omega_1 t$$

and

$$p_2 = P_2 \sin (\omega_2 t + \theta).$$

Then, the combined signal can be written in the form

$$p = P \sin (\omega_1 t + \phi)$$

where $P^2 = P_1^2 + P_2^2 + 2P_1P_2 \cos (\Delta\omega.t + \phi)$.

Thus, amplitude P fluctuates with beat frequency $\Delta\omega = \omega_2 - \omega_1$ between a maximum value of $(P_1 + P_2)$ and a minimum of $|P_1 - P_2|$.

TABLE E-6. MAXIMUM BEAT FREQUENCIES FOR FIRST HARMONIC

Test Series	Aircraft Speed kts	Engine rpm	Frequency of 1st Harmonic Hz	Beat Frequency Hz
I	0	2100	68	1.09
	0	2400	76	2.65
	0	2600	82	1.50
	0	2600	82	1.33
II	0	2600	82	1.18
	0	2600	82	1.29
	0	2600	82	1.50
	45	2600	86	0.30
	55	2600	88	0.63
	70	2600	82	0.55

The difference in sound level between maximum and minimum values of the combined signal will be

$$(\Delta SPL)_1 = 10 \log_{10} \left[\frac{P_1 + P_2}{P_1 - P_2} \right]^2 \quad dB. \qquad (E.1)$$

Obviously, the closer the two original signals are in amplitude, or in sound level, the greater will be the value of $(\Delta SPL)_1$. This is demonstrated in Figure E.8, which plots $(\Delta SPL)_1$ as a function of the difference between the sound pressure levels SPL_1 and SPL_2 of the two original signals.

The time history of P will be in the form of a simple cosine function. When plotted logarithmically, in terms of sound pressure level, the time history shows the typical broad peak and narrow trough pattern observed in the test data.

The time-averaged mean square value of the beat amplitude averaged over several beat periods is $(P_1^2 + P_2^2)/2$. Thus, the difference between peak and time-averaged sound pressure levels is given by

$$(\Delta SPL)_2 = 10 \log_{10} \left[\frac{(P_1 + P_2)^2}{P_1^2 + P_2^2} \right] \quad dB. \qquad (E.2)$$

This simplified analysis will be valid for Aero Commander data only for those harmonics that have values of the sine-wave-to-noise ratio significantly greater than unity.

Equations (E.1) and (E.2) can now be applied to the Aero Commander data to estimate the differences in sound level between the contributions from the two engines and the difference $(\Delta SPL)_2$

between the beat maximum and average sound levels. As an example, take run 2 of Test Series I. For harmonic m = 1, Table E-5 gives $(\Delta SPL)_1$ = 23 dB. From Figure E.8, the difference in sound levels for the contributions from the two propellers is 1.3 dB. Thence, from Eq. (E.2) the predicted difference between maximum and average levels is 3.0 dB and the predicted average sound level is 105.0 dB compared to a measured value of 104.4 dB. Thus, the simple method seems to work reasonably well for the first harmonic which has a very high value of the sine-wave-to-noise ratio. As harmonic order increases and the sine-wave-to-noise ratio decreases, the simple analytical model shows less agreement with measurements. For example, when averaged over the static and taxi runs that provide adequate sine-wave-to-noise ratios, the analytical model overpredicts the harmonic average sound level by about 0.2 dB for m = 1, 1.0 dB for m = 2, 2.7 dB for m = 3, and 2.6 dB for m = 5.

The analytical model has also been used to estimate the differences in sound level contributions from the two propellers. The results for static and taxi run data presented in Table E-5 are shown in Table E-7. It is seen that the predicted differences in level vary considerably from run to run and show some fairly high values. Measured differences for the 2100 rpm condition (runs 4-6 of Test Series I) show similar, or even larger, differences. Thus, the analytical model can be used to obtain an estimate of the difference in contributions from the two propellers,* but some additional validation tests seem warranted.

The maximum beat frequencies measured for the first harmonic of the propeller blade passage frequency have been listed in Table E-6 for each run of interest. Over all runs, the maximum beat frequency is 2.65 Hz for static tests and 0.63 Hz for taxiing

*Note that the beat analysis does not determine which propeller contributes the higher sound level at the measurement location.

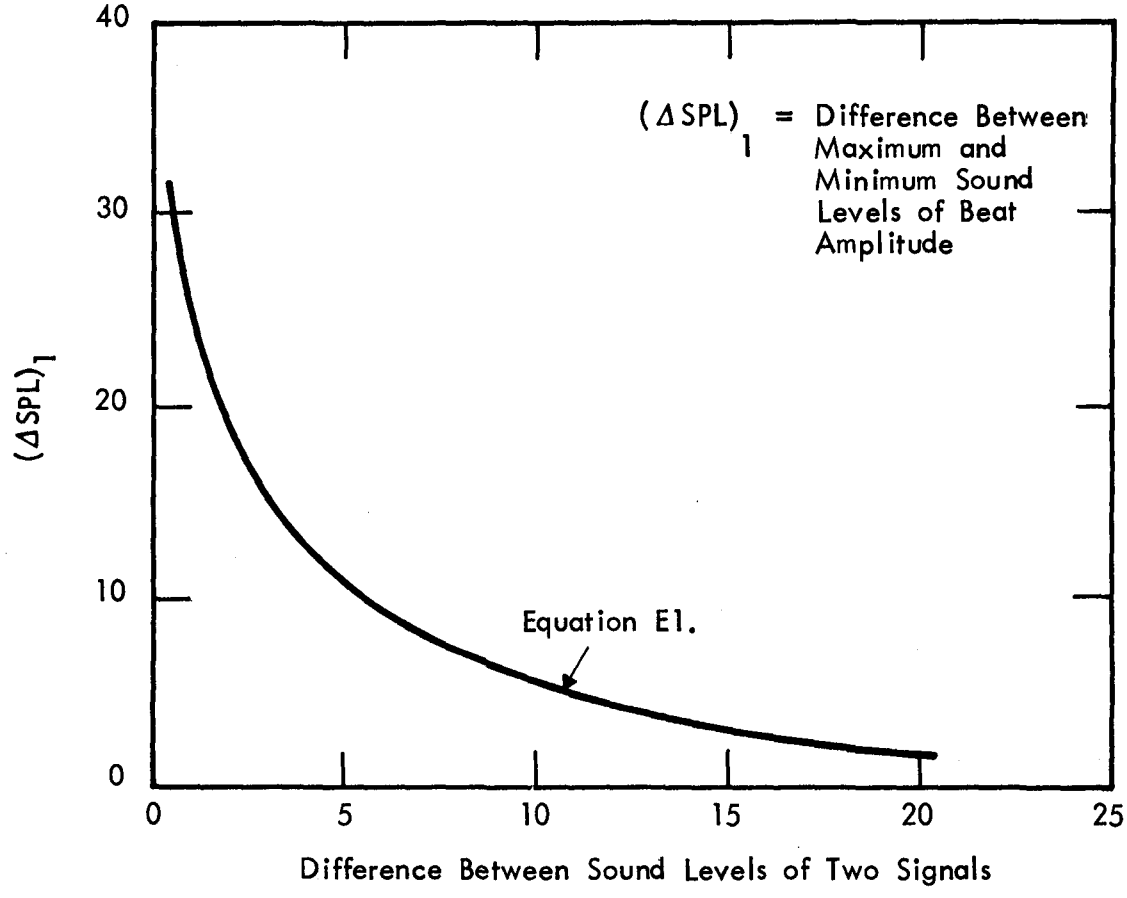

FIGURE E8. PREDICTED RELATIONSHIP BETWEEN DIFFERENCE OF CONSTITUENT SIGNAL SOUND LEVELS AND PEAK-TO-TROUGH DIFFERENCE OF BEAT AMPLITUDE

TABLE E-7. ESTIMATED AND MEASURED DIFFERENCES BETWEEN SOUND PRESSURE LEVEL CONTRIBUTIONS FROM THE TWO PROPELLERS (INTERIOR MICROPHONE LOCATION #11)

Harmonic Order	Predicted Difference* (dB)		Measured Difference (dB) Test Series I, 2100 rpm
	Average Value	Range of Values	
1	2.1	0.5 to 4.0	7.4
2	5.1	2.7 to 7.5	9.7
3	5.8	4.0 to 9.8	7.8
5	7.5	7.5	10.9

*Predicted using simple analytical model and Figure E.8.

tests. These data imply that the engine speeds must have been synchronized to within 0.7 percent for the taxi tests but only 3.5 percent for the static tests.

E.4 Difference Between Exterior and Interior Levels

Table E.4 has presented the difference between sound levels measured by exterior microphone #5 and interior microphone #11, and the discussion in Section E.2 cautioned against the interpretation of these results in terms of noise reduction. In this section the data will be explored a little further, with exterior microphone locations 1 and 8, and the effect of forward velocity being considered also.

The data presented in Table E.4 for the static case are plotted in Figure E.9. The figure distinguishes between data points for single and twin engine operation but there is no readily apparent difference between the results for the two conditions. Detailed analysis for the 2100 rpm case, the only tests for which there are data for simple and twin engine operation, shows, however, that the difference between exterior and interior sound levels is, on the average, 3.0 dB lower (with a standard deviation of 3.3 dB) for two-engine operation than for right-hand engine operation alone. The data points in Figure E.9 are for propeller harmonics only, and cover a range of engine rpm from 1700 to 2600. The contributions from different harmonic orders are not identified separately, although there is an indication at the bottom of the figure of the frequency ranges associated with the five lowest order harmonics. It is seen that there is considerable overlap of the frequency ranges for the higher order harmonics.

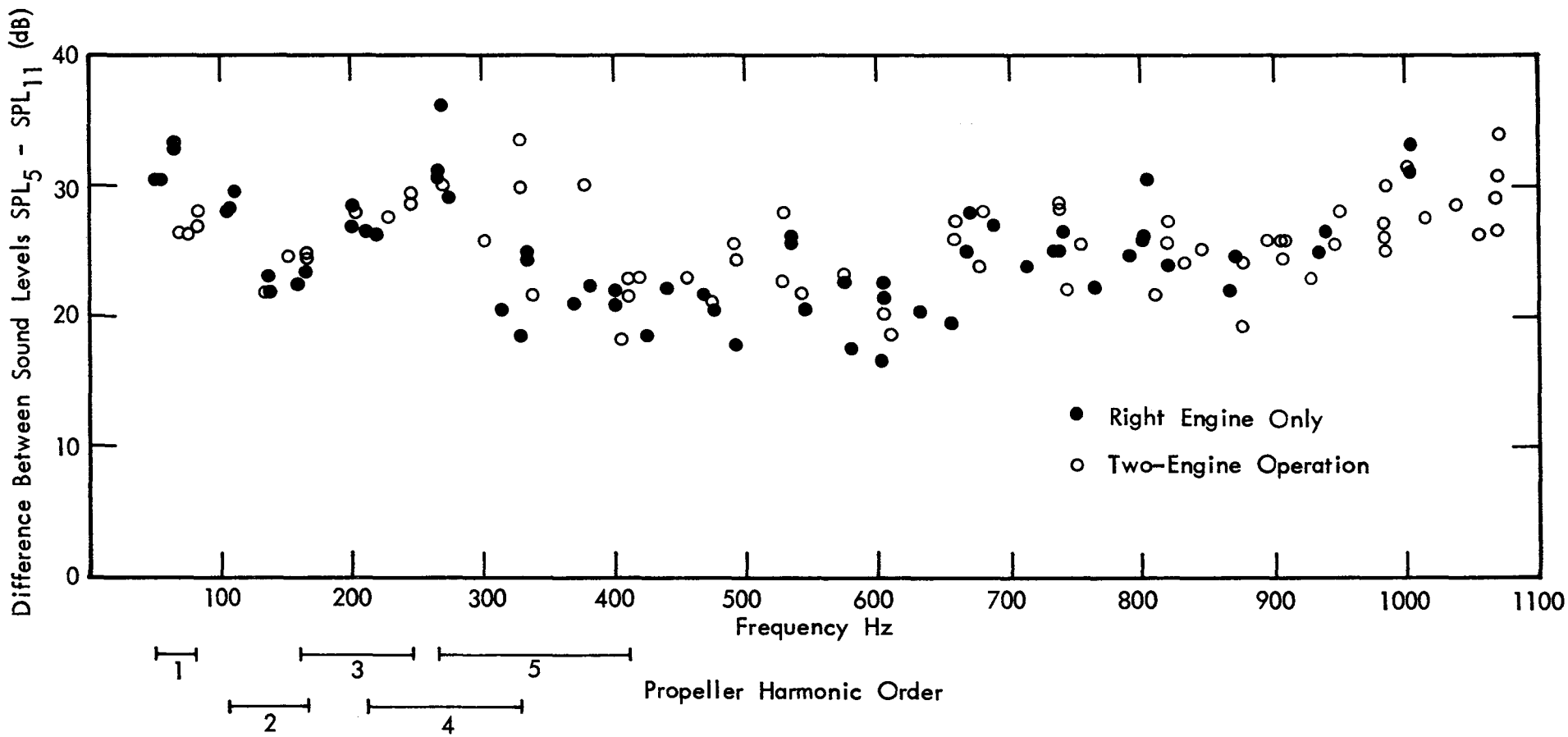

FIGURE E9. DIFFERENCE BETWEEN EXTERIOR (LOCATION #5) AND INTERIOR (LOCATION #11) SOUND LEVELS AT PROPELLER HARMONICS IN TEST SERIES I. VARYING ENGINE RPM.

The data in Figure E.9 show an irregular pattern, particularly at frequencies below 400 Hz., with the spectrum having a series of roughly-defined peaks and troughs. At the higher frequencies there is a general trend of increasing sound level difference with increasing frequency, as would be expected with mass law noise transmission loss. For example, the predicted increase in mass law transmission loss associated with a frequency change from 400 to 1000 Hz is 8.8 dB. This change is similar to that shown by the test data in Figure E.9.

When measurements for microphone pairs (1,11) and (8,11) are included, it is seen that the microphone pair (5,11) is associated with the largest sound level difference at low frequencies and the smallest difference at high frequencies. Figure E.10 compares results for the 2600 rpm test condition, with data points associated with microphone pair (5,11) being connected by a broken line in order to emphasize the different trends. Similar relationships are found in the data for lower engine speeds.

The introduction of forward motion produces a marked change in the measured difference between exterior and interior sound levels, as can be seen in Figure E.11. The data, for microphone pair (5,11), show little influence of forward motion at frequencies below 300 Hz., but at higher frequencies there is a large (5 to 15 dB) increase in the sound level difference. This is a consequence of the trend observed in Figure E.2 that, for the higher order harmonics the sound levels at microphone location 11 decrease with forward motion whereas those at location 5 show little change.

Data for microphone pairs (1,11) and (8,11) can be included but,

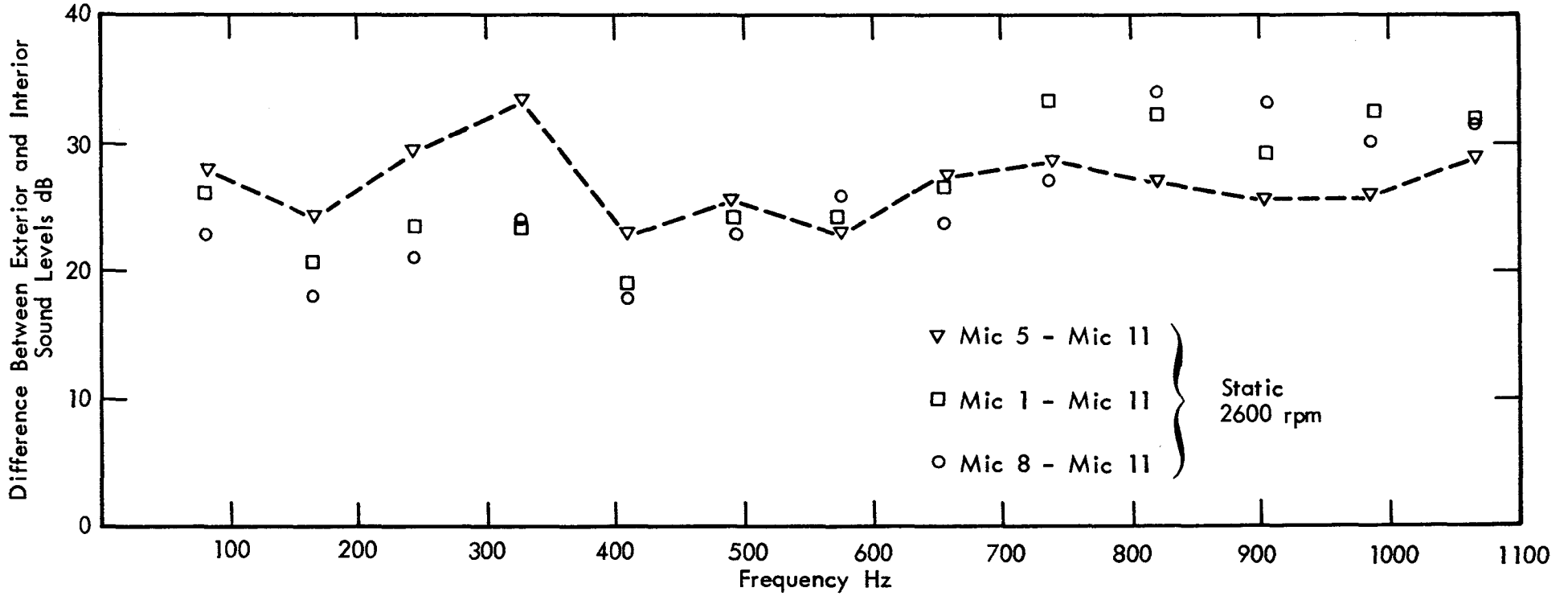

FIGURE E10. DIFFERENCE BETWEEN EXTERIOR AND INTERIOR SOUND LEVELS FOR DIFFERENT EXTERIOR MICROPHONE LOCATIONS. TEST SERIES I, 2600 RPM, STATIC.

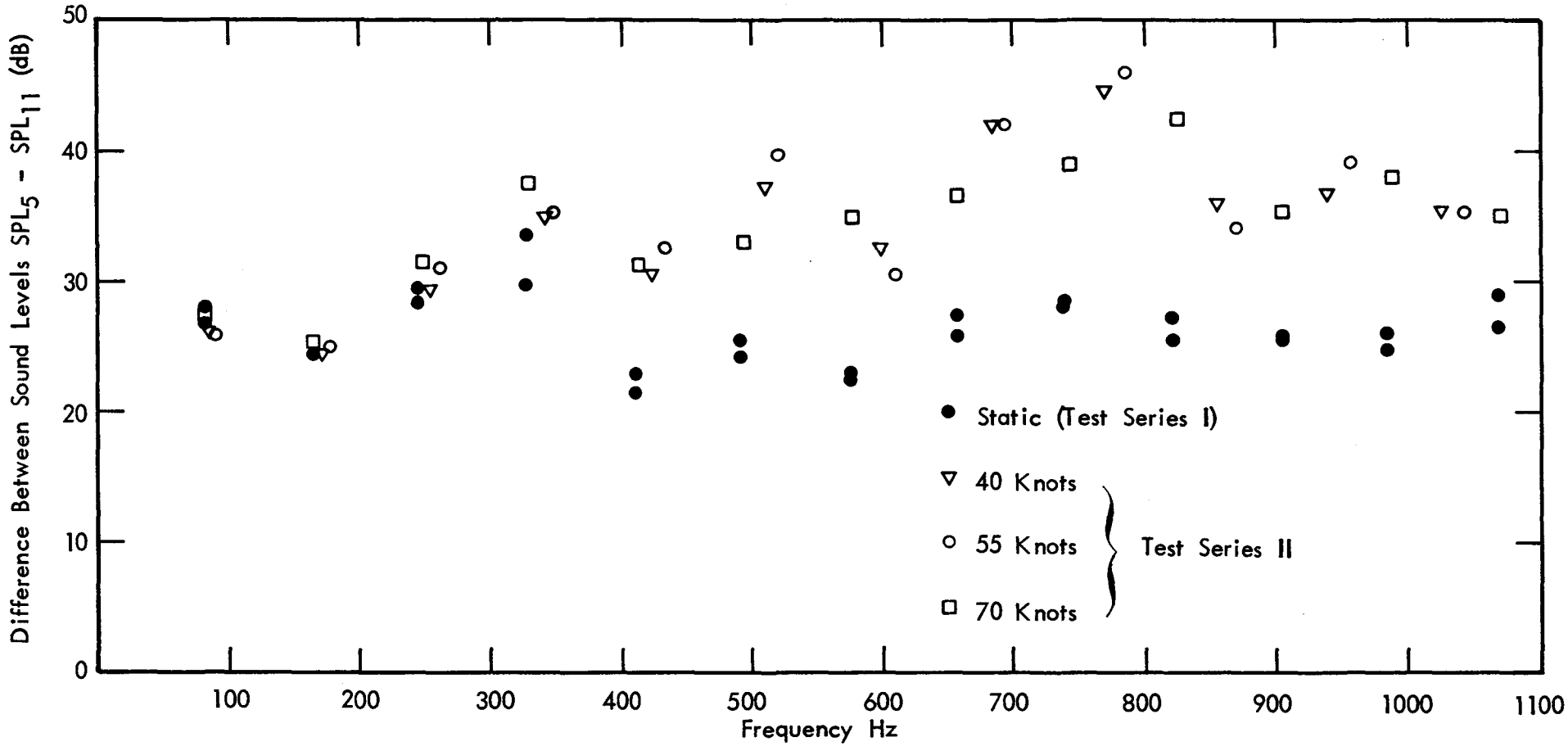

FIGURE E11. DIFFERENCE BETWEEN EXTERIOR (LOCATION #5) AND INTERIOR (LOCATION #11) SOUND LEVELS AT PROPELLER HARMONICS. TEST SERIES I AND II, 2600 RPM, FORWARD MOTION.

as data for microphone locations 1 and 8 were recorded during test runs which were different from those for microphone location 11, an indirect computation procedure was used with microphone location 5 as the common reference. Thus, the difference between levels at exterior location 1 and interior location 11 was computed from the difference between locations 1 and 5 on run 3 and the difference between locations 5 and 11 on run 5. A similar procedure was followed for microphone pair (8,11). A comparison of the computed differences in sound level is contained in Figure E.12 where it is seen that values for microphone pair (5,11) are now greater than the corresponding values for the other pairs, throughout the frequency range of interest.

Before concluding the discussion some comment should be made regarding the interpretation of the data in Figures E.9 through E.12 in terms of sidewall noise reduction. Firstly, it is apparent from data such as is in Figure E.2 that the sound levels at location 11 (at least for the static case) are due to the integrated effect of noise transmission through a region of the fuselage sidewall which is larger than that exposed to the high pressures in the plane of rotation of the propeller. Secondly, when forward motion is introduced, the external sound levels away from the plane of rotation of the propeller fall significantly for the higher order harmonics. Thus it is more likely that the sound level difference between locations 5 and 11 will be a measure of sidewall noise reduction when there is forward motion than when the airplane is static. Thirdly, even under forward motion conditions the left hand propeller can make significant contribution to the interior sound level at location 11, thereby contaminating a measure of sidewall noise reduction.

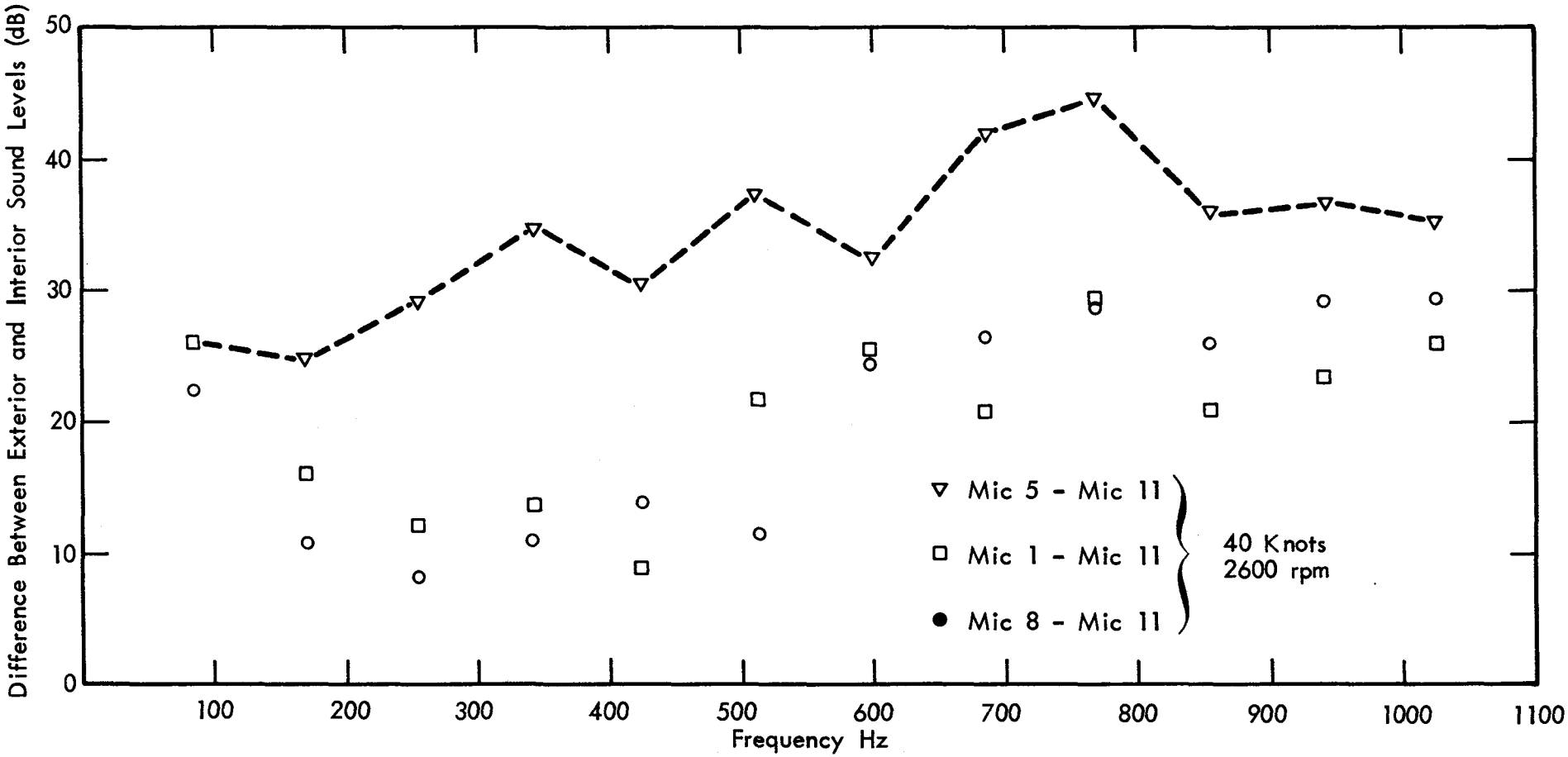

FIGURE E12. DIFFERENCE BETWEEN EXTERIOR AND INTERIOR SOUND LEVELS FOR DIFFERENT EXTERIOR MICROPHONE LOCATIONS. TEST SERIES II, 2600 RPM, 40 KNOTS.

In summary it seems that all the above measurements of the difference in sound level between exterior location 5 and interior location 11 provide values which are lower than those attributable to sidewall noise reduction. The best estimate of sidewall noise reduction for the structure in the plane of rotation of the propeller would be obtained when taxiing the airplane with only the right hand propeller operating and when the three lowest order modes are excluded from consideration. Alternatively, the test would be performed with two engine operation where the engine speeds are well separated so that associated harmonic levels can be identified.

E.5 Summary

This appendix has presented interior noise data for a single microphone location and, on this basis, has attempted to provide some analysis and interpretation of the results. Obviously, from such a limited amount of information, particularly with respect to the spatial variation of the interior noise levels, it is difficult to deduce general conclusions. Certain comments can, however, be made and these are given below:

(a) The highest external sound levels occur in the plane of rotation of the propeller and these levels change only slightly with forward motion. In contrast, interior levels in the plane of rotation decrease as forward speed increases. Thus it is deduced that the levels at the interior measurement location are not dominated by the inplane exterior pressures under static conditions.

(b) As a consequnce of (a) it is deduced that the difference between exterior and interior sound levels, for static

conditions, does not give an accurate estimate of local sidewall noise reduction. It may underestimate the noise reduction by a significant amount. More accurate estimates might be obtained under forward motion conditions, but only in the plane of rotation of the propeller.

(c) Beating between contributions from left and right hand propellers results in fluctuating pressure levels in the five lowest order harmonics. The beat amplitude increases as the sound levels from the two propellers approach the same value at the measurement location. Conversely, the beat amplitude can be used to estimate the difference in levels for the sound pressures from the two propellers. However, the method cannot identify the propeller generating the higher sound level.

(d) Several of the problems associated with the analysis of cabin interior noise levels of the Aero Commander are associated with twin-engine operation. It is recommended that for future diagnostic tests the engines be deliberately operated at different rpm so that the harmonics of left and right hand propellers can be identified. Unfortunately, for reciprocating engines the spectra will become a complicated collection of propeller and exhaust frequencies making harmonic identification very difficult. An alternative approach would be to operate only one engine at a time. In addition it is recommended that forward motion and static conditions be always included in the test procedure as an aid to data analysis and because forward motion conditions represent the true practical flight situation.